# THE SYNTHESIS AND DEVELOPMENT OF BHQ-DERIVED COMPOUNDS: A PROBE FOR DYNAMIC BIOLOGICAL STUDIES

by

YUE ZHU

(Under the Direction of Timothy M. Dore)

## ABSTRACT

Caged compounds have been used in biochemistry and physiology for over two decades. BHQ compounds were found to protect bioactive functional groups and release the substrate effectively upon irradiation of light. BHQ-protected carboxylates, phosphates, and glycerol derivatives were synthesized and tested for their photochemical and photophysical properties. BHQ protected compounds were found to be sensitive to both 1PE and 2PE processes. The one-photon quantum efficiencies were found to be 0.29–0.39 upon irradiation with 365-nm UV light. The two-photon uncaging action cross-sections were determined to be 0.43–0.90 GM upon irradiation with 740-nm IR laser light. The dark hydrolysis rates of BHQ-caged compounds under simulated physiological conditions were found to be 69–105 h. Stern-Volmer quenching experiments, a photolysis in oxygen-18 labeled water, NMR observation of BHQ-OAc photolysis in acetonitrile-$d_3$, and time-resolved spectroscopic studies were executed to understand the photolysis mechanism of BHQ, which is proposed to be a solvent assisted heterolysis mechanism involving a short-lived triplet state.

BHQ-caged ATP was synthesized and examined for its photochemistry as a biologically useful, temporally and spatially controlled ATP releasing reagent.

INDEX WORDS: two-photon sensitive photoremovable protecting group, BHQ as biologically useful caging group, the photolysis mechanism of BHQ-OAc, BHQ-caged ATP

# THE SYNTHESIS AND DEVELOPMENT OF BHQ-DERIVED COMPOUNDS: A PROBE FOR DYNAMIC BIOLOGICAL STUDIES

by

YUE ZHU

B.S., Peking University, China, 2000

A Dissertation Submitted to the Graduate Faculty of The University of Georgia in Partial Fulfillment of the Requirements for the Degree

DOCTOR OF PHILOSOPHY

ATHENS, GEORGIA

2008

# THE SYNTHESIS AND DEVELOPMENT OF BHQ-DERIVED COMPOUNDS: A PROBE FOR DYNAMIC BIOLOGICAL STUDIES

by

YUE ZHU

| | |
|---|---|
| Major Professor: | Timothy M. Dore |
| Committee: | George F. Majetich<br>Robert S. Phillips |

Electronic Version Approved:

Maureen Grasso
Dean of the Graduate School
The University of Georgia
August 2008

ACKNOWLEDGEMENTS

My academic goals were achieved with the help and encouragement of many individuals. First, I would like to express my gratitude to my advisor, Timothy M. Dore. I want to thank him for his patience, encouragement, and guidance. Professor Dore was always helpful whenever I was in trouble. I will always appreciate his kindness.

I also want to thank the members of my committee, Professor George Majetich and Professor Robert Phillips, for their time and precious advice. I am also grateful to Dr. John Shields, Ramona Urbauer, Dr. Jeffrey Urbauer, Dr. Jon Amster, Franklin Leach, Dr. Dennis Phillips, and Dr. Greg Wylie for their help with instruments.

I want to thank my lab colleagues, Dr. Lesya Fedoryak, Min Lu, and Dr. Khalilah Reddie for their assistance with instrumentation and experimental techniques. I appreciate my friends for their support.

Finally, I thank my parents and relatives in China for their love and support.

TABLE OF CONTENTS

LIST OF TABLES

Page

LIST OF FIGURES

Page

LIST OF SCHEMES

Page

## Chapter 1

## The Caging Groups: History and Current Research

### *Introduction*

Investigations in biochemistry and physiology require tools that enable temporal and spatial control of biochemical substrates in biological and physiological systems. With easy accessibility, compared to other methods initiating chemical processes, the photoactivated release of bioactive particles has received considerable attention since Engels and Schlaeger's[1] first report about the release of free cAMP upon photolysis of the *ortho*-nitrobenzyl (2-nitrobenzyl or NB) ester of cAMP, which controls both the temporal and spatial release of cAMP in biological and physiological environments. Subsequently, Kaplan, Forbush, and Hoffman[2] reported the efficient photorelease of ATP and inorganic phosphates from the corresponding NB and the *ortho*-nitrophenethyl (1-(2-nitrophenyl)ethyl or NPE) esters (Figure 1). These authors gave the general term "cage" to the NB group to emphasize its application as a photoremovable protecting group. Since then, other chromophores have been developed to control the activity of

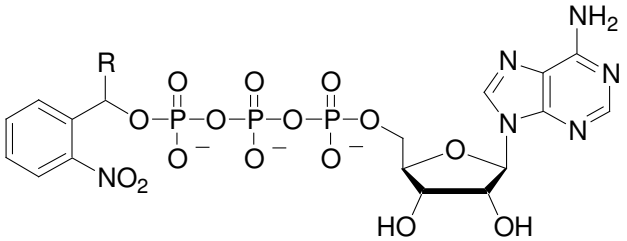


**1**: R = H (NB)
**2**: R = $CH_3$ (NPE)

**Figure 1.** NB-ATP and NPE-ATP structure

bioactive particles, and collectively, photoremovable protecting groups used in biology are all called "caging groups" and "caged compounds" are now extensively employed to study molecular processes in biochemistry, biophysics, cell biology, and neurobiology.

A caged compound consists of a bioactive substrate and a caging group. The caging group is connected to the bioactive particle through a covalent bond and renders its biological activity inert. Irradiation causes the covalent bond to break and the biologically active particle to be released; thus, the temporal and spatial release of the bioactive substrate can be achieved by controlling the light irradiation, as depicted in Figure 2.

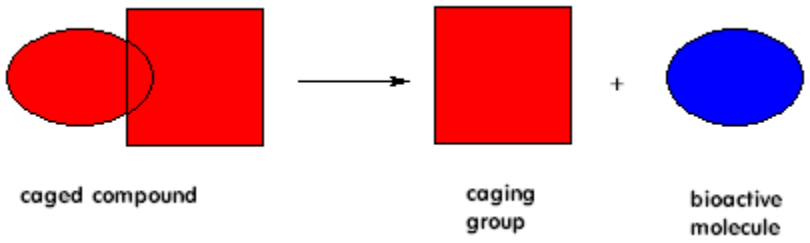


**Figure 2.** Release of bioactive substrate by a caged compound upon photolysis

An effective caging group in a biological system needs to fulfill the well-established criteria for common protecting groups[3] and be compatible with biological systems.[4] The necessary properties of a photoremovable protecting group to be applicable in biological systems for common bioactive substrates, such as ATP, L-glutamate, or γ-aminobutyric acid (GABA), are as follows: (1) The caged compound should not affect the biological system being studied; (2) any photoproducts other than the desired bioactive molecule should not interact or interfere with the biological system; (3) the caged compound should release the bioactive molecule rapidly in high yield at wavelengths of light that are not lethal to the biological system;[*] (4) the caged

[*] The one-photon quantum efficiency of the photochemistry should be high and the activating light wavelength should be more than 300 nm to avoid competition for light absorption by native

compound must be hydrolytically stable under physiological conditions (high ionic strength aqueous buffer, pH 7–7.4, 37°C) in a dark environment; (5) the caged compound should be soluble in water; and (6) the caged compound must be easily synthesized.

***Caging groups***

Many potential chromophores have been synthesized and tested for caging applications, but few have met the requirements or been successfully developed for biological use.[5-7] In this chapter, I will discuss selected photoremovable protecting groups that have been used in a biological system, pointing out the strengths and weaknesses of each one.

***2-Nitrobenzyl (NB)***

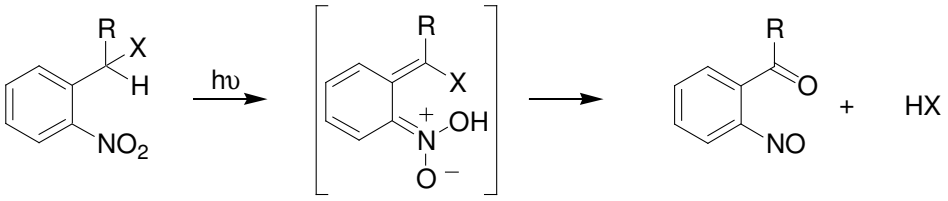


**3**: R = H (NB)
**4**: R = $CH_3$ (NPE)

**5** aci-nitro intermediate

**6** nitroso byproduct

Over 80% of the publications on caged compounds are applications of the NB chromophore and its derivatives. The NB caging group was the first developed photoremovable protecting group and is the most widely used one. The only commercially available caged ATP is based on the NB chromophore. The photolysis process of the NB group has been thoroughly studied,[8-10] and the overall mechanistic sequence is outlined in Scheme 1.

To better understand the factors that affect the rates and mechanism for the NB chromophore, the mechanism has been divided into five major steps: (1) excitation; (2) photored-ox to the aci-nitro intermediate **5**; (3) cyclization to the oxazole **10**; (4) ring opening to the hemi-

---

biological chromophores, and the rate-limiting step for the photorelease of the bioactive substrate should be faster than the physiological event under study.

**Scheme 1.** Photolysis mechanism of NB

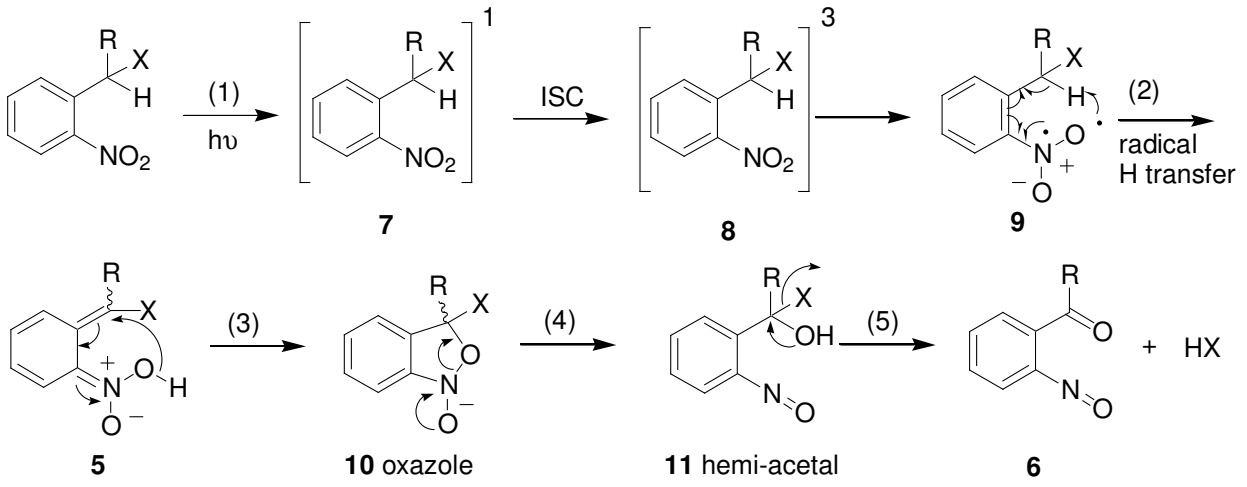


acetal **11**; and (5) collapse of the hemi-acetal with release of the substrate. The complexity of the reaction and the competing kinetic pathways make it important that those investigating dynamic effects using caged substrates become particularly aware of the limiting kinetics of the key step: the release of substrate from the hemi-acetal intermediate. While the rate constants vary with pH, media, and the nature of the substrate, it is the slowest step under physiological conditions requiring seconds to complete. The formation and decomposition of all the intermediates (aci-nitro intermediate, isomeric isoxazoles, and hemi-acetals) are pH dependent.[8] The leaving abilities of the substrates are also important. For example, photolysis of NPE-caged ATP will release ATP, a superior leaving group, but not methanol, which is a poor leaving group. At pH < 6, where the hemi-acetal is very unstable, and hydrolyzes as soon as it formed, the decomposition of isoxazole becomes the rate limiting step.

***NB derived caging groups***

Derivatives of NB (Figure 3) were developed to improve the photochemical and photophysical properties of the chromophores. Instead of a hemi-acetal, the photolysis of NPE[11-13] proceeds through a hemi-ketal, which is unstable and decomposes faster, thus it provides a

better leaving effect for the substrate, yet it is weakly absorbing over 340 nm. The dinitrobenzyl (DNB, **12**) derivative improves the quantum efficiency of the photolysis, but the absorptivity is not improved, and the uncaging sensitivity is not high. Dimethoxynitrobenzyl (DMNB, **14**)[11,14,15] has improved light absorption with the two methoxy groups on the phenyl ring, the absorption at high wavelength is greatly improved with lower quantum yield, and the uncaging sensitivity is several times better than that of NB and NPE. Carboxynitrobenzyl (CNB, **16**)[16-18] possesses better solubility and faster release kinetics; the carboxylate group on benzyl position improves the solubility of the compound in aqueous buffers. The photo-byproduct of CNB, nitrosopyruvate **17**, decomposes rapidly.

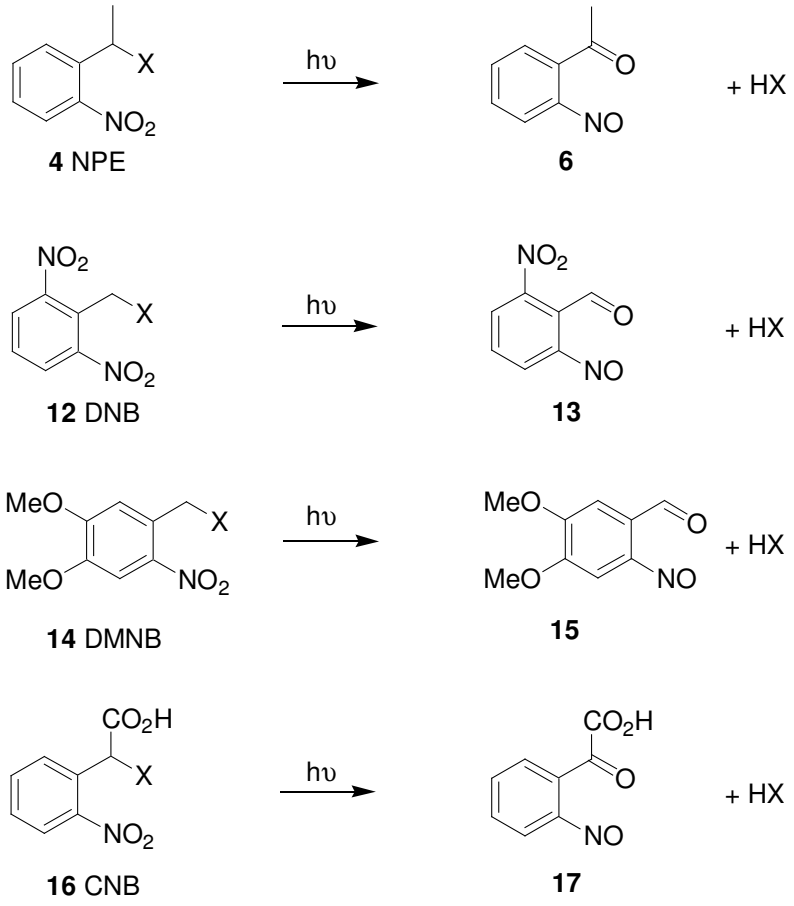


**Figure 3.** Photolysis of NB derived caging groups

In Figure 4, some examples of applying NB and its derivatives to caging small biological molecules, including nucleotides, carboxylates, amines, amides, alcohols, phenols, phosphates, protons, $Ca^{2+}$, and fluorophores are presented. The basic photochemical properties of these

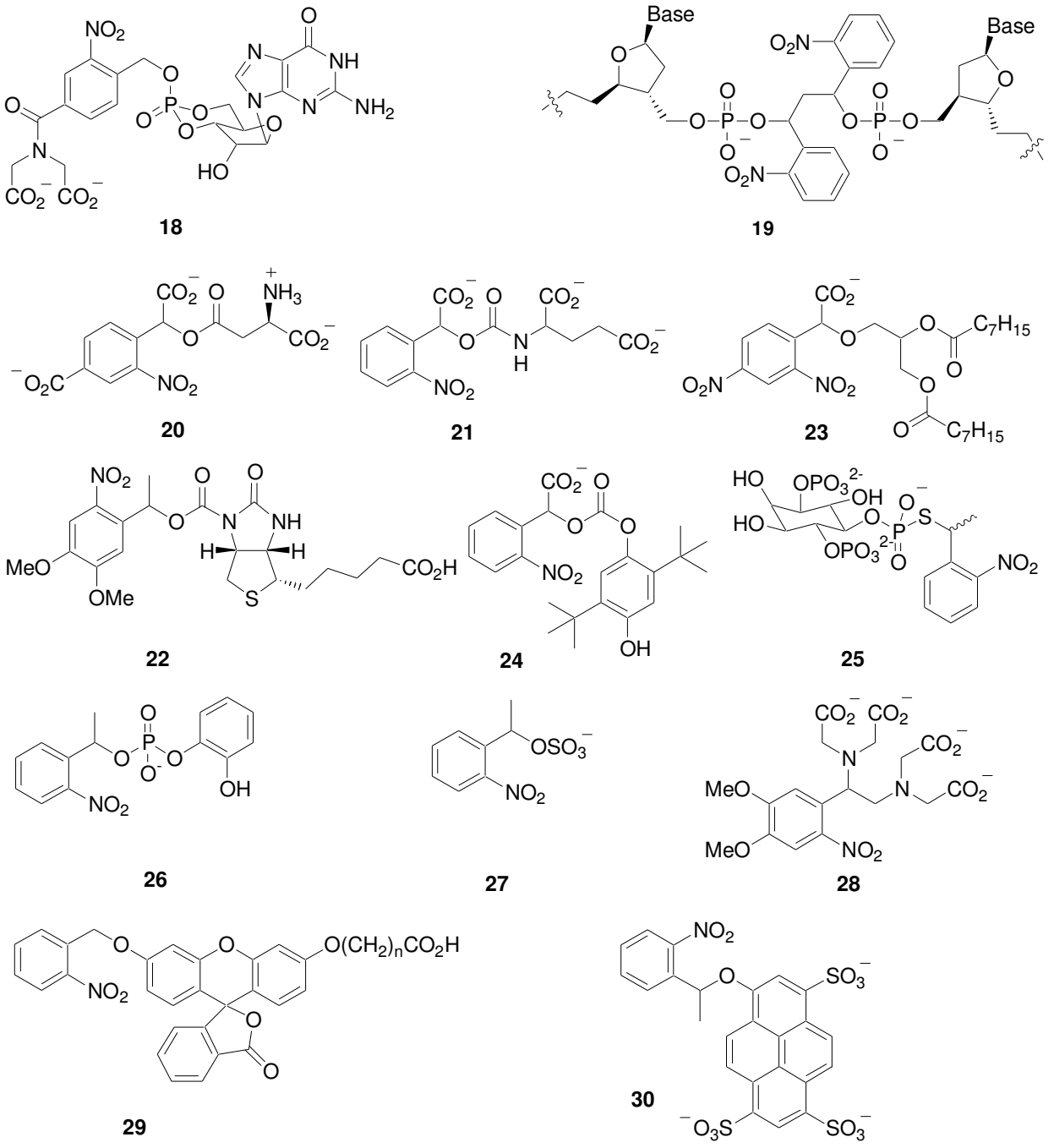


**Figure 4.** NB and derivatives caged biological molecules

compounds are shown in Table 1. Most of the NB-caged molecules have good absorption at wavelengths <300 nm, but the absorptivity over 340 nm is poor. DMNB is the only caging group among NB derivatives with good absorption at long wavelengths. The quantum yield of NB-derived caged compounds ranges from 0.07 to 0.57; it relies on the leaving ability of the protected functional groups.

**Table 1.** Photochemical properties of NB-caged compounds

| Caged compounds | $\lambda_{max}$ (nm) | $\varepsilon$ ($M^{-1}\cdot cm^{-1}$) | $\phi$ | Reference |
|---|---|---|---|---|
| **18** | 251 | 20300 | 0.24 | 19, 20 |
| **19** | — | — | — | 21, 22 |
| **20** | 440 | 3000 | 0.14 | 23 |
| **21** | 270 | — | 0.11 | 24 |
| **22** | 346 | 9400 | — | 25, 26 |
| **23** | — | — | 0.18 | 27 |
| **24** | 270 | — | 0.10 | 28 |
| **25** | — | — | 0.57 | 29 |
| **26** | 270 | 4600 | 0.095 | 30 |
| **27** | 263 | 4700 | 0.47 | 31 |
| **28** | 350 | 4330 | 0.18 | 32 |
| **29** | 350 | 47 | 0.07 | 33 |
| **30** | 403 | 18500 | 0.13 | 34 |

Although we have gained an understanding of the photochemistry of NB-derived caging groups and their advantages in many applications, limitations exist. For example, the photo-byproduct nitroso functional group is poisonous to most biological systems, and experiments must be designed to minimize its effects. The quantum efficiency and release kinetics of most NB derivatives are not impressive. The slow release of substrates, which is on the second timescale, is a limiting factor for applications in biological studies. Thus, there is still a strong need for other efficient caging groups.

***Nitroindolyl (NI)***

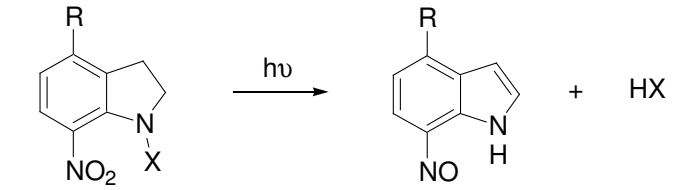


**31**: R = H (NI)
**32**: R = OMe (MNI)

**33**: R = H
**34**: R = OMe

Compared to the 100-year old observation of the photoisomerization of 2-nitrobenzaldehyde, photocleavage of 1-acyl-7-nitroindolines has a much shorter history. Patchornik and co-workers found that 1-acyl-5-bromo-7-nitroindolines were photolyzed in organic solvents containing a low proportion of water, alcohols, or amines.[35] The products were nitroindoline and a carboxylic acid, ester or amide, depending on the nucleophile existing in the system. The work was intended for peptide synthesis,[36] but put aside for over twenty years because the purities of the products did not meet the demands. The Corrie group began to use NI for the release of neuroactive amino acids.[37-40]

**Scheme 2.** Photolysis mechanism of NI

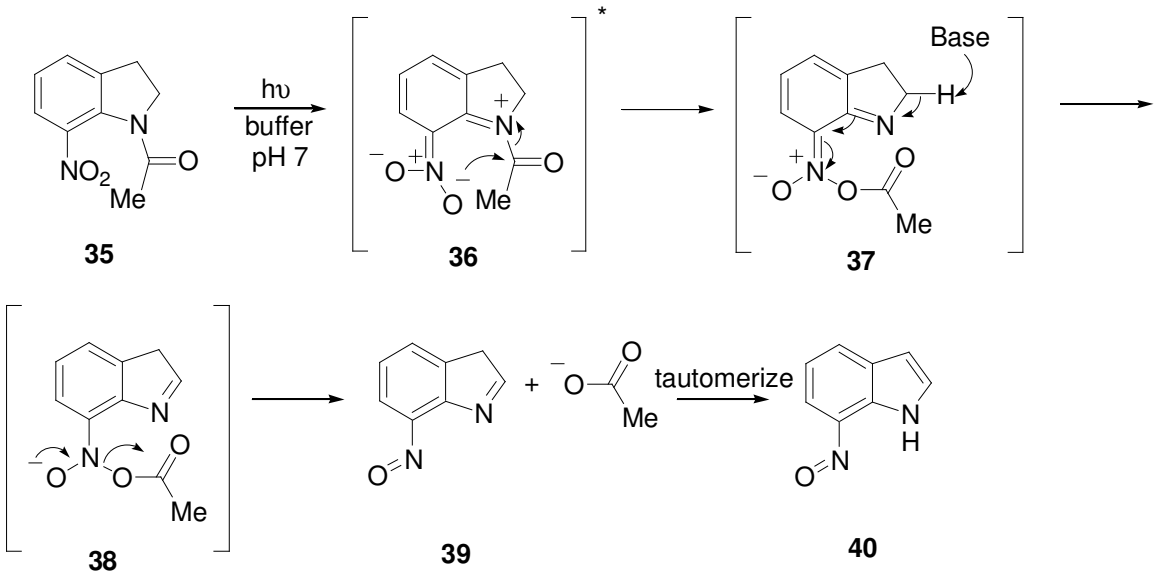

Based on the study of 1-acyl-7-nitroindolines, the photolysis mechanism is considered to proceed through a triplet excited state and involve an intramolecular attack of one oxygen atom of the nitro group on the carbonyl (Scheme 2). A methoxy group on the aromatic ring of the NI group also improves its light absorption and photolysis efficiency. Thus, methoxy nitroindolyl (MNI) is a caging group with improved properties. The kinetics of NI and MNI deprotection are on the microsecond timescale, significantly faster than the NB derivatives. Widespread application of these two photoremovable protecting groups is limited, because they are only capable of protecting carboxylates. Several examples of applying NI and MNI for calcium regulation and fluorophore caging are shown in Figure 5.[9,41,42]

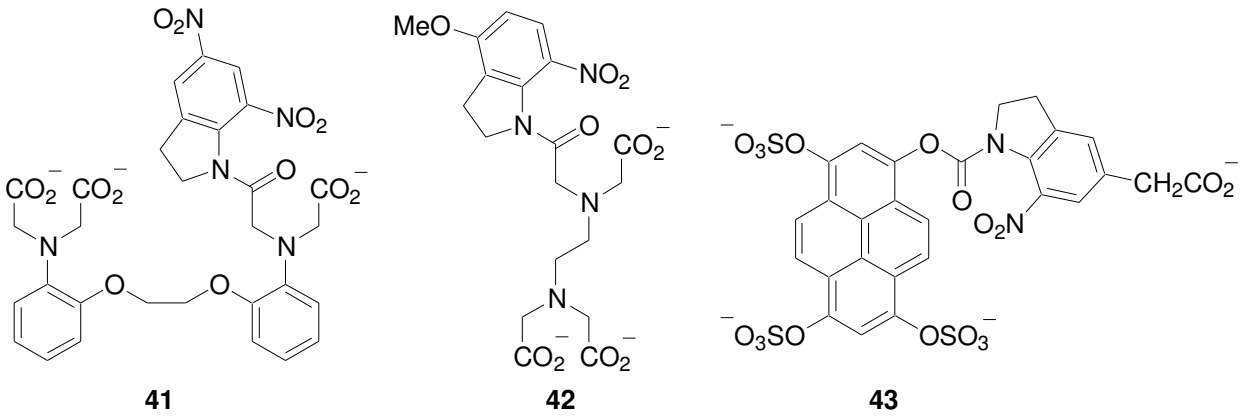


**41** **42** **43**

**Figure 5.** NI and MNI caged compounds for $Ca^{2+}$ regulation and fluorophore activation

***Benzoin***

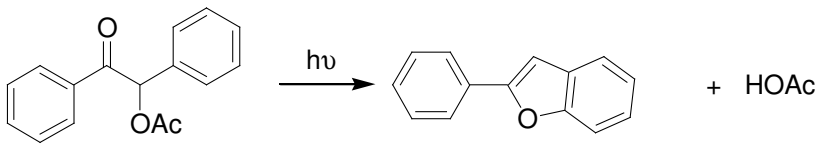


**44** **45**

Benzoin acetates rearrange to 2-arylbenzofurans upon photolysis with release of acetic acid.[43] During the past decade, the benzoin (**44**) or desyl group have been popular photoremovable protecting groups because this chromophore has strong absorptivity in the near

UV region, high quantum efficiency, and an unreactive side product of photolysis (**45**). Although the functional groups that can be protected by benzoin are limited to only carboxylic acids or phosphates, the use of benzoin as a caging group is an attractive alternative to NB as a caging group for a number of applications.[44-47] Another advantage is that benzoin-caged derivatives are synthesized in good yields by straightforward procedures.

With nanosecond laser flash photolysis studies, Wan[48] proposed a singlet intramolecular reaction mechanism for 3,5-dimethoxybenzoin-OAc photolysis (Scheme 3). He also suggested that a short-lived cationic intermediate **48** was generated.

**Scheme 3.** Photolysis mechanism of benzoin (desyl)

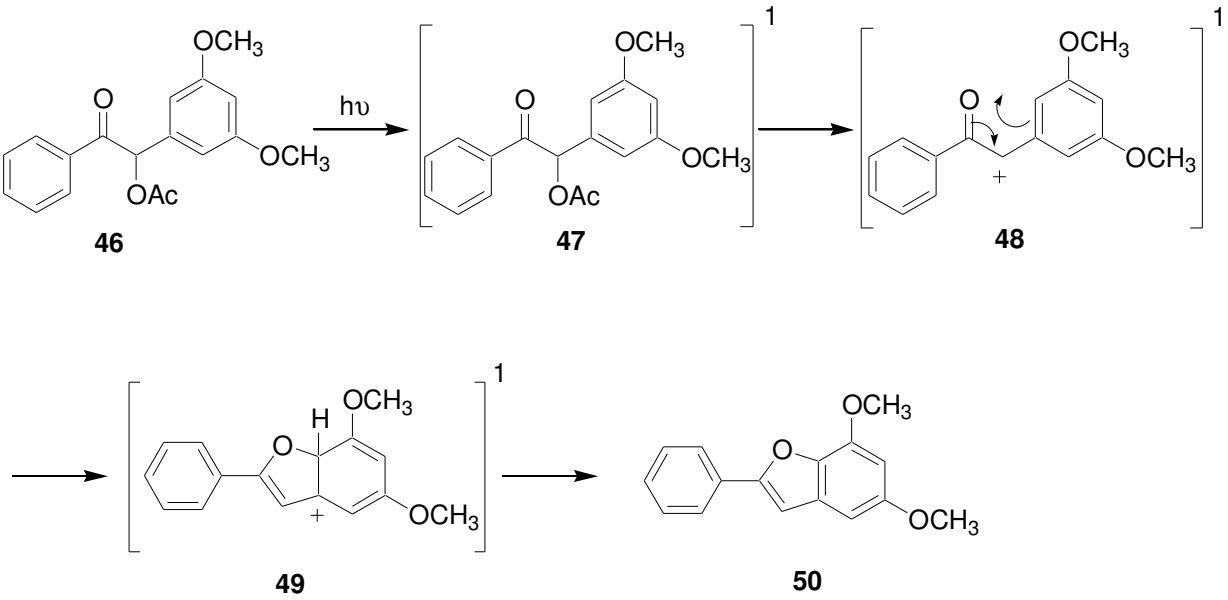


After the molecule is excited to the singlet excited state, an intramolecular charge transfer exciplex is generated between the electron rich dimethoxybenzyl and the electron deficient [n, $\pi^*$] excited carbonyl.[48] Consequently, after the loss of the protected group (acetyl in this case), the formation of the cyclized, protonated furan is followed by proton loss to give 2-phenylbenzofuran **50** as the product.

Methoxy substitution on the benzyl ring helps the transformation to the 2-phenylbenzofuran, and the reactive state was assigned as either a singlet excited state or an untrapable, short-lived triplet excited state.[43] On the other hand, unsubstituted benzoin derivatives will undergo fast intersystem crossing from the singlet to the triplet state. Givens and Wirz[49] reported that benzoin phosphates photocyclize through the triplet excited state.

The methoxy substituent on the benzyl group is crucial for efficient photolysis. For example, photolysis at 366 nm converted the 3-methoxybenzyl and 3,5-dimethoxybenzyl derivatives to the corresponding 2-phenylbenzofurans in excellent yields,[48] while the 4-methoxybenzyl analogs gave only 10% of 4-methoxy-2-phenylbenzofuran along with other byproducts.

The high quantum yield of 0.64 observed for 3,5-dimethoxybenzoin-OAc (**46**) indicated that the photorelease was efficient. The rate-determining step of the photolysis is the cyclization and protected group loss, which are assumed to occur within 20 ns at room temperature based on a picosecond resolved pump-probe study.[49] The photorelease is also rapid. Despite the limitation on the type of protected groups and the solubility issue, benzoin is still an attractive caging group for carboxylates and phosphates, both of which are commonly used bioactive functional groups.

***Phenacyl***

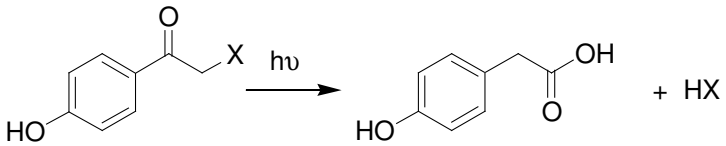


**51** *p*HP **52**

The suitability of the *para*-hydroxyphenacyl (*p*HP)[6,7,50] group as a photoremovable protecting group was discovered in the mid 1990s. Development of this group continues today, yet the number of applications is still limited. The functional groups that can be protected and

efficiently released include carboxylates, phosphates, sulfonates, sulfides and halides. There are two important features of the *p*HP group photolysis: (1) the first-order photochemical heterolytic cleavage of the substrate-phenacyl bond and (2) the rearrangement of the conjugated chromophore skeleton leading to an intermediate insensitive to the light used during the heterolysis. The side product (**52**) structure does not have a strong absorption over 300 nm. The release of the substrate occurs on a nanosecond timescale with quantum yields of 0.1–0.4, as the result of the first-order heterolytic cleavage process. The rearrangement assures that the conversion of the caged moiety to the free substrate will be completed. These properties assure the deprotection of molecules with high quantum efficiency, rapid release rate of substrates, and high conversion of the released substrate.

The reaction mechanism is best described as an excited state "Favorskii-like" rearrangement (Scheme 4)[44,50-53]. The photochemical "Favorskii" process was first suggested by Reese and Anderson[51] in 1962 for the photorearrangement of 2-chloro-4'-hydroxyacetophenones that includes a cyclopropanone intermediate. In the photolysis of *p*HP, molecule **51** will be excited to the singlet excited state **53** and the singlet excited state **53** will undergo intersystem

**Scheme 4.** Photolysis mechanism of *p*HP

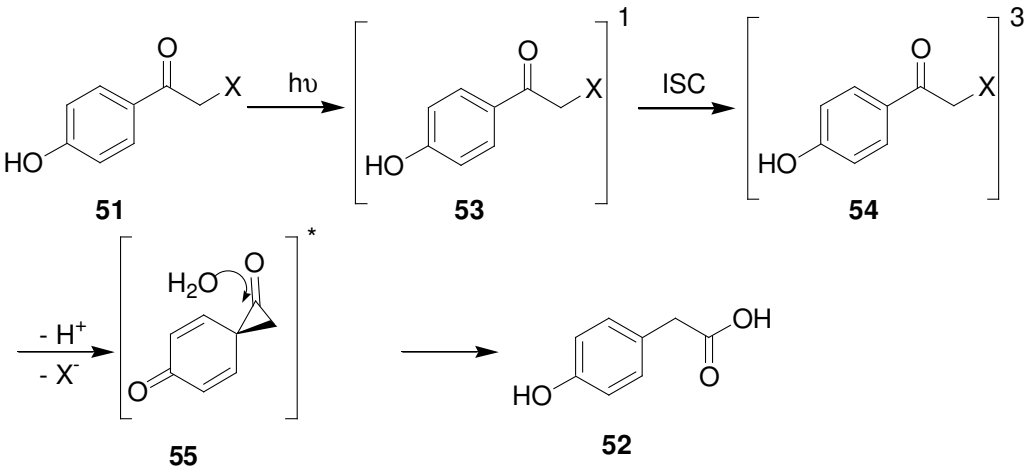

crossing (ISC) to form the triplet excited state **54**. With the heterolytic cleavage of the substrate phenacyl bond, a "Favorskii" cyclopropanone ring **55** will be formed. The resulting spirodienedione, an unstable intermediate in this rearrangement, will be hydrolyzed in aqueous media to form *para*-hydroxyphenylacetic acid immediately.

Corrie and Wan[54] proposed an alternative mechanism, that suggests that the release of substrate and formation of cyclopropanone occur from the *p*HP singlet excited state (Scheme 5). The phenolic proton is effectively transferred to the carbonyl oxygen to form a *para*-quinone methide **57** in aqueous media. Corrie and Wan termed this process as a formal Excited-State Intramolecular Proton Transfer (ESIPT). In their laser flash photolysis experiment, a singlet state intermediate absorption at 330 nm was observed. Kinetic studies at different pHs showed that this absorption band consists of two species with very similar UV absorptions and related by a prototropic equilibrium. With evidence from other photosolvolysis reactions,[55] these two species are assigned to **54** and its conjugate base.

**Scheme 5.** Corrie and Wan's mechanism of photolysis of *p*HP

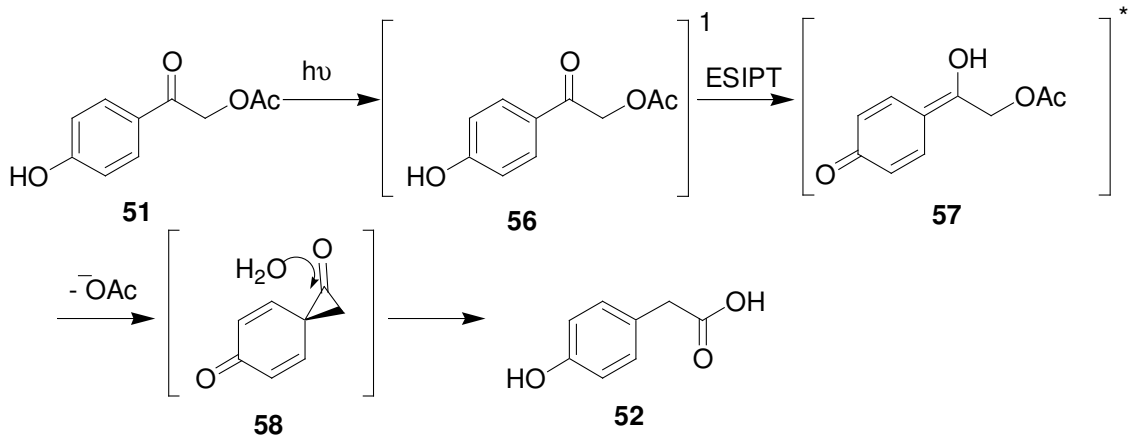


The photochemistry of the *p*HP provides a good tool for rapid and efficient photorelease of biologically active substrates if they have a relatively good leaving group. The sensitive wavelength range is limited to less than 300 nm in organic solvent and 330 nm in water, but

other properties such as solubility in aqueous buffers, synthetic accessibility, and stability in the dark are excellent.

The rapid release rates of substrates from the *p*HP caging group enables the study of many biological processes that need rapid increases in local concentration of substrates. Some examples of *p*HP caged biological substrates (neurotransmitters and nucleotides) are shown in Figure 6, and their basic photochemical properties are reported in Table 2.

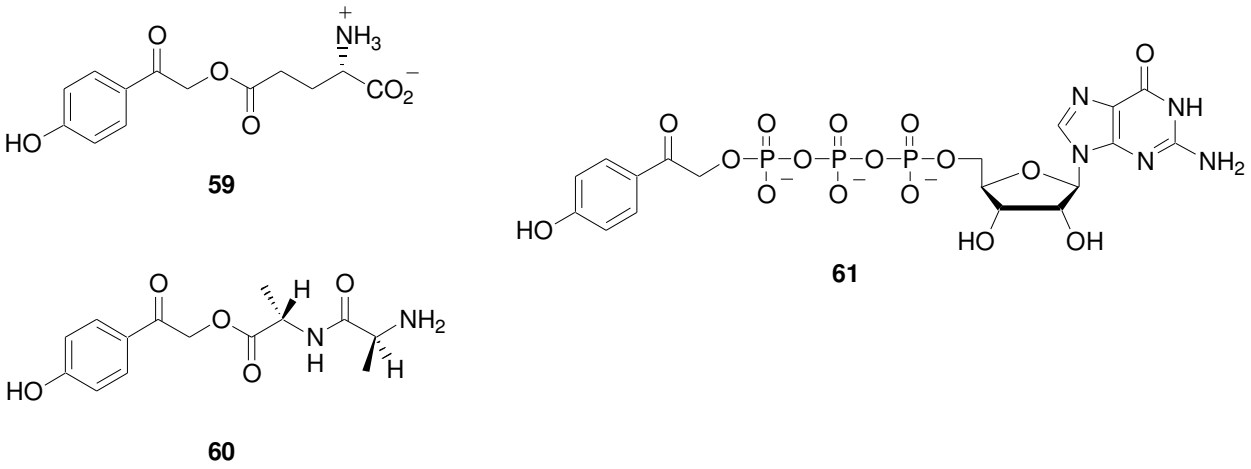


**Figure 6.** *p*HP-caged biomolecules

**Table 2.** Photochemical properties of *p*HP-caged compounds

| Caged compounds | $\lambda_{max}$ (nm) | $\varepsilon$ ($M^{-1}\cdot cm^{-1}$) | $\phi$ | Reference |
|---|---|---|---|---|
| **59** | 282 | 14500 | 0.21 | 56 |
| **60** | — | — | 0.25 | 57 |
| **61** | 286 | 14600 | 0.30 | 53 |

***Aryl methyl***

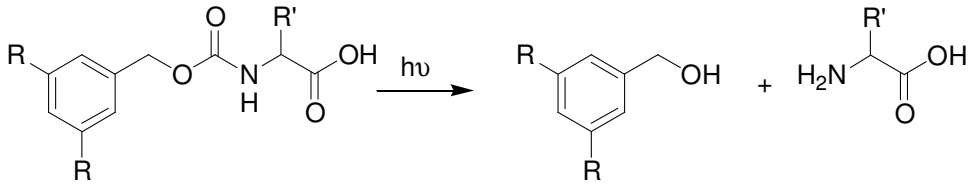


**62 Bz** $CO_2NH$ gly glycine (R, R' = H) **63** **64**

An aryl methyl caging group is mainly designed for protection and release of amino acids. Barltrop[58] first reported the photochemistry to release glycine from *N*-benzyloxycarbamoyl glycine in aqueous buffer at 254 nm. Four years later Chamberlain developed 3,5-dimethoxybenzyl chromophores, which have now become the most popular benzyl derivatives as caging groups.[59]

The photolysis process is believed to be a photosolvolysis reaction through its singlet excited state by heterolysis, for which the reactive excited state has been characterized. At the present time, this is accepted as the general mechanism (Scheme 6). Zimmerman[60] showed that electron donating groups on either the *ortho* or *meta* positions cause preferential photoheterolysis and give higher quantum efficiencies and photolysis rates comparing to the photoreactions of the *para* analogs. Zimmerman further reported that the 3,5-dimethoxybenzyl acetate cleanly produced the product in 77% yield with a quantum efficiency of 0.10.

**Scheme 6.** Photolysis mechanism of aryl methyl caging groups

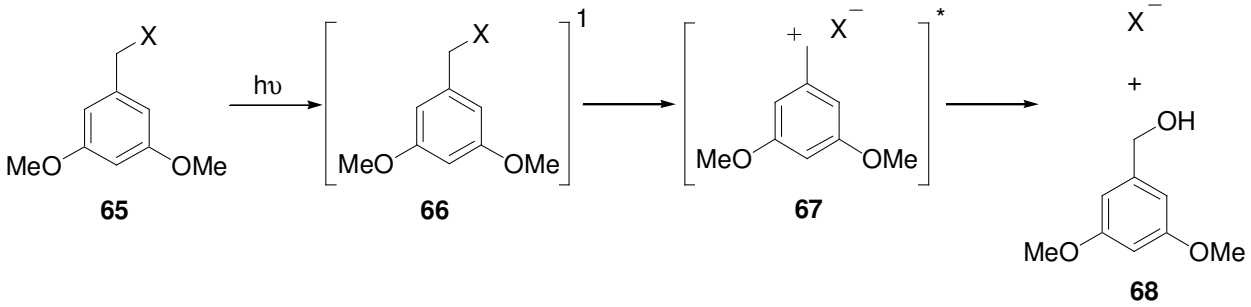


**65** **66** **67** **68**

Givens[61] and Pincock[62] have independently done preliminary mechanistic work on naphthylmethyl derivatives. Their results indicated that the photochemical reactions are similar to the benzyl and methoxybenzyl analogs. These reactions generally require polar, protic solvents to trap the cation, otherwise it will undergo a radical reaction to form unwanted products. The quantum efficiencies of these naphthylmethyl compounds tend to be lower than benzyl analogs.

***Coumaryl derivatives***

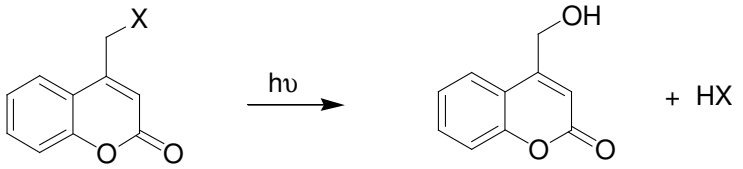


**69** Coumaryl **70**

Coumaryl analogs are known for their high fluorescence efficiency, and many analogs with known physical and photophysical properties exist. The coumaryl ring is found to be stable under intense photolysis conditions through many laser dye experiments. These compounds have drawn great interest as photoremovable protecting groups.

Most of these compounds are highly fluorescent, while many of the protected molecules are weakly fluorescent. With the introduction of light into the studied system, the bond cleavage between the coumaryl group and bioactive molecule causes a change of fluorescence intensity. This change in fluorescence has been used to monitor the process of the photolysis reaction. Recent work has shown that the 6-bromo-7-hydroxycoumarylmethyl (Bhc) group has a good two-photon action cross-section[15] and can be applied in two-photon uncaging studies (more discussion on this subject later). Coumaryl-protected compounds are easy to synthesize.

Bendig and Hagen[63,64] proposed a mechanism that outlines the major steps in the release of substrate from the [π, π*] singlet excited state of coumaryl compounds (Scheme 7). The

coumaryl chromophore is excited to the singlet state, followed by heterolytic C-O bond fragmentation. The resulting ion-paired species is trapped by the solvent to afford the coumaryl residue and the bioactive substrate. According to Bendig and Hagen's mechanism, the rate-limiting step is the heterolysis step. A significant coumarin-X bond weakening takes place upon excitation of the substrate to singlet excited state **72**. Strong electron donating abilities from the substituents on the coumarin ring stablizes the coumaryl cation **73**. On the other hand, the stablization of $X^-$ is achieved by selecting anions with large $pK_b$ values.[65]

**Scheme 7.** Bendig and Hagen's mechanism of photolysis of coumaryl caging group

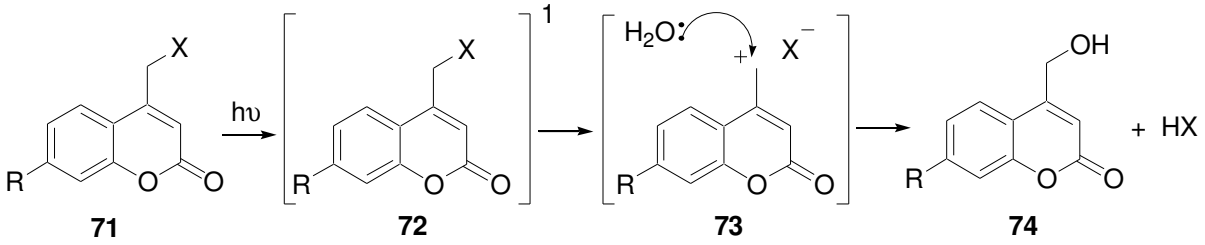


A large number of substituted coumaryl derivatives have been tested for the substituent effect at the 6- and 7-position of the coumaryl chromophore. The 7-hydroxyl, 7-carboxymethoxy and the 7-diethylamino coumaryl cages[63,64,66-69] were synthesized, and their release quantum efficiencies were determined using a phosphate leaving group. The 7-diethylamino coumaryl derivative chromophore extended the excitation wavelength range to over 400 nm without compromising the efficiency (0.20-0.25). The 7-carboxymethoxy coumaryl chromophore derivatives have a narrower effective wavelength range, which is less than 365 nm, and the photolysis efficiencies were lower (0.08-0.16). The 7-hydroxy coumaryl chromophore was the most hydrophilic of all three, and it had the best thermal stability among all the derivatives tested. Its quantum efficiency for photolysis ranged from 0.08 to 0.24.

Like most of the other caging groups mentioned, coumaryl derivatives also require a good leaving group so that the release of the substrate will be completed. Alcohols and amines are not

efficiently released. The alternative method for photoreleasing alcohols and amines involves the formation of free carbonate or carbamate, which will hydrolyze, releasing carbon dioxide and the bioactive alcohol or amine. This process occurs on the millisecond scale, which is quite comparable to the diffusion rate of substrates in biological systems. The release of free alcohols or amines is not rapid enough for some biological studies that require a localized fast change of the concentration of substrates.

Hagen and Bendig synthesized a series of 7-methoxycoumarylmethyl caged compounds[63,64] and determined the photorelease efficiency. *n*-Heptanoate, benzoic acid, *para*-substituted benzoic acid, sulfonate, and diethyl phosphate can be protected and photoreleased with a quantum yield of 0.037-0.081. When the leaving groups were *n*-heptanoate, sulfonate, and diethyl phosphate, >95% yields were achieved.

Furuta has also examined the photolysis of 7-substituted coumarins.[66] Electron-donating substituents on the 6- and 7-positions and electron withdrawing groups at the 3-position help to extend the absorption wavelength. Furuta's recent work in this area has led to the development of 6-bromo-7-hydroxy-coumarinyl-4-methyl (Bhc) as a photoremovable protecting group for two photon activated photolysis. Bhc esters and carbamates efficiently release carboxylates and amines upon photolysis by both one- and two-photon excitation processes.

In Figure 7, examples of Bhc-caged phosphates, carboxylates, sulfates, amines, alcohols, phenols, diols, ketones, and aldehydes are shown. The photochemical data are given in Table 3.

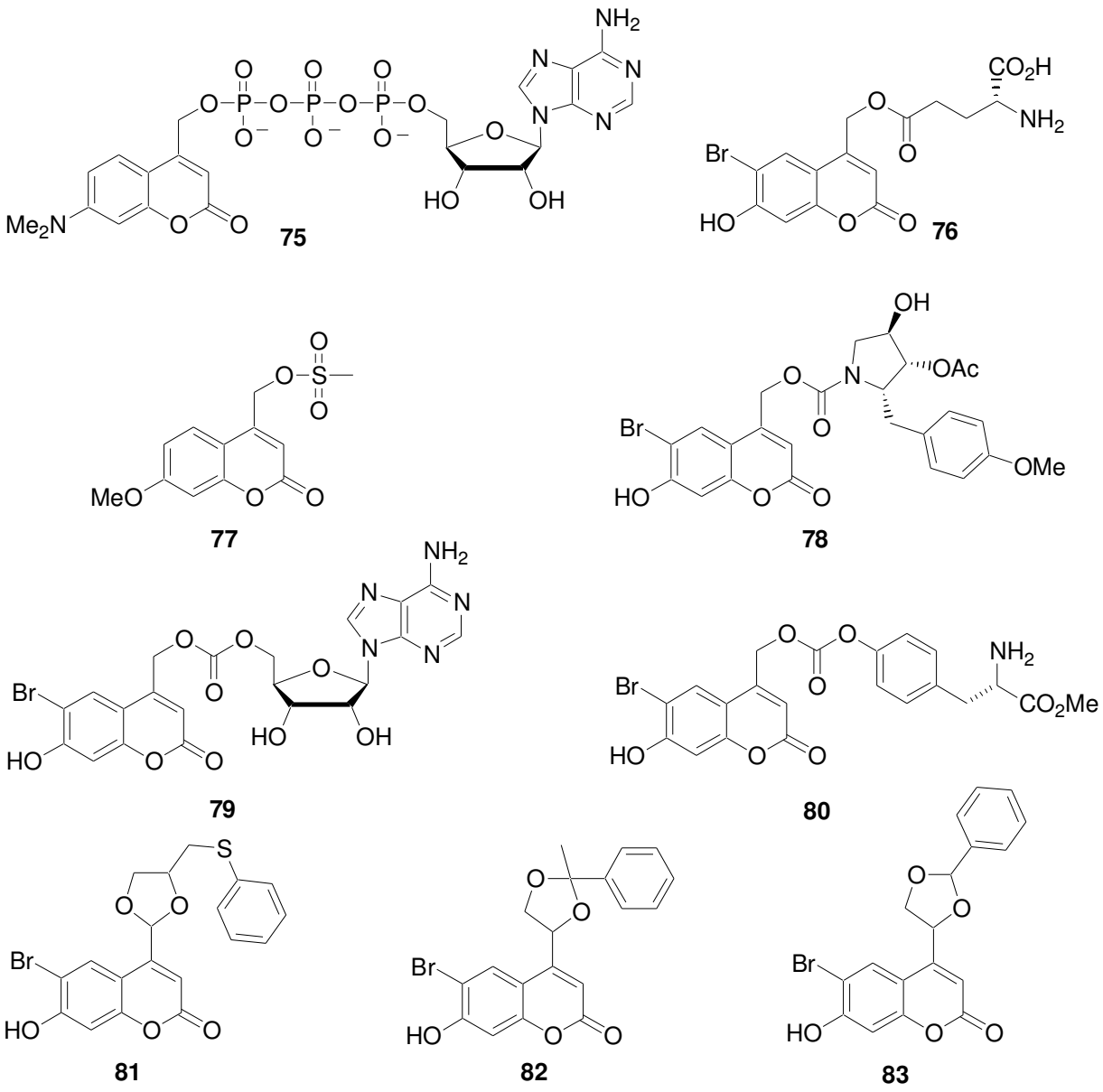


**Figure 7.** Coumaryl-caged compounds

**Table 3.** Photochemical properties of coumaryl-caged compounds

| Caged compounds | $\lambda_{max}$ (nm) | $\varepsilon$ ($M^{-1}\cdot cm^{-1}$) | $\phi$ | Reference |
|---|---|---|---|---|
| **75** | 385 | 15300 | 0.086 | 70 |
| **76** | 369 | 19550 | 0.019 | 15 |
| **77** | 325 | 13000 | 0.081 | 63 |
| **78** | 373 | 14500 | 0.040 | 71 |
| **79** | 373 | 13700 | 0.012 | 72 |
| **80** | 372 | 13900 | 0.020 | 72 |
| **81** | 348 | 8500 | 0.053 | 73 |
| **82** | 370 | 18400 | 0.030 | 74 |
| **83** | 370 | 18400 | 0.057 | 75 |

***Applications of caging groups in biological studies***

***Caged cyclic nucleotides***

The photorelease of cyclic nucleotides in living cells is a powerful method to study their cellular activities and control their downstream effects. Many different caging groups can be used to protect cyclic nucleotides. The cyclic nucleoside monophosphates (cNMP) control a variety of important cellular processes. Their primary targets are cAMP and cGMP regulated phosphodiesterases, cAMP and cGMP dependent kinases, cyclic nucleotide gated ion (CNG) channels, hyperpolarization activated and cyclic nucleotide gated (HCN) channels, guanosine nucleotide exchange factors, and bacterial transcription factors.

The most widely used caging groups in this area can be categorized into two divisions. The first one comprises NB, NPE and their derivatives,[11,19] which are the first developed photoremovable protecting groups. The second one comprises coumaryl derivatives. DMNB, NPE and 4,5-bis(carboxymethoxy)-2-nitrobenzyl (BCMNB) derivatives are the most important NB-caged cyclic nucleotides. NPE and BCMNB derivatives have high photochemical quantum yields and low absorption at wavelength >300 nm. DMNB-caged compounds absorb at longer

wavelength with quantum yield of 0.005–0.05. The NPE-, BCMNB- and DMNB-caged cyclic nucleotides are found to have low sensitivity at wavelength >330 nm. Consequently, relatively intense UV light is needed for successful uncaging of cyclic nucleotides. The coumaryl caged cNMPs[63,64,67,75] with electron donor substituents at the 7-position of the coumaryl ring possess a set of favorable properties, making them ideal tools for intra- and extra-cellular studies of cyclic nucleotide signaling. They show no background activity, are stable to solvolysis, and are photolyzed efficiently and extremely quickly using long wavelength UV–Vis light (330–440 nm). The hydrophilicity of the coumaryl-caged compounds can be adjusted, by changing substituents on the coumaryl ring. The coumaryl-caged compounds are superior to the NB analogs.

Caged cyclic nucleotides have been used to elucidate several cAMP and cGMP dependent signaling pathways. Karpen and co-workers[76] were the first to study CNG channels using DMNB-caged cGMP. When cAMP and cGMP are bounded to a site on the C-terminal end of the channel polypeptide, CNG channels are directly gated open. In Karpen's experiment, membrane patches were exposed to a DMNB-caged cGMP solution. With flash irradiation of UV light (≥ 14 ns), cGMP was released, and CNG channels became activated with a time course fitted in a single exponential with a time constant of 2.1 ms.

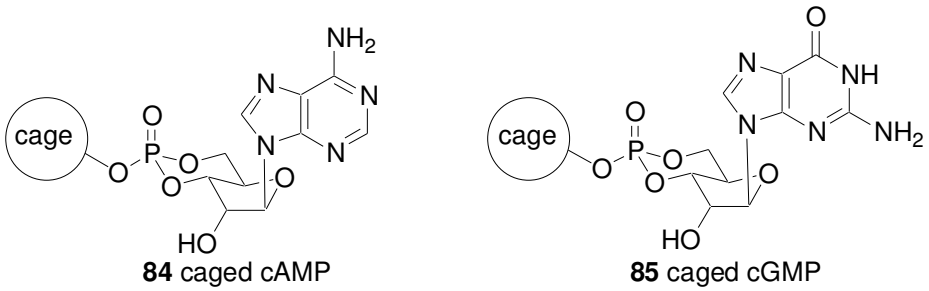


**84** caged cAMP **85** caged cGMP

**Figure 8.** Caged cNMP

Kaupp and co-workers[77,78] used caged cAMP to study hyperpolarization-activated and cyclic nucleotide-gated (HCN) channels. Compared to CNG's direct cAMP and cGMP binding dependence, HCN channels are activated by hyperpolarized membrane potentials. Cyclic nucleotides can directly enhance the activation of the channels. To activate these channels, the required concentration level of cAMP is significantly lower than cGMP. Kaupp's work showed that the activation of HCN channels by photo-released cAMP occurs with almost no delay.

***Caged calcium***

Calcium ions are important second messengers, and several caged calcium ion chelators have been synthesized based on the NB caging groups. NITR-5, NITR-7, NP-EGTA, and DM-Nitrophen[79-83] (Figure 9) all employ the NB caging group as the key structure initializing the photo-process. NITR-5 **86** and NITR-7 **87** are based on 1,2-bis(*ortho*-aminophenoxy)ethane-*N*,*N*,*N*',*N*'-tetraacetic acid (BAPTA) chelating structure; DM-nitrophen **88** is based on ethylene

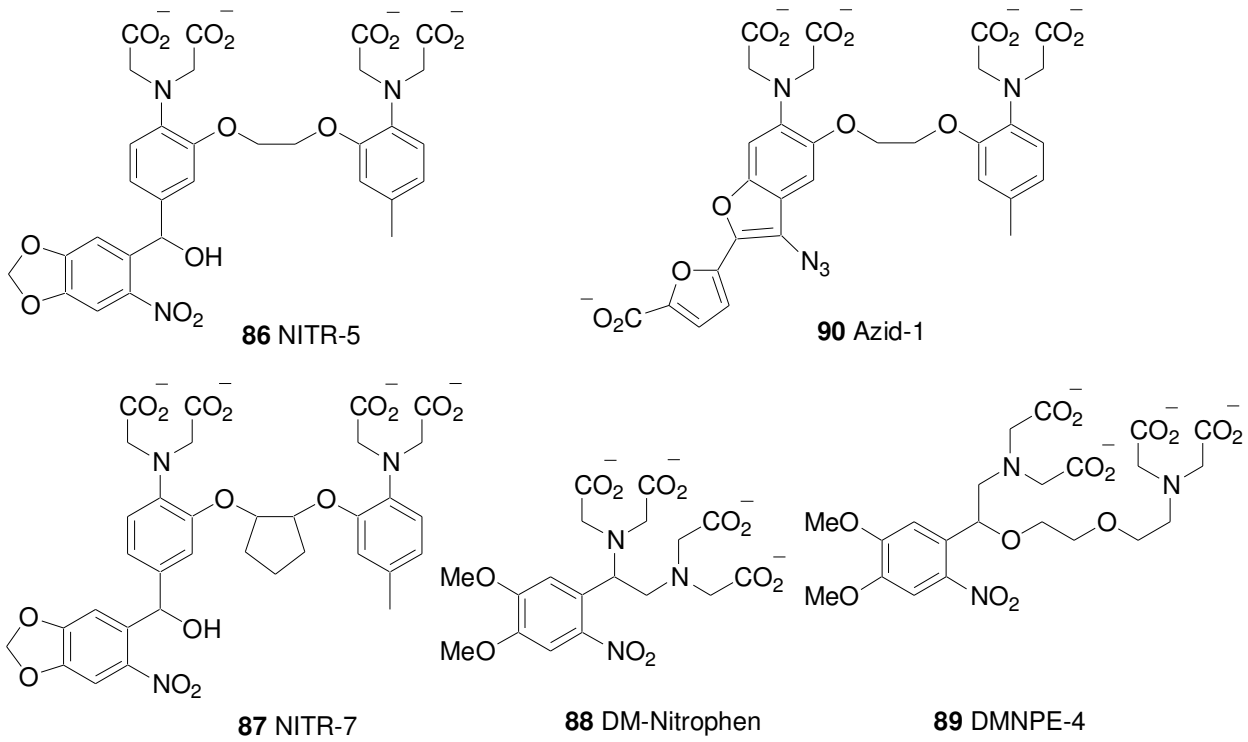


**Figure 9.** Caged $Ca^{2+}$ chelators

dinitrilo tetraacetic acid (EDTA) chelator; and NP-EGTA **89** is based on ethylene glycol tetraacetic acid (EGTA) chelator. These caged calcium compounds' release of $Ca^{2+}$ is caused by the destruction of the ligand. Azid-1[79,83] **90** was invented by Tsien, and the change of chelating property upon photolysis is caused by an intramolecular charge transfer.

Using DM-Nitrophen:$Ca^{2+}$, Troullier and co-workers[84] studied the calcium binding at the high-affinity transport sites of the sarcoplasmic reticulum $Ca^{2+}$-ATPase with time-resolved Fourier transfer infrared (FTIR) spectroscopy. With the photo-release of the calcium ion, the authors confirmed the main features of the spectral bands induced by calcium binding. Moreover, by studying the calcium binding reaction at low temperature, they were able to measure the kinetics of the reaction. Before that, the kinetic measurements were only executed on the photoactivable proteins. Their experiments demonstrated a possible method for measuring kinetics by FTIR difference spectroscopy on nonphotoactivable proteins.

***Caged neurotransmitters***

Almost all the different caging groups have been employed into the area of neurotransmitter photorelease. Hess and co-workers have put great effort in using NB-caged carbamoylcholine **91** (which will release carbamoylcholine), NB-caged glutamate **92**, and NB-caged GABA **93**[18,24,85] for various biological studies (Figure 10). There are also other examples of using MNI, *p*HP, and Bhc caged neurotransmitters to investigate biological processes.[15,86,87]

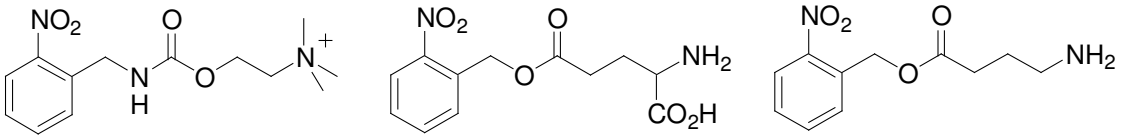


**91** NB-caged carbamoylcholine **92** NB-caged glutamate **93** NB-caged GABA

**Figure 10.** NB-caged neurotransmitters

One example of using caged neurotransmitters is the mechanistic study of reactions mediated by membrane-bound receptors. Understanding the mechanism of inhibition of the nicotinic acetylcholine receptors (nAChR) has been a major subject for over two decades.[88,89] Before the laser pulse photolysis technique of uncaging carbamoylcholine, the only method to determine the effects of inhibitors was to use a single-channel current-recording technique, which illustrates the channel-closing rate. Two different mechanisms were proposed prior to the development of caged neurotransmitters. In the first mechanism, the inhibitor binds in the open channel and blocks it,[88,89] while in the second mechanism, the inhibitor binds to both the open-channel and closed-channel forms. The form to which the inhibitors bind can not form an open channel.[90] The first application of photolyzing caged compounds in this problem showed that the nAChR has two inhibitory sites.[91] Collectively with results of other laser pulse photolysis experiments,[92,93] the proposed second mechanism fits the data: The inhibitor binds to an allosteric site on both the closed- and opened-channel forms of the receptor and shifts the channel-opening equilibrium constant toward the closed-channel form, thereby inhibiting the receptor.

***Caged peptides***

Photoremovable protecting groups can be employed as a protecting group for the synthesis of peptides. They can be used to protect the amino group, carboxyl group, carboxyamide, hydroxyl group, and imidazole.[94-98] NB is primarily used because of its ability to protect various functional groups with straightforward syntheses and efficient photorelease. There are many applications of its use in peptide synthesis, as recent reviews confirm.[99,100]

Caged peptides have also been used to study and understand biological activities. For example, Fay and co-workers reported the first application of a caged peptide to a biological

system.[101] The peptide inhibitors of Ca/calmodulin and myosin light chain kinase were caged at a tyrosine side chain. These caged inhibitors were used to examine the role of the proteins in cell locomotion. Since then, many caged peptides have been synthesized and used for biological studies. Recently, the application of caged peptides has been applied into two new areas: peptides with post-translationally modified residues[102,103] and peptide-based sensors.[104,105]

***Caged enzymes and proteins***

Normally, a covalent bond formation that prevents the biological activity of an enzyme or protein is permanent and irreversible. However, because the accessibility of heat, acid or base in biological system is limited, once an enzyme or protein is rendered inert by forming a covalent bond, it is almost impossible to deprotect and release the active enzyme or protein. A photoremovable protecting group can be used to solve this problem. Upon the irradiation at appropriate wavelength, the enzyme or protein can be quickly and efficiently activated. There are many applications reported, and there is a good review.[106]

Majima and coworkers[107] developed this strategy for the design of photochemically controllable endonuclease *Bam*HI by manipulating the salt-bridge network at the dimer interface, which consists of four amino acids: Lys132, His133, Glu167, and Glu170. The DMNB caging group was introduced to Lys132, Glu167, and Glu170. The caged enzyme was irradiated and the results demonstrated that the key amino acid in *Bam*HI for control of the enzymatic activity is the Lys132. The photochemical activation of the enzyme and protein was achieved by introducing the caging group to the dimer interface followed by irradiation of light.

***Caged nucleotides***

The first application of caged compounds used NB-caged ATP because a phosphate is a very good leaving group. Almost all of the caging groups previously discovered can successfully

and efficiently release phosphates upon photolysis. The photochemistry of caged ATP has been thoroughly studied. In addition to studies with mononucleotides and dinucleotides, oligonucleotide sequences have been photoregulated either by uncaging or by generating strand breaks. For example, caged RNA sequences have been accessed by using an NB-caged precursor that can be used in oligonucleotide synthesis;[108] RNA can also be caged by non-specific protection of the phosphate in the RNA backbone.[109] The Bhc caging group was linked to the phosphate moiety of the sugar backbone of mRNA encoding green fluorescent protein (GFP). Bhc-caged mRNA of GFP has severely reduced expression of GFP until it is illuminated with long wavelength UV light, which causes GFP expression and fluorescence is observed.

***Two-photon excitation (2PE)***

Most photoreaction processes of caged compounds for biological use are initiated by UV light, which is harmful to biological samples and lacks 3-dimensional selectivity. A non-linear optical processs, called multiphoton excitation (MPE), has been recently employed to activate photo triggers and photo switches and release bioactive particles. MPE normally refers to excitation by two or more photons. One advantage of MPE lies in the application to uncaging caged compounds, which will enable the release of the bioactive substrate in a volume as small as 1 fL, or about the size of an *E. coli* bacterium (Figure 11). MPE-based activation of caged compounds aids in the exploration of complex biological systems. The photoactivation of phototriggers, photoswitches, and caged compounds is more powerful with MPE, and it has the pontential to become one of the most important techniques for studying and understanding biological function in real time and living tissue.

In 1931, Maria Goeppert-Mayer first predicted that an atom or molecule could be excited through the simultaneous absorption of two photons. The sum of the frequencies is equal to the

frequency required for excitation of the atom or molecule with one photon.[110,111] This hypothesis could not be validated until 1961 and the invention of the laser, which provided a light source that has enough photon intensity to enable the two-photon excitation (2PE). Kaiser and Garrett revealed the 2PE-induced fluorescence of $CaF_2:Eu^{3+}$.[112] The early applications of 2PE were quite limited to spectroscopic purposes. However in 1990, Denk and co-workers[113] introduced 2PE to microscopy and spatially controlled photochemistry. Denk also executed the release of a neurotransmitter by 2PE in a living cell,[85] which opened the area of multiphoton uncaging for development.

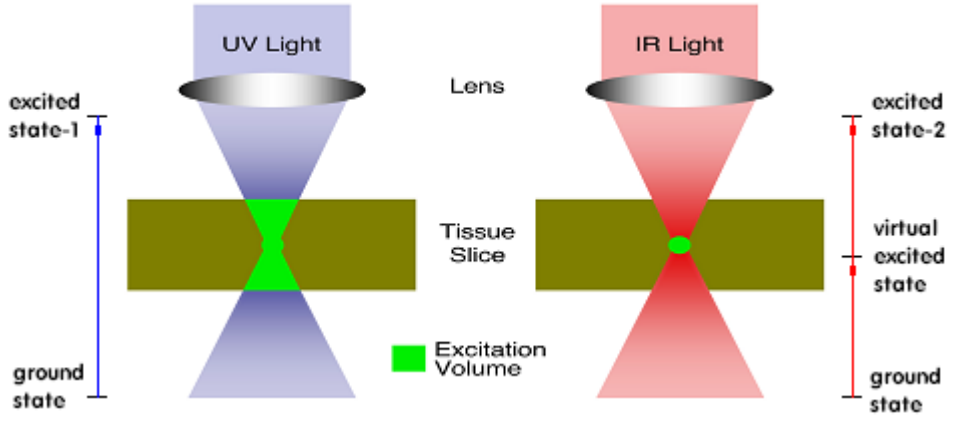


**Figure 11.** 1PE vs 2PE

2PE means that two non-resonant photons are nearly simultaneously absorbed by one choromophore, and the chromophore will be excited as if it absorbs one photon with double frequency. The photochemical and photophysical process from the excited states is as that excited by one photon, such as fluorescence, intersystem crossing to the triplet excited state, phosphorescence, and uncaging. The only difference between 2PE and 1PE is in the excitation step. In 2PE, the chromophore collides with 1 photon and absorbs its energy, reaching a virtual excited state (Figure 11). This state has a lifetime of around 1 fs. Before the chromophore loses the energy and relaxes back to the ground state, a second photon must collide with the

chromophore and the energy of second photon will be absorbed. The chromophore will be excited to a singlet excited state. High light intensity, such as those obtained from pulsed lasers, and stability of the virtual excited state of the chromophore are both critical for successful 2PE. Because the probability of simultaneous two photon absorption depends on the square of the intensity of light, the result is that 2PE occurs only at the focus of the laser beam, the focal volume, which can be as small as 1 fL for a tightly focused laser. No excitation will occur outside of this space because the light intensity is too low. A single photon process lacks 3-D selectivity of excitation because all of the chromophore molecules, not just the ones at the focus of the laser, can absorb a single photon with sufficient energy to cause excitation. Since the excitation probability is proportional to the square of the light intensity rather than having a linear dependence to light intensity as in one-photon excitation (1PE), it is called a non-linear process. The quantum mechanical rules for these excitations vary, which can cause large differences between 1PE and 2PE spectra.[114,115] The most sensitive 2PE wavelength for a chromophore is not always twice of the 1PE $\lambda_{max}$, but it is a good predictor for possible 2PE.

To excite common organic or biological chromophores with 1PE, the wavelength of light used is typically in the near UV–Vis region. For 2PE, the wavelength needed generally falls into the near IR region. In the UV region, the energy of photons is high and causes damage to living cells and tissues; near IR light does not damage cells and tissues, which are relatively transparent to IR light, as there are few chromophores with absorption in this range. The longer wavelength also reduces light scattering, enabling deeper penetration into tissues. These advantages assure that MPE has the potential to become an important technique in the exploration of physiology.

***The two-photon cross section***

For 1PE photochemistry, the quantum efficiency and extinction coefficient (also known as the 1PE absorption cross-section) are used to evaluate the quality of phototriggers and caged compounds. Quantum efficiency informs us of the yield of the chemical transformation, and the extinction coefficient evaluates the ability of the chromophore to absorb photons. The sensitivity of 1PE uncaging process is defined as the product of the quantum efficiency and extinction coefficient. Similar to these, the sensitivity of 2PE uncaging is quantified by its two-photon action cross-section ($\delta_u$), given in Goeppert-Mayer (GM, $10^{-50}$ $cm^4 \cdot s$ $photon^{-1}$), which is 2PE absorption cross-section ($\delta_a$) times the quantum efficiency ($Q_u$) of the photochemical process. The 2PE absorption cross-section represents the probability that the chromophore absorbs two photons simultaneously, and it is analogous to molar absorptivity (extinction coefficient, ε) for a 1PE process.

The first applications of two-photon excitation in microscopy utilized dye chemistry and the general technique for acquiring two-photon absorption cross-section is based on the use of laser pulses with two-photon induced fluorescence.[116] The two-photon induced fluorescence cross-section is the product of the two-photon absorption cross-section ($\delta_a$) and fluorescence quantum yield ($\phi_f$). The time averaged fluorescence photon flux is proportional to the product of two-photon induced fluorescence cross-section and laser power. The two-photon absorption cross-section is calculated from 2PE fluorescence emission, laser power, and known fluorescence quantum yield of 1PE. The measurement of the two-photon absorption cross-section is simplified if a reference dye with a known two-photon absorption cross-section and fluorescence quantum yield is used.[117] This method requires the chromophore or the uncaged

product to be fluorescent. If the caged compound can be detected by using a fluorescent indicator, this method is also applicable.

Tsien and co-workers[15] developed a method that relates the 2PE action cross-section of a chromophore with the two-photon absorption cross-section and fluorescence quantum yield of fluorescein. The fs-pulsed, mode locked IR laser is directed by a mirror through a lens into a cuvette with a side window (Figure 12). The solutions of chromophores and fluorescein are placed in the cuvette. A radiometer is placed beside the side window of the cuvette to collect two-photon induced fluorescence emission of fluorescein. The solutions of chromophores are photolyzed and analyzed. The calculation equation is as follows:

$$\delta_u = \frac{N_p \phi Q_{fF} \delta_{aF} C_F}{< F(t) > C_S} \qquad (1)$$

$N_p$ is the number of molecules that undergo photochemical transformation; $\phi$ is the collection efficiency of the fluorescence detector; $Q_{fF}$ is the fluorescence quantum yield of fluorescein, which is 0.9; $\delta_{aF}$ is the absorption cross-section of fluorescein, which is 30 GM; $C_F$ is the concentration of fluorescein solution; $<F(t)>$ is the time averaged fluorescent photon flux from the fluorescein solution sample; and $C_S$ is the concentration of the chromophore before

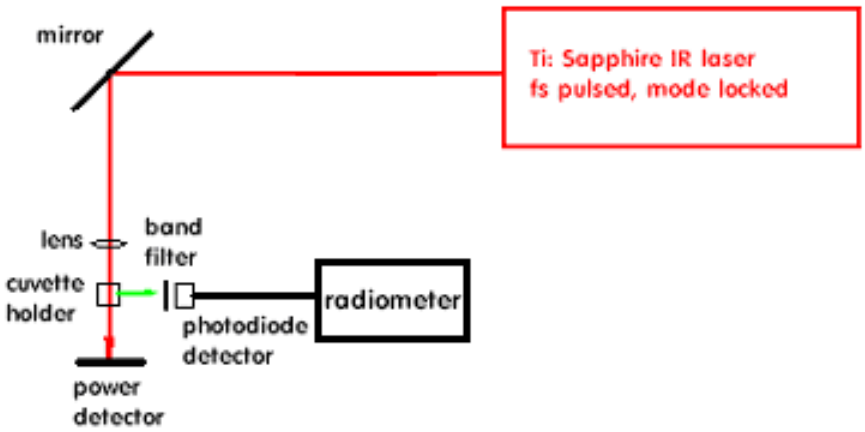


**Figure 12.** 2PE cross-section measurement apparatus using Tsien's method

photolysis. Using the fluorescein solution as a standard, the number of photons that pass through the reaction vial can be calculated, and the 2PE uncaging action cross-section can be acquired.

In practical terms the measurement of $\delta_u$ is made as follows. The fluorescein solution is placed in the cuvette holder in the dark. The fluorescein solution is excited by the laser, and emits fluorescence through the side window on the cuvette. The intensity of the 2PE induced fluorescence is measured by a radiometer. The substrate solution is then put in the cuvette and the sample is exposed to the laser beam for a period of time. Three samples of each irradiation time are acquired. After laser photolysis, the samples are analyzed by HPLC, plotted, and fit to a single exponential decay curve. $N_p$ is calculated from the decay curve.

The measurement of two-photon uncaging action cross-section can be further simplified by using a reference two-photon sensitive caged compound with a known two-photon uncaging action cross-section. Two-photon photolysis of the unknown compound and the reference are performed using the same laser. The photolysis rate is assumed to be proportional to the two-photon uncaging action cross-section, so HPLC analysis will show the uncaging reaction rate difference, which indicates the two-photon uncaging action cross-section difference.[86,118]

***Chromophores for 2PE***

Two factors determine the success of two-photon uncaging: (1) high light intensity and (2) 2PE absorption cross-section $\delta_a$. The molecules with a large two-photon absorption cross-section require the molecule's virtual excited state to be more stable, which can typically be achieved by extending conjugation on the molecule.[119,120] Syntheses of new materials with large two-photon absorption cross-section and theory have revealed the importance of certain basic structural properties that are required for an optimized two-photon sensitive organic molecule.[119,120] The most efficient two-photon absorption materials are the ones with various electron-donor and

electron-acceptor substituents attached to a conjugate linker in symmetric or asymmetric ways. Such as: (acceptor)—(aromatic core)—(acceptor), (donor)—(aromatic core)—(donor), and (acceptor)—(aromatic core)—(donor).

Simply increasing the molecule's two-photon absorption cross-section is not sufficient for the chromophore to be a good two-photon sensitive phototrigger. The quantum yield of the photochemical process is also crucial, and the chromophore needs to fulfill the criteria that are needed for a photoremovable protecting group discussed in Section 1.1. One advantage of 2PE over 1PE is the high 3-D selectivity. To make better use of this advantage, 2PE uncaging must be faster than the diffusion in aqueous media for spatial-selectively release of the bioactive messengers. With these critical requirements, not many photoremovable protecting groups are found suitable for 2PE uncaging applications.

DMNB, NPE, CNB have been explored for applications in 2PE uncaging studies in biological systems, but the 2PE uncaging action cross-section is determined to be 0.03 GM for DMNB at 740 nm and 0.019 GM for NPE at 640 nm. Based on a suggestion by Tsien,[15] 0.10 GM is the lower limit for a successful 2PE sensitive caging group to be applicable in biological study. Clearly, these NB derivatives are not sensitive enough to activate the release of bioactive substrates with 2PE.

Jullien and co-workers have designed and synthesized photoremovable protecting groups based on the NB platform, seeking for a better uncaging cross-section in both 1PE and 2PE.[121] The methodology used is to extend conjugation and add extra donors and acceptors. The authors hoped that the quantum efficiency was not decreased with the improvement of two-photon absorption cross-section. Compounds **94** and **95** (Figure 13) have shown a significant increase in the two-photon uncaging action cross-section, which are 0.065 GM and 0.05 GM at 750 nm,

respectively. Goeldner and coworkers developed another NB-based protecting group that possess high 1PE and 2PE sensitivities.[122] Compound **96** has an absorption maximum and extinction coefficient of 317 nm and 9900 $M^{-1}\cdot cm^{-1}$, perspectively. Glutamate is recovered at 90% yield from photolysis. The 1PE disappearance quantum efficiency of **96** is determined to be 0.1. The two-photon uncaging action cross-section is determined to be 0.45 GM at 800 nm.

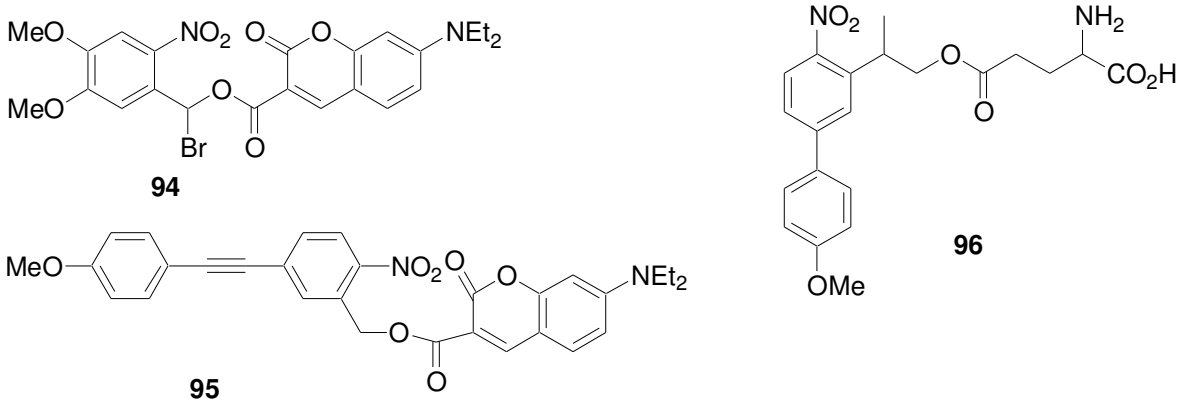


**Figure 13.** Next generation of NB derivative caging groups with 2PE sensitivity

Bhc (**97**, Figure 14), introduced by Furuta and coworkers, is found to possess good 2PE sensitivity of 0.72 GM, and it is capable of protecting carboxylates, phosphates, diols, carbonyl groups, amines (as the carbamate), and alcohols and phenols (as the carbonate).[15,72,73,123] Other coumaryl caging groups have sensitivity to 2PE. The DMACM chromophore (**98**) is reportedly sensitive to 2PE.[124] The fluorescent chromophore was attached to a non-fluorescent dextran. Exposure of the system to 728- and 750-nm laser light caused a significant decrease of the

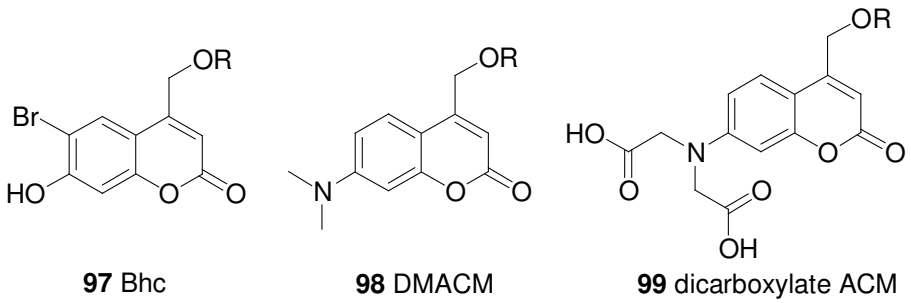


**Figure 14.** Caging groups on coumaryl platform

fluorescence of dextran, which demonstrates that photocleavage was achieved. Adding carboxylates to the amine (**99**) increases solubility in aqueous buffers, making it more suitable for biological studies.

MNI (Figure 15) is another caging group that has been used for 2PE uncaging of certain small organic molecules (**100**)[86] and metal ions ($Ca^{2+}$).[86] With a two-photon uncaging action cross-section close to 0.06 GM at 730 nm, the low sensitivity of MNI to 2PE might be the limiting factor for widespread application.

Nitrodibenzofuran (**101**) has been developed for two-photon uncaging of $Ca^{2+}$.[118] The two-photon photolysis was accomplished in a cuvette on the stage of a two-photon microscope. Comparison of HPLC analyses with MNI-glutamate showed that the nitrodibenzofuran caging group has a two-photon uncaging cross section of about 0.60 GM.

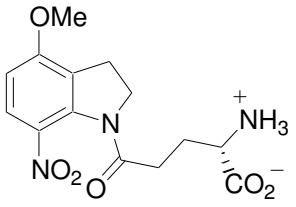


**100** MNI-glutamate

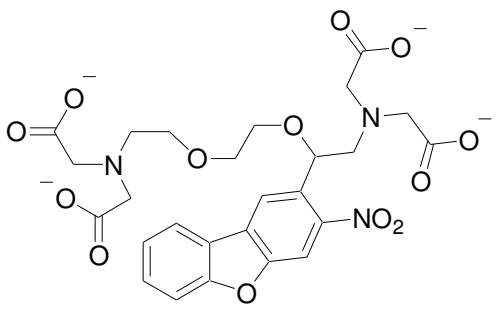


**101** nitrodibenzofuran-EGTA

**Figure 15.** MNI-glutamate and nitrobenzofuran cages

Jullien and coworkers[125,126] have quantitatively studied the two-photon uncaging of *ortho*-hydroxycinnamic acid analogs (Figure 16), which were introduced by Porter and coworker.[127] With the *ortho*-hydroxycinnamic acid platform, alcohols and amines can be protected and photoreleased from their respective esters and amides. For example, ethyl 3,5-dibromo-2,4-dihydroxycinnamate (**102**), which has a strong absorption beyond 350 nm and has a 0.05 quantum efficiency and uncaging cross section over 60 $M^{-1}\cdot cm^{-1}$ at $\lambda_{max}$ = 369 nm, releases

ethanol with concomitant formation of a coumarin fluorophore (**103**). This photoremovable protecting group also possesses a two-photon uncaging action cross-section of 1.6 GM at 750 nm. The fluorescence emission changes from non-fluorescent caged compound **102** to fluorescent coumarin **103** can be used for quantitative control of delivery of the bioactive messenger.

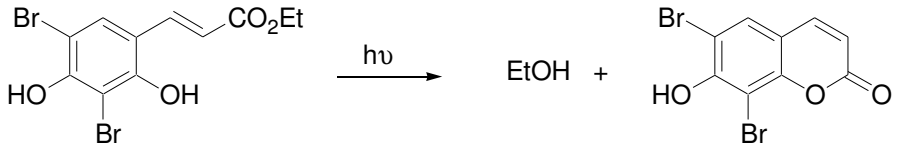


**102** ethyl 3,5-dibromo-2,4-dihydroxycinnamate **103**

**Figure 16.** Photolysis of *o*-hydroxycinnamic acid platform

***Applications of 2PE of caged compounds***

The photochemistry of caging groups excited by 2PE and 1PE are not qualitatively different. The difference lies in the potential for the 2PE process to enable a high 3-D spatial selectivity of effector release, minimize damage to living cells and tissues, and penetrate deeper into tissues. 2PE phototriggers have been used for the caged compounds of neurotransmitters, second messengers, fluorophores, photodynamic therapy molecules, and drugs have been synthesized and studied in appropriate biological systems.

***Caged neurotransmitters***

Denk first applied 2PE photorelease of a neurotransmitter into a biological system.[85] CNB-caged carbamoylcholine was irradiated to release a mimetic of the acetylcholine neurotransmitter and the whole cell current was recorded to determine the distribution of ligand-gated ion channels. A more important landmark was established by Tsien and co-workers in 1998.[15] Bhc-caged glutamate (Bhc-glu, Figure 17) was synthesized and irradiated in brain tissue slices from the hippocampus and cortex of rats. With a raster-scanned pulsed IR laser, Bhc-glu was

photolyzed, releasing glutamate, which enabled the recording of the first three-dimensional map of glutamate sensitivity of neurons in rat brain slices. The Ti:sapphire IR laser and the technique of using 2PE reduce technical difficulties in conducting high-resolution mapping. For Bhc-glu, however, the slow kinetic release of glutamate was a limiting factor. The glutamate was linked to the Bhc chromophore through a carbamate functional group, and the directly released compound from Bhc-glu photolysis is a carbamic acid, which will undergo hydrolysis to give rise of the glutamate. The process of hydrolysis of the carbamic acid takes several milliseconds. Diffusion occurs, which limits the tight spatial release of glutamate.

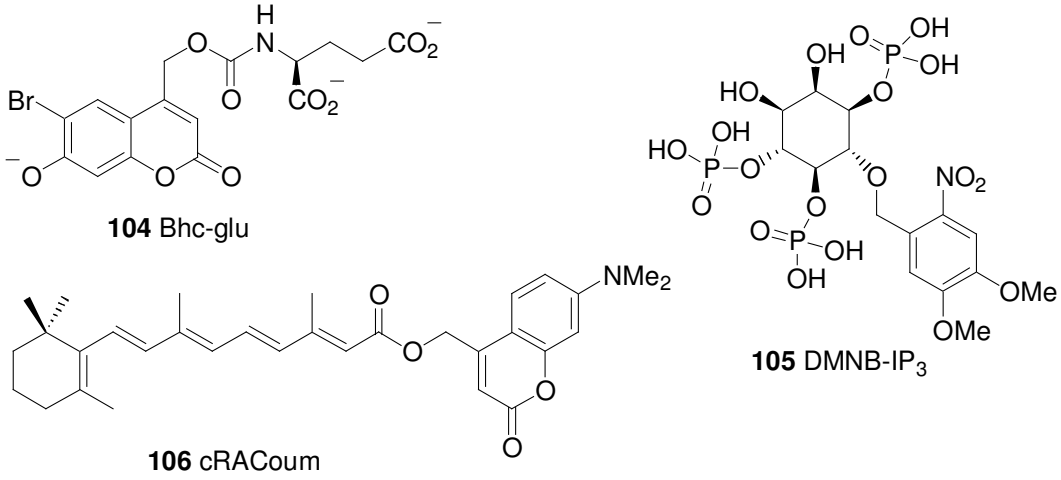


**Figure 17.** Caged compounds for 2PE applications

***Caged signaling molecules***

Inositol-1,4,5-triphosphate ($IP_3$) binds to receptors on the endoplasmic reticulum (ER), triggering $Ca^{2+}$ release. Recently, different groups have tried using different caged $IP_3$ with two-photon uncaging for biological studies. Ellis-Davies and co-workers used DMNB-caged $IP_3$ (**105**), which has a two-photon action cross-section of 0.035 GM at 730 nm, to release $Ca^{2+}$ in HeLa cells.[128] Using a near-IR laser (5mW, 710 nm, 80 MHz, pulsewidth 70 fs), a concentration jump of $IP_3$ was produced and a $Ca^{2+}$ concentration image was revealed. Wang and co-workers used NPE-caged $IP_3$ to probe the synapse specificity of calcium release.[129] A comparison study

using caged $IP_3$ and caged $gPIP_2$ (glycerophosphoryl-*myo*-inositol 4,5-bisphosphate, a poorly metabolized $IP_3$ analog) indicated that $Ca^{2+}$ release lasts several hundred milliseconds and is terminated by intrinsic receptor dynamics.

Retinoic acid (RA) is another signaling molecule. It is one of the key components in patterning the body axis and formation many of organs. Jullien and co-workers caged retinoic acid with DMACM (**106**) and DMNPE.[130] The caged compound was found to be stable and did not interfere with the normal development of the zebrafish embryos. With IR laser at 730 nm with 1 mW power, retinoic acid was released at a rate constant of 0.015 $s^{-1}$ and monitored by fluorescence of RA binding to RA binding protein. With successfully release of RA using 1PE and 2PE, caged RA could be a useful tool to study important developmental events.

***Drug delivery***

With the temporal- and spatially-controlled release of bioactive compounds, 2PE can enhance the spatial and temporal selectivity of drug delivery. The stable caged drug can be taken by a patient and exist in the patient's body without harm. Training light from an IR laser onto the target tissue will release the drug at the desired place and time.

1400W is a nitric oxide synthase (NOS) inhibitor. At pM concentration, nitric oxide (NO) is an important second messenger and is involved in critical bioregulatory processes including neuroransmission, blood clotting, and blood pressure control. Macrophages can release large amounts of NO to kill cancerous tumor cells and intracellular parasites, but over-production of NO by inducible NOS (iNOS) causes tissue damage. The selectivity of a drug for iNOS is important. Most of the drugs for iNOS are non-sepcific NOS inhibitors, they inhibit NOS as well as iNOS. Guillemette and co-workers used Bhc-1400W (**107**, Figure 18) to release 1400W and inhibited iNOS at the desired place.[131,132] The in vivo experiment with murine macrophage cells

showed promising results; the NO production in 2PE uncaging cells is similar to a cell media with 10 μM 1400W.

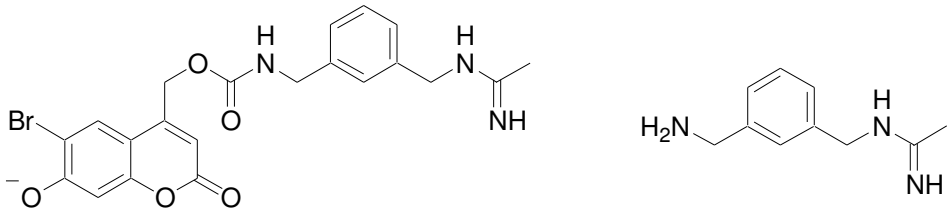


**107** Bhc-1400W **108** 1400W

**Figure 18.** 1400W and Bhc-1400W

Tegafur (**110**, Figure 19) is widely used in cancer treatment. Yuan and coworkers have applied NB cages on tegafur.[133] MCF-7 mammary cancer cells were incubated with prodrug **109** or tegafur (**110**). Tegafur induced up to 91% cell death. Caged compound **109** only induced 7% cell death. After irradiation of 25 min, 67% of the cancer cells with **109** were observed to be dead. This is consistent with the fact that 69% of cells died when incubating with prodrug **109** that has been irradiated for 25 min, and prodrug **109** releases 70% tegafur after 25 min of irradiation. This 2PE approach provides a temporal and spatial delivery method for drugs.

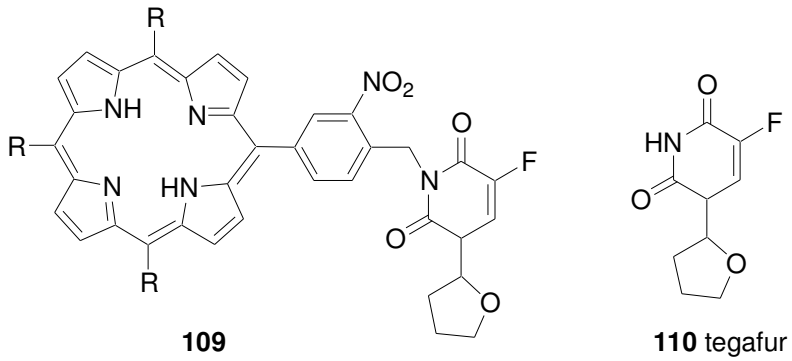


**109** **110** tegafur

**Figure 19.** Caged tegafur and tegafur

***Conclusions***

Caged compounds provide a powerful tool for studying fast processes in biology and physiology. Biologically active compounds can be caged and photoreleased in a timely and local

manner, which makes the studies of fast kinetics in biology possible. The high 3-D selectivity achieved with 2PE uncaging will provide localized phototriggering and release of bioactive substrates. The near IR region of light used causes less harm, minimal scattering, and deeper penetration in tissue. All these unique features of the 2PE uncaging process has made 2PE uncaging an excellent tool for biological studies. Limiting this, however is the lack of qualified 2PE-sensitive caging groups. In this document, my efforts to develop biologically useful, 2PE-sensitive photoremovable protecting groups will be discussed.

## Chapter 2

## Synthesis and Photochemistry of BHQ Derivatives

### *Introduction*

Caging groups and MPE are widely used in biological and physiological studies. The combination of these two new concepts provides many advantages. Fast and efficient release of bioactive substrates in a small volume enable the study of fast kinetics of biological transformations, but few caging groups have sufficient sensitivity for application in 2PE mediated uncaging. Bhc[15,71-74,109,123,131,132,134] has one of the highest two-photon action cross-sections among the known 2PE caging groups. It can protect and efficiently release carboxylates, phosphates, diols, carbonyl groups, amines, and hydroxy groups. The solubility of Bhc in high ionic strength aqueous buffer is limited, and the high fluorescence emission of the Bhc chromophore upon excitation might limit applications that use fluorescent indicators as readouts of biological function.

Fedoryak in the Dore lab found that the 8-bromo-7-hydroxyquinolinyl group (BHQ, **111**, Figure 20)[135] is efficiently photolyzed by 1PE and 2PE under simulated physiological conditions to release acetate. BHQ has a large quantum efficiency, better solubility in aqueous buffers than Bhc, and low levels of fluorescence.

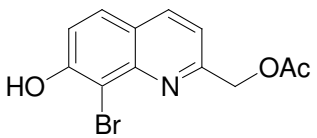


**111** BHQ-OAc

**Figure 20.** BHQ-OAc

In this chapter, BHQ-caged compounds of other common bioactive functional groups will be discussed. Mechanistic studies of the photolysis of BHQ will be reported. This chapter also discusses how substituents on the quinoline skeleton modulate the photochemical and photophysical properties of the quinoline chromophore so that the next generation of caging groups can be developed with better photophysical and photochemical properties.

***Synthesis of BHQ derivatives***

***Synthesis of BHQ-protected carboxylates***

The synthesis of BHQ-protected benzoate and piperonylate started from *tert*-butyldiphenylsilyl-protected quinoline **112**[135] (Scheme 8). Alcohol **112** was treated with triethyl amine, dimethylaminopyridine and benzoyl chloride in chloroform, and benzoate **113** was acquired in 73% yield. The subsequent bromination of benzoate **113** gave only one regioisomer in 67% yield, which is the desired isomer **114**. The isomer's regioselectivity was determined by $^1$H NMR spectra. Benzoate **113** has 5 aromatic hydrogen atoms on the quinoline ring and 5 aromatic hydrogen atoms on the benzoate. The H-5, H-6, H-8 of the quinoline ring couple with each other. H-6 is coupled with H-8 and H-5, causing the peak to split into a doublet of doublets ($\delta$ 7.10 ppm, $J$ = 8.8, 2.8 Hz); H-8 is only coupled with H-6, it is mixed with other aromatic protons from TBDPS protecting group and benzoate ($\delta$ 7.41 ppm, 10 H). The $^1$H NMR of **114** showed the disappearance of the H-8 peak ($\delta$ 7.41 ppm, 9 H) and the doublet of doublets peak at 7.10 ppm condensed to a doublet ($\delta$ 7.12 ppm, $J$ = 8.8 Hz). The disappearance of the H-8 peak at 7.41 ppm suggests the substitution occurs at the 8 position of quinoline. The coupling constant of 8.8 Hz of H-6 indicates that it is coupled with a hydrogen atom in the *ortho* position. No other bromine substituted quinoline compound fits this pattern. Benzoate **114** was treated with

tetrabutylammonium fluoride (TBAF) to remove the bulky silyl group, to yield BHQ-protected benzoate **115** in 90% yield.

BHQ-protected piperonylate was synthesized similarly. The only difference is the removal of the bulky silyl protecting group was conducted before the bromination. The bromination turned out to be faster than the bromination with the 7-hydroxy group protected. The analysis of $^1$H NMR confirmed the regiochemistry of the bromination. The doublet of doublets corresponding to H-6 (δ 7.19 ppm, $J$ = 8.8, 2.4 Hz) in the spectrum of **117** gave way to a doublet (δ 7.36 ppm, $J$ = 8.4 Hz) in the spectrum of **118**, and the signal for H-8 (δ 7.29, d, $J$ = 2.0 Hz) in the spectrum of **117** was absent in the spectrum of **118**.

**Scheme 8.** Synthesis of BHQ-protected benzoate[a]

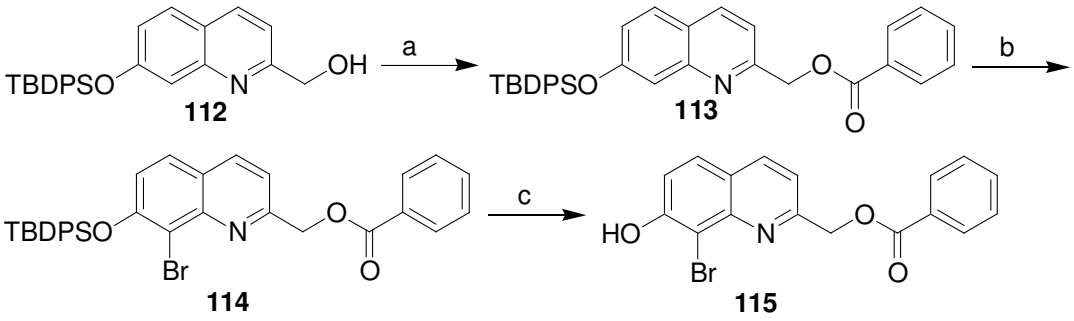


[a] Reagents and conditions: (a) BzCl, $Et_3N$, DMAP, $CH_3Cl$, rt, 12 h, 73%; (b) $Br_2$, AcOH, rt, 24 h, 67%; (c) TBAF, THF, rt, 90%;

**Scheme 9.** Synthesis of BHQ-protected piperonylate[a]

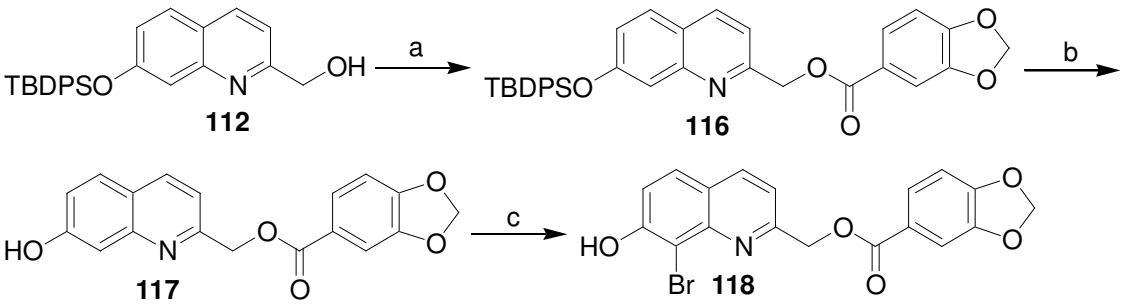


[a] Reagents and conditions: (a) piperonyloyl chloride, $Et_3N$, DMAP, $CH_3Cl$, rt, 12 h, 66%; (b) TBAF, THF, rt, 87%; (c) $Br_2$, AcOH, rt, 5 h, 64%.

***Synthesis of BHQ-protected phosphates***

BHQ-protected dimethylphosphate **124** was synthesized starting from quinaldine (**119**)[135] (Scheme 10). Compound **119** was treated with bromine in acetic acid followed by protection of the phenol with an acetyl group. The regiochemistry of the bromination was determined by $^1$H NMR as before. The peak corresponding to H-8 in **119** (δ 7.33 ppm, d, *J* = 1.9 Hz) was not present in the spectrum of **57**, and the H-6 signal in the spectrum of **119** collapsed from a doublet of doublets (δ 7.08 ppm, *J* = 8.8, 1.9 Hz) to a doublet in **120** (δ 7.22 ppm, *J* = 8.0 Hz). Acetic anhydride in pyridine protected BHQ **120** smoothly to yield bromoquinaldine **121**. Selenium dioxide in *para*-dioxane oxidized the benzylic methyl group of **121** to an aldehyde. The aldehyde **122** was treated with tosylhydrazine in ethanol to precipitate out the corresponding tosylhydrazone **123** in decent yield. Tosylhydrazone **123** was treated with sodium methoxide to generate BHQ-diazo, and the addition of dimethylphosphoric acid phosphorylated the benzylic carbon. The target compound, BHQ-caged dimethylphosphate **124**, was acquired in poor yield.

**Scheme 10.** Synthesis of BHQ-protected phosphates.[a]

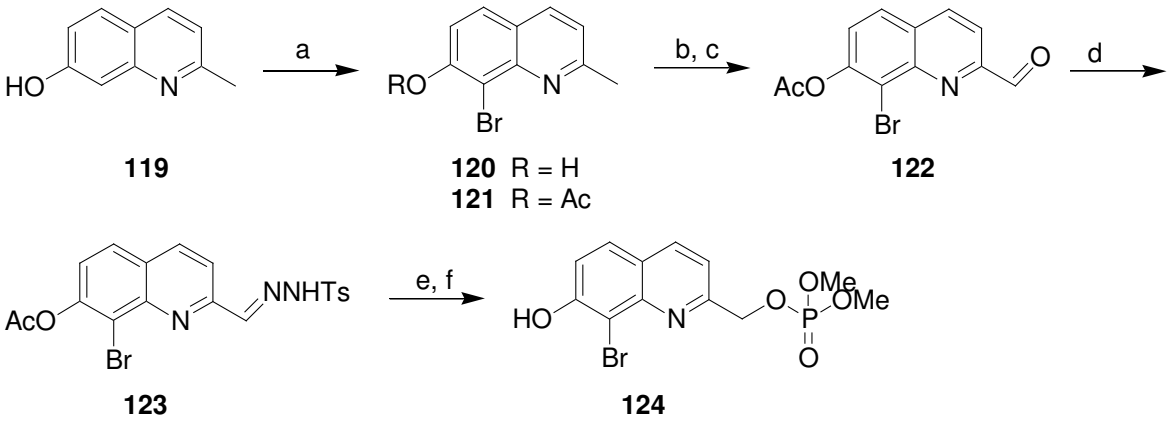


[a] Reagents and conditions: (a) $Br_2$, AcOH, rt, 8 h, 71%; (b) $Ac_2O$, pyridine, DMAP, rt, 4 h, 83%; (c) $SeO_2$, dioxane, 80 °C, 18 h, 60%; (d) $H_2NNHTs$, EtOH, rt, 48 h, 74%; (e) NaOMe, MeOH, rt, 10 min; (f) dimethylphosphoric acid, $CH_3CN$, rt, 48 h, 20%.

***Synthesis of BHQ-protected glycerol derivatives***

The BHQ-protected glycerol derivatives **127** and **128** were synthesized in a single step from aldehyde **122** and 1-phenoxypropane-2,3-diol (**125**)[136] and 1-phenthioxypropane-2,3-diol (**126**),[137] by heating the aldehyde with the diol in the presence of pyridinium *para*-toluenesulfonic acid and anhydrous magnesium sulfate in toluene. With the acid-catalyzed ketal formation, the byproduct water was removed by anhydrous magnesium sulfate, and longer heating time caused the acid catalysed deprotection of the acetyl protecting group. The desired BHQ-proteceted glycerol derivatives **127** and **128** were acquired as the major products in modest yields (55-60%).

**Scheme 11.** Synthesis of BHQ-protected diols

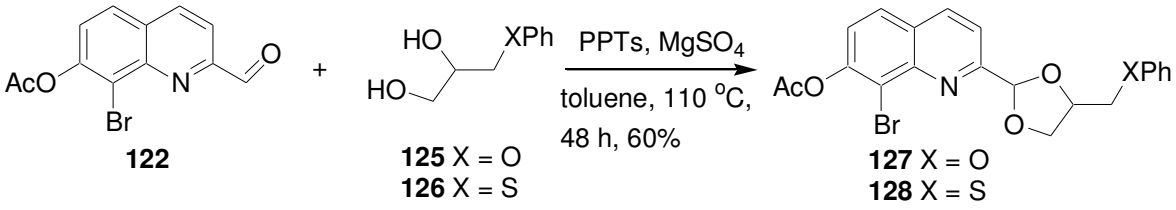


***Photochemistry of BHQ-caged compounds***

In Fedoryak's early work,[135] BHQ-OAc (**111**) has good sensitivity to 1PE and 2PE. The 1PE quantum efficiency is 0.29 and the 2PE uncaging action cross-section is 0.59 at 740 nm. Photochemical experiments of BHQ-caged carboxylates, phosphates, and diols were conducted to elucidate the usefulness of BHQ caging group for bioactive effectors.

***One-photon and two-photon photolysis***

BHQ-caged compounds were dissolved in KMOPS buffer (10 mM 4-morpholinepropanesulfonic acid and 100 mM potassium chloride titrated to pH 7.2 with potassium hydroxide) at a concenctration of 100 μM. The $pK_a$ of the phenol group in BHQ-OAc is 6.8.[135] Under these conditions, the free hydroxy of the BHQ is partially deprotonated; the UV

spectra indicates a mixture of phenolate and phenol. The phenoxide form of quinoline-caged compounds has an absorption maximum of 370 nm, compared to around 320 nm of the phenol form. Nevertheless, the singlet excited state of hydroxyquinoline is extremely acidic and the hydroxy is rapidly deprotonated.[138,139] Solutions of **129a**, **129b**, **129c**, **132d**, and **132e** (100 μM) in KMOPS buffer were excited with light from a 365-nm mercury lamp passed through a pair of filters that narrow the spectral output to 365 ± 15 nm. The photolysis results in the deprotection of each carboxylic acid, phosphate, and glycerol derivative, respectively and leaving the BHQ-OH or BHQ-CHO remnant (Scheme 12).

**Scheme 12.** Single- and two-photon photolyses of BHQ-caged compounds[a]

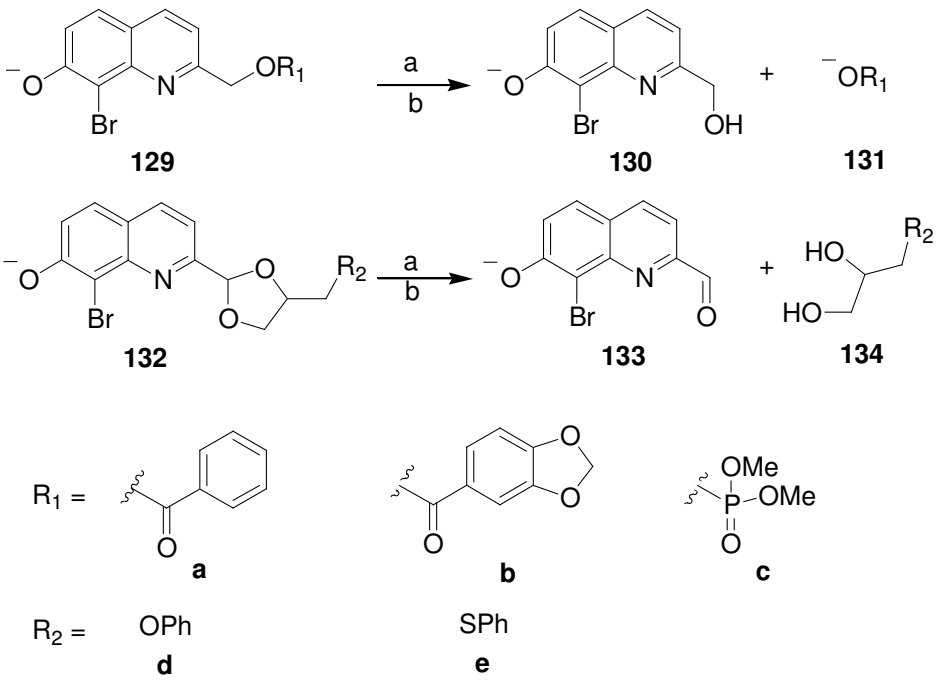


[a] Reagents and conditions: (a) hν (365 nm), KMOPS, pH 7.2; (b) hν (740 nm), KMOPS, pH 7.2.

The photolyses of **129a**, **129b**, and **129c** were monitored by HPLC analysis of 20-μL aliquots taken at periodic intervals (10, 20, 40, and 60s). The chromatograms of these HPLC traces were quantified using an external standard to relate the detector response to the

concentrations of **129a-c** and **131b** (Figure 21). Authentic samples of **130** and **131b** were analyzed by HPLC, and the retention time and UV absorption spectra confirmed their identities in the reaction mixture. For BHQ-OBz (**129a**) and BHQ-caged dimethylphosphate (**129c**), the product of the reaction is benzoate (**131a**) and dimethylphosphate (**131c**), respectively. These two compounds do not possess sufficient UV absorption to be monitored by HPLC. In the case of BHQ-OPip (**129b**), the product of the reaction, piperonylate (**131b**), has sufficient UV absorption signal at 296 nm for observation of its formation. The yield of piperonylate approaches to 75%.

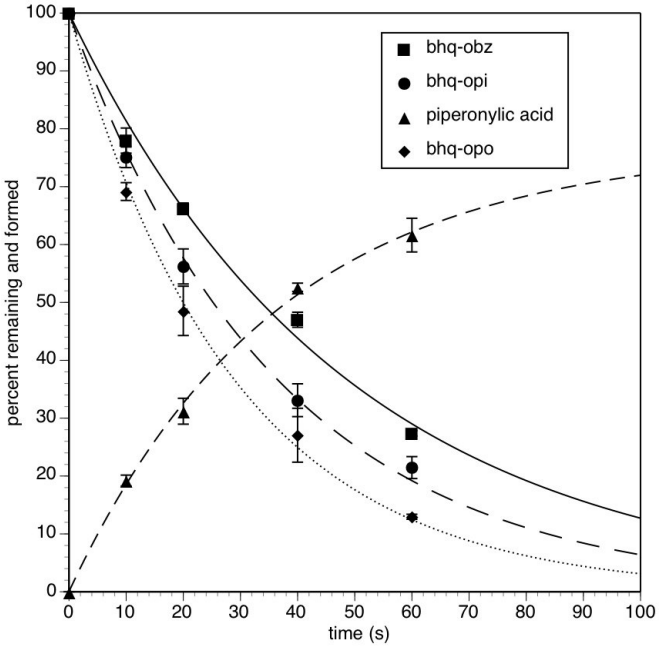


**Figure 21.** Time course of one-photon photolysis of BHQ-protected carboxylates **129a** and **129b** and phosphate **129c** at 365 nm. The percent remaining was determined by HPLC and is the average of 3 runs. Also shown is the relative amount of piperonylate **131b** released from **129b**, which was also determined by HPLC from average of 3 runs. Lines are fits of a single decaying exponential or exponential rise to max. Error bars represent the standard deviation of the measurement.

Similarly, HPLC was used to monitor the photolyses of BHQ-caged diols **132d** and **132e** and the generation of **134e** (Figure 22). Glycerol derivative **134d** lacks sufficient UV absorption to be detected, so **134e** was used for monitoring the formation of the desired diol at 260 nm.

Authentic samples of **133** and **134e** were analyzed by HPLC, and the retention time and UV absorption spectra confirmed their identities in the reaction mixture. The yield of **134e** approached to 65%.

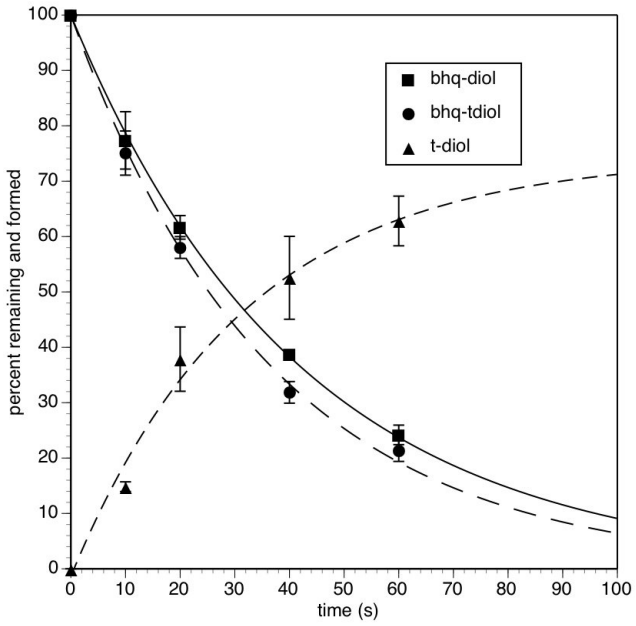


**Figure 22.** Time course of one-photon photolysis of BHQ-protected diols **132d** and **132e**. The percent remaining was determined by HPLC and is the average of at least 3 runs. Also shown is the relative amount of 1-phenthioxypropane-2, 3-diol **134e** released from **132e**, which was determined by HPLC from at least 3 runs. Lines are fits of a single decaying exponential or exponential rise to max. Error bars represent the standard deviation of the measurement.

From these data, the one-photon uncaging quantum efficiency, $Q_u$, for each compound was calculated from the following equation:[140,141]

$$Q_u = (I\sigma t_{90\%})^{-1} \quad (2)$$

where $I$ is the light intensity (determined by potassium ferrioxalate actinometry[142]), $\sigma$ is the decadic extinction coefficient ($1000 \times \varepsilon$, the molar extinction coefficient) at 365 nm, and $t_{90\%}$ is the irradiation time for 90% of the starting material to be consumed. The quantum efficiencies for the BHQ-protected carboxylates and phosphates were found to be 0.30-0.32 mol·ein$^{-1}$, while the protected diols had slightly higher values of 0.37 and 0.39 mol·ein$^{-1}$ (Table 4).

**Table 4.** Photochemical properties of BHQ-caged compounds.[a]

| Caged Compound | $\lambda_{max}$ (nm) | $\varepsilon_{max}$ ($M^{-1}\cdot cm^{-1}$) | $\varepsilon_{365}$ ($M^{-1}\cdot cm^{-1}$) | $Q_u$ (mol/ein) | 1p sensitivity | $\delta_u$ (GM)[b] | $\tau_{dark}$[c] (h) |
|---|---|---|---|---|---|---|---|
| **111**[d] | 369 | 2600 | 2580 | 0.29 | 748 | 0.59 | 71 |
| **129a** | 368 | 2400 | 2400 | 0.30 | 720 | 0.64 | 100 |
| **129b** | 296 | 6400 | 2900 | 0.32 | 928 | 0.76 | 94 |
| **129c** | 370 | 3900 | 3800 | 0.31 | 1178 | 0.43 | 105 |
| **132d** | 375 | 2300 | 2200 | 0.37 | 814 | 0.78 | 79 |
| **132e** | 374 | 2500 | 2400 | 0.39 | 936 | 0.90 | 69 |

[a]Measured in KMOPS, pH 7.2. [b]Measured at 740 nm, GM = $10^{-50}$ $cm^4\cdot s$/photon. [c]Time constant for hydrolysis in the dark. [d]Values taken from ref.135.

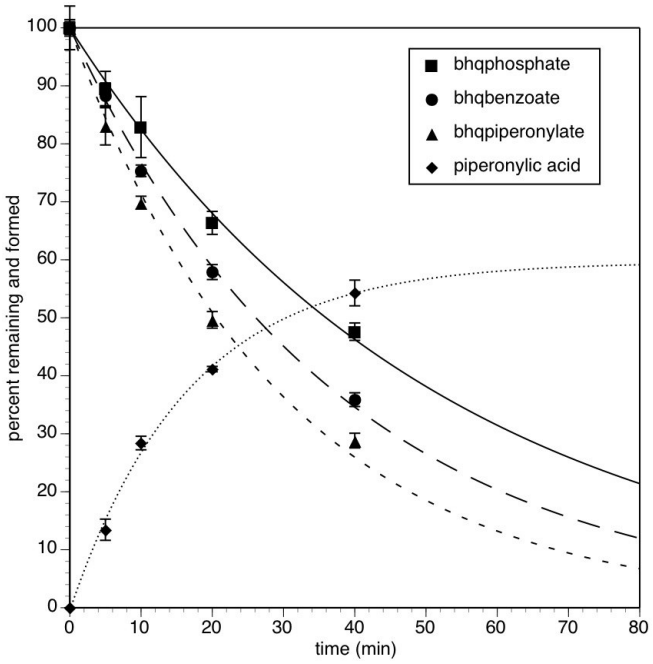


**Figure 23.** Time course of two-photon photolysis of BHQ-protected carboxylates **129a** and **129b** and phosphate **129c** at 740 nm. Also shown is the relative amount of piperonylate **131b** released from **129b**. The percent remaining was determined by HPLC and is the average of 3 runs. Lines are fits of a single decaying exponential or exponential rise to max. Error bars represent the standard deviation of the measurement.

The two-photon uncaging action cross-section was determined using a method described previously.[15,74,135] The time course of photolysis with 2PE of compounds **129a**, **129b**, and **129c**, was acquired in a similar way as that for 1PE quantum efficiency measurement. Briefly, 20-μL samples were irradiated with a fs-pulsed, mode-locked Ti:sapphire laser tuned to 740 nm (287 fs pulse width and 160-200 mW average power). HPLC analysis of the sample (at 5, 10, 20, and 40 min) was used to determine the time course of the photolysis (Figure 23). In the case of **129b**, the formation of piperonylate **131b** was also observed, which approached 60%.

The 2PE uncaging action cross-section, $\delta_u$ (in GM), was determined using equation (1):[15]

$$\delta_u = \frac{N_p \phi Q_{fF} \delta_{aF} C_F}{< F(t) > C_S} \quad (1)$$

The time-averaged fluorescence photon flux, $<F(t)>$, was from the radiometer readout of the fluorescence of a fluorescein solution upon irradiation of the sample with the Ti:sapphire laser in the same set-up. The initial rate of photolysis was used to determine the number of molecules photolyzed per second, $N_p$. $\phi$ is the collection efficiency of the detector; $Q_{fF}$ is the fluorescence quantum yield of fluorescein (0.9); $\delta_{aF}$ is the absorbance cross-section of fluorescein (30 GM);[116,143] $C_F$ is the concentration of fluorescein, which is measured by UV at 490 nm; and $C_S$ is the concentration of the BHQ-protected substrate.

The time courses for the BHQ-protected diols **132d** and **132e** were measured similarly (Figure 24), and $\delta_u$ calculated. Values of $\delta_u$ for **129a-c** and **132d-e** ranged from 0.43-0.90 GM (Table 4).

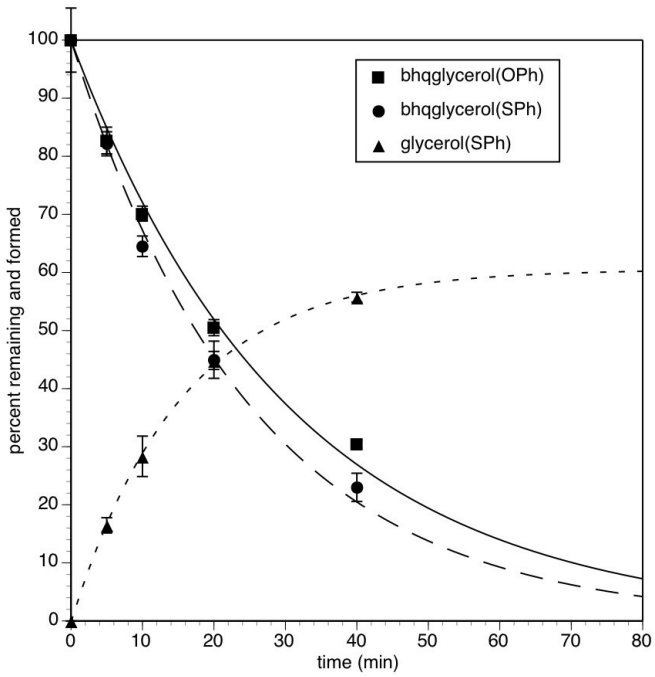


**Figure 24.** Time course of two-photon photolysis of BHQ-protected diols **132d** and **132e**. Also shown is the relative amount of phenthioglycerol **134e** released from **132e**. The percent remaining was determined by HPLC and is the average of 3 runs. Lines are fits of a single decaying exponential or exponential rise to max. Error bars represent the standard deviation of the measurement.

***Dark hydrolysis***

Each of the BHQ-caged compounds was tested for its hydrolytic stability in the dark at room temperature in KMOPS buffer. Compounds **129a-c** and **132d-e** were dissolved in KMOPS and stored in the dark at room temperature. Periodically, 20-μL aliquots were removed and analyzed by HPLC to measure the dark solvolysis rate. The time constants for the dark hydrolysis were measured to be from 69 to 105 h (Table 4). BHQ-caged compounds are stable enough for biological applications.

***Mechanistic studies of the photolysis of BHQ-caged compounds***

The photolysis mechanism of BHQ-caged compounds is not known yet. Because of its structural similarity to coumarin and other benzoates, the photolysis mechanism should be similar to coumarin, which photolyzes through a solvent-assisted heterolysis.[63,64] A number of

experiments have been carried out to understand the nature of the excited state (*i.e.*, singlet or triplet), the identity of intermediates, and the reaction kinetics.

***Stern-Volmer quenching experiments***

Stern-Volmer quenching experiments were conducted on BHQ-OAc (**111**). The quantum efficiency, $Q_u$, of the one-photon photolysis of BHQ-OAc was determined in the presence of 1, 2, and 3 times the concentration of a triplet quencher, sodium 2-naphthalene sulfonate (SNS) or potassium sorbate (PS). No statistically relevant change in $Q_u$ was observed with either quencher (Table 5). The calculated diffusion rate of SNS in water was determined to be $7.4 \times 10^9$ $M^{-1}$ $s^{-1}$.[144] Assuming it is a diffusion-controlled quenching, the product of the diffusion rate, the concentration of quencher, and the lifetime of triplet excited state is related to the quantum efficiency change with the Stern-Volmer relation. The result of Stern-Volmer quenching experiments suggests two possibilities: (1) the photolysis process proceeds through singlet excited states, and the triplet quenchers do not interfere the photochemistry; (2) the photolysis proceeds through a triplet excited state, but the liftime of the triplet state is too short for the quenchers to effectively quench it.

**Table 5.** Stern-Volmer quenching data of BHQ-OAc

| **[SNS]**[a] (μM) | **[BHQ-OAc]** (μM) | **$Q_u$** (mol/ein) | **[PS]**[b] (μM) | **[BHQ-OAc]** (μM) | **$Q_u$** (mol/ein) |
|---|---|---|---|---|---|
| 0 | 100 | 0.29 | 0 | 180 | 0.29 |
| 100 | 100 | 0.30 | 180 | 180 | 0.30 |
| 200 | 100 | 0.31 | 360 | 180 | 0.30 |
| 300 | 100 | 0.29 | 720 | 180 | 0.30 |

[a]SNS = sodium 2-naphthalene sulfonate, [b]PS = potassium sorbate

***Oxygen-18 labeling photolysis experiment***

Two photo-solvolysis pathways are possible. Nucleophilic attack by the solvent can occur either at the benzylic carbon–oxygen bond or at the carbonyl carbon–oxygen bond (Scheme 13). To distinguish between these pathways, the photolysis of BHQ-OAc was conducted in $^{18}O$-labeled water. If the oxygen on the remnant of the BHQ-chromophore comes from the solvent, which means that the bond between benzylic carbon and oxygen is cleaved, then the product observed will be the labeled BHQ-$^{18}$OH (**136**). On the contrary, if unlabeled BHQ-OH (**135**) is observed, then the source of the oxygen would be from the ester, and that means the bond between the carbonyl carbon and oxygen is cleaved.

**Scheme 13.** Oxygen-18 labeling experiment

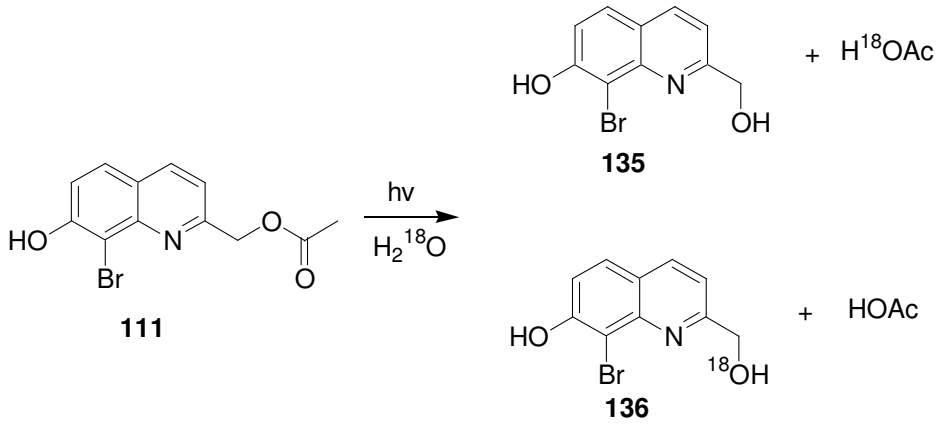


A solution of BHQ-OAc (**111**) in either $H_2O$ or $H_2{}^{18}O$ (97% label) was irradiated with a 365-nm mecury lamp light for several seconds. The solutions were then analyzed by LC-MS. For the reaction in $H_2O$, mass spectral analysis of the peak on the chromatogram corresponding to BHQ-OH gave *m/z* 254/256 (Figure 25), while the reaction in $H_2{}^{18}O$ gave almost exclusively *m/z* 256/258 (Figure 26). A direct comparison of the MS data of the labeled and unlabeled water reaction revealed that 96% of the oxygen atoms in the BHQ chromophore remnant were $^{18}O$. Compound **136** is the dominant product.

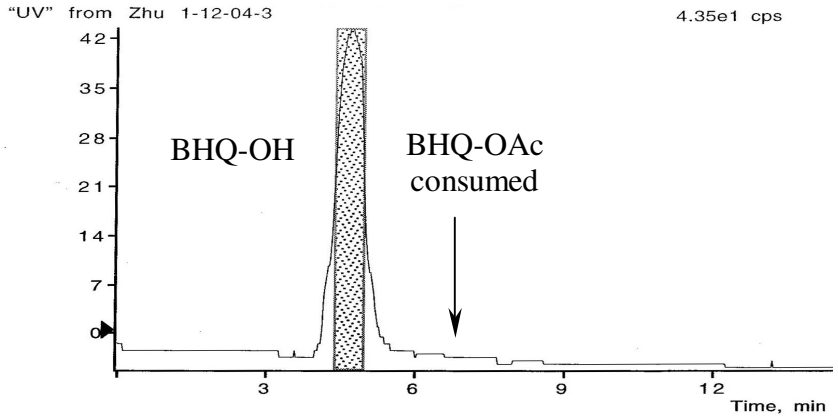


MS of highlighted peak in chromatogram above

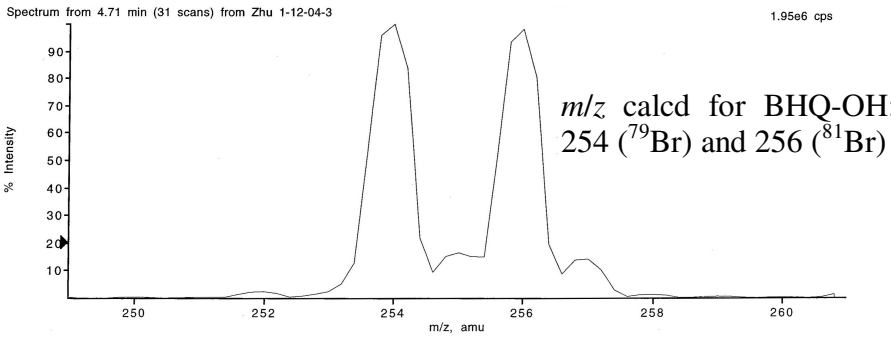


**Figure 25.** Photolysis of BHQ-OAc in water

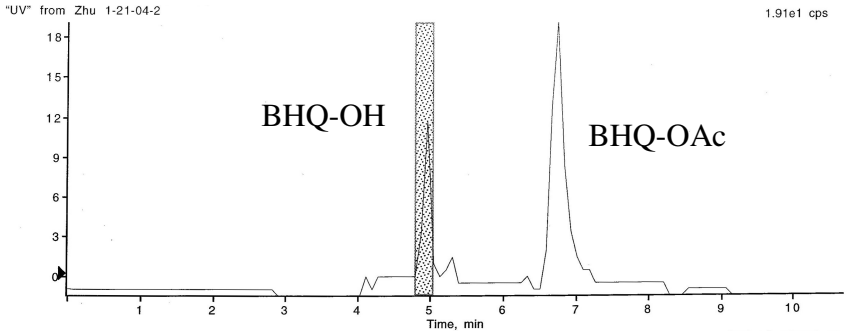


MS of highlighted peak in chromatogram above

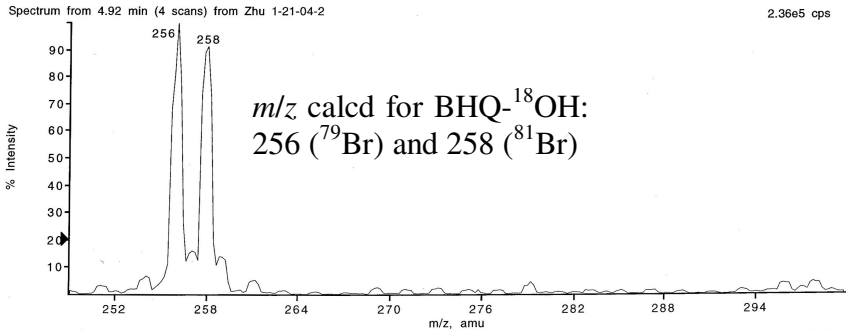


**Figure 26.** Photolysis of BHQ-OAc in $^{18}O$ labeled water

### *$^1$H NMR experiment of BHQ-OAc photolysis in acetonitrile-$d_3$*

To beter understand time-resolved studies on BHQ, which were conducted in acetonitrile and with 266 nm laser light, photolysis of BHQ-OAc in a non-nucleophilic solvent was conducted. The photolysis of BHQ-caged compounds in aqueous media undergoes through a solvent-assisted heterolysis. The solutions of BHQ-OAc in acetonitrile-$d_3$ with a trace of water and in dry acetonitrile-$d_3$ were irradiated by 254 nm UV light. The sample containing a trace of water showed some changes in the $^1$H NMR after irradiation for 4 h (Figure 27 and Figure 28). The water peak at 2.2 ppm disappeared. The original peaks in the aromatic region shifted downfield, two of which overlapped with each other. Four doublet peaks in the aromatic region grew with concomitant decrease of the original peaks. In comparing this spectrum to the $^1$H NMR spectrum of BHQ-OH in acetonitrile-$d_3$ (Figure 29), these new aromatic peaks do not represent BHQ-OH. Interestingly, the benzylic methylene signal at 5.4 ppm in BHQ-OAc, which is different from 4.8 ppm in BHQ-OH, did not move. The photolysis of BHQ-OAc in dry acetonitrile-$d_3$ gave similar results. The aromatic peaks moved upfield after irradiation for 0.5 h (Figure 31). The peak at 7.3 ppm moved downfield most. And there were some new small peaks generated. After irradiation for 2 h (Figure 32), the peak originally at 7.3 ppm moved further downfield and overlayed with another doublet; new peaks remained the same as that from the photolysis experiment with a trace of water. After irradiation for 16 h (Figure 33) and 40 h (Figure 34), most of the BHQ-OAc was consumed due to non-specific photo degradation. New peaks did not arise after more than 0.5 h of irradiation time. The photochemistry in acetonitrile is quite different from that in aqueous media. Traces of nucleophilic solvent (water in this case) do not quench the reactive excited state of BHQ-OAc to release the acetate. These experimental observations can be explained given that the singlet excited state of hydroxyquinoline is

extremely acidic, which protonates the acetonitrile or another hydroxyquinoline molecule. The downfield shift of aromatic peaks and formation of new peaks are possibly caused by the solvent protonation, dimerization of the BHQ-OAc, or formation of some charged complex. The possible formation of a charged complex might be the reason of the unsuccessful reaction of BHQ-OAc and water in acetonitrile-$d_3$. More work is needed to understand this interesting photolysis process better. The results from these experiments demonstrate that the photolysis of BHQ-caged compounds does not lead to successful release of bioactive effector without the assistance from solvent.

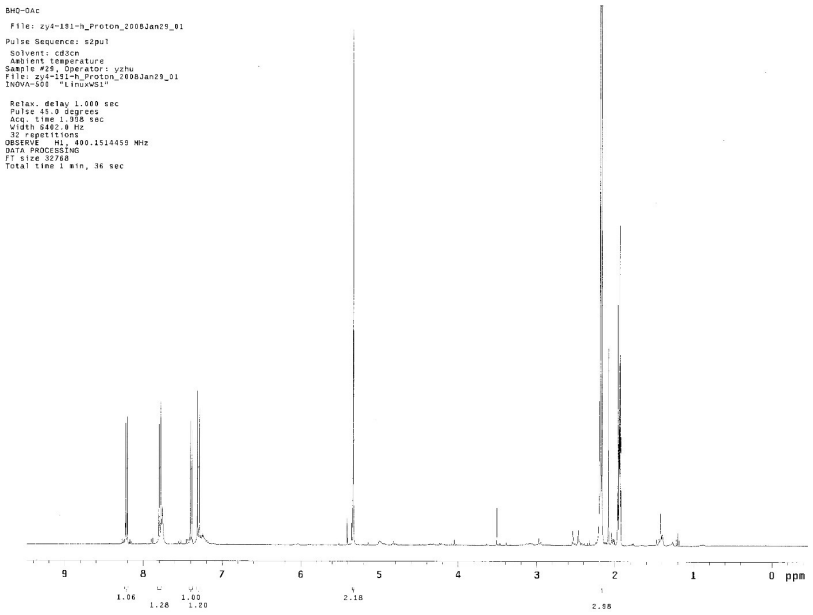


**Figure 27.** $^1$H NMR of BHQ-OAc in acetonitrile-$d_3$ with trace of water

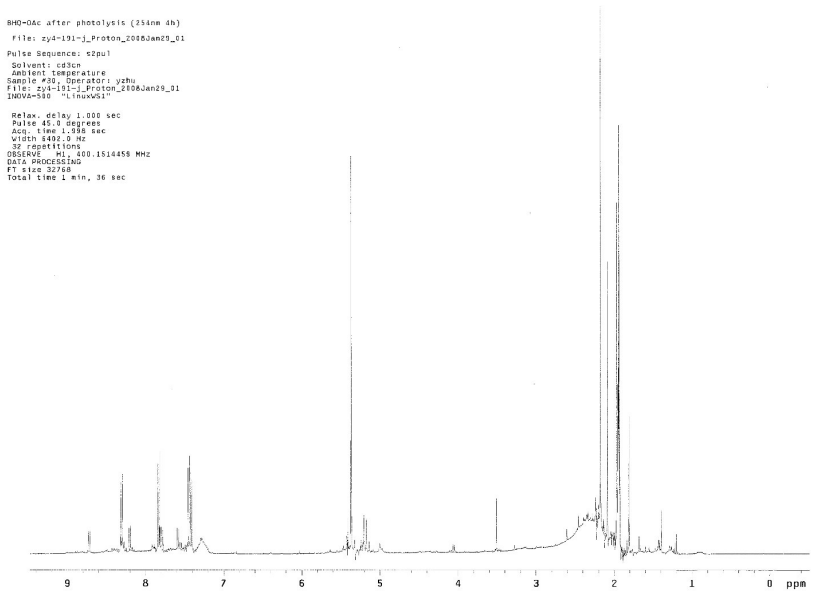


**Figure 28.** $^{1}$H NMR of BHQ-OAc after irradiation of 4 h in acetonitrile-$d_3$ with trace of water

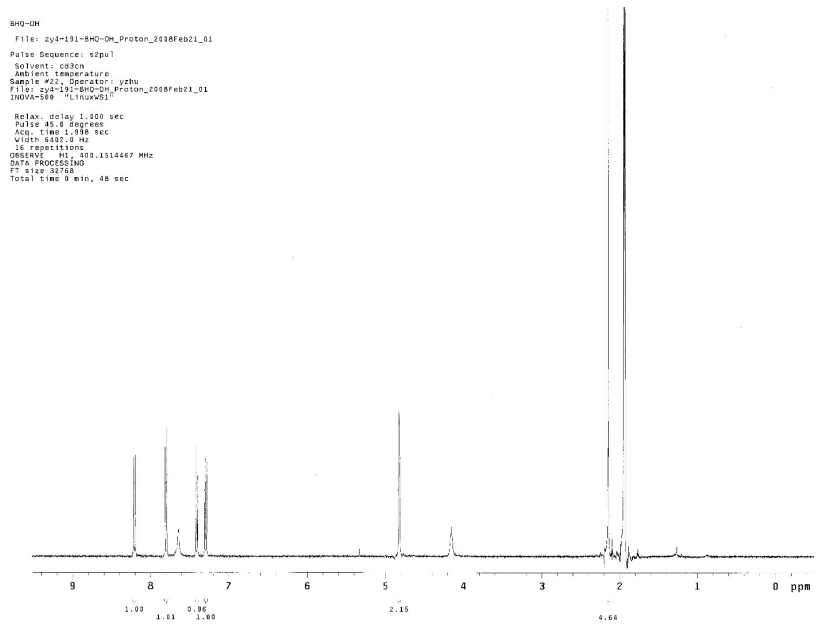


**Figure 29.** $^{1}$H NMR of BHQ-OH in acetonitrile-$d_3$

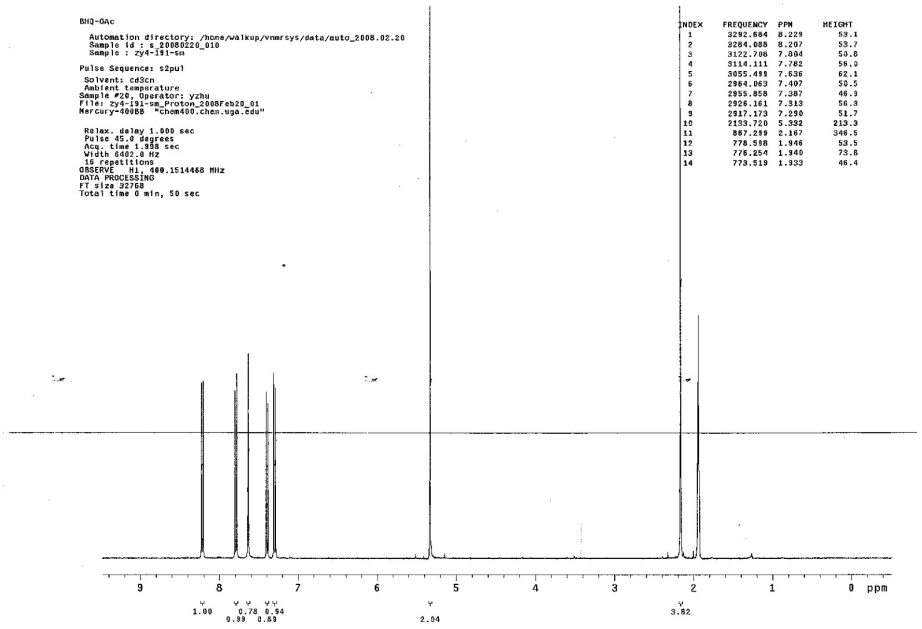


**Figure 30.** $^{1}$H NMR of BHQ-OAc in dry acetonitrile-$d_3$

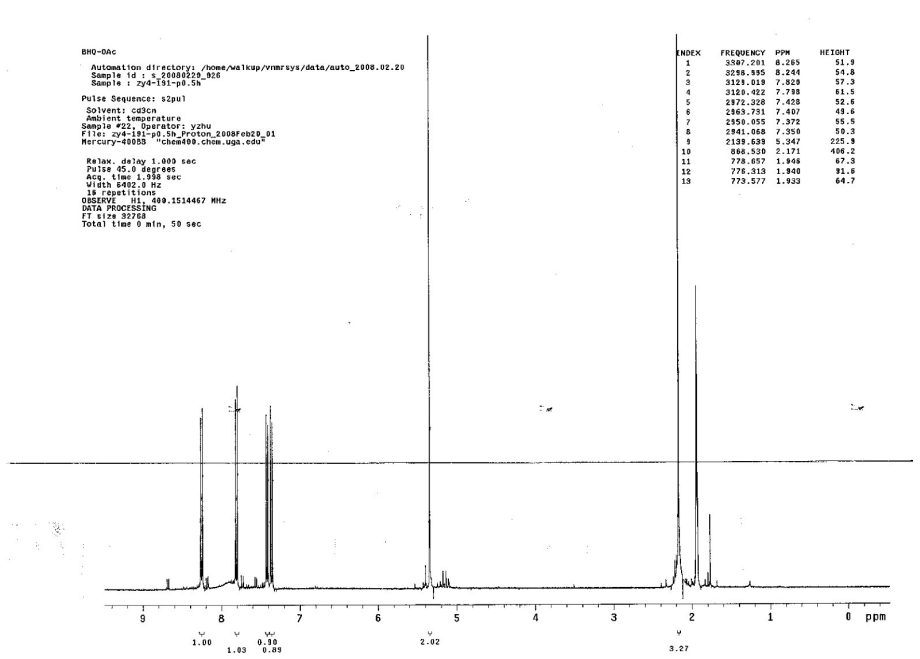


**Figure 31.** $^{1}$H NMR of BHQ-OAc after irradiation of 0.5 h in dry acetonitrile-$d_3$

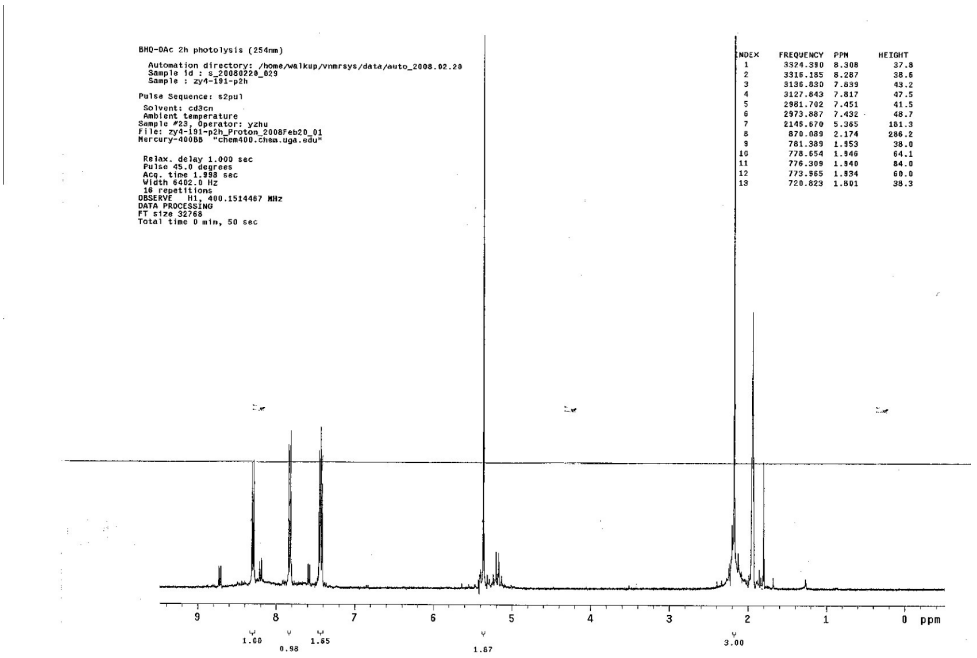


**Figure 32.** $^{1}$H NMR of BHQ-OAc after irradiation of 2 h in dry acetonitrile-$d_3$

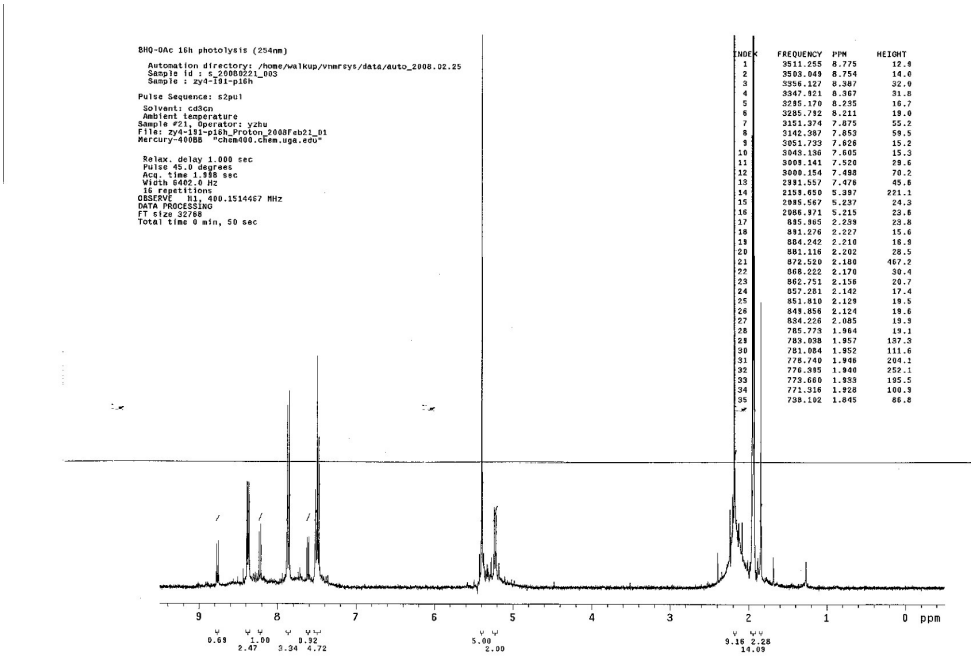


**Figure 33.** $^{1}$H NMR of BHQ-OAc after irradiation of 16 h in dry acetonitrile-$d_3$

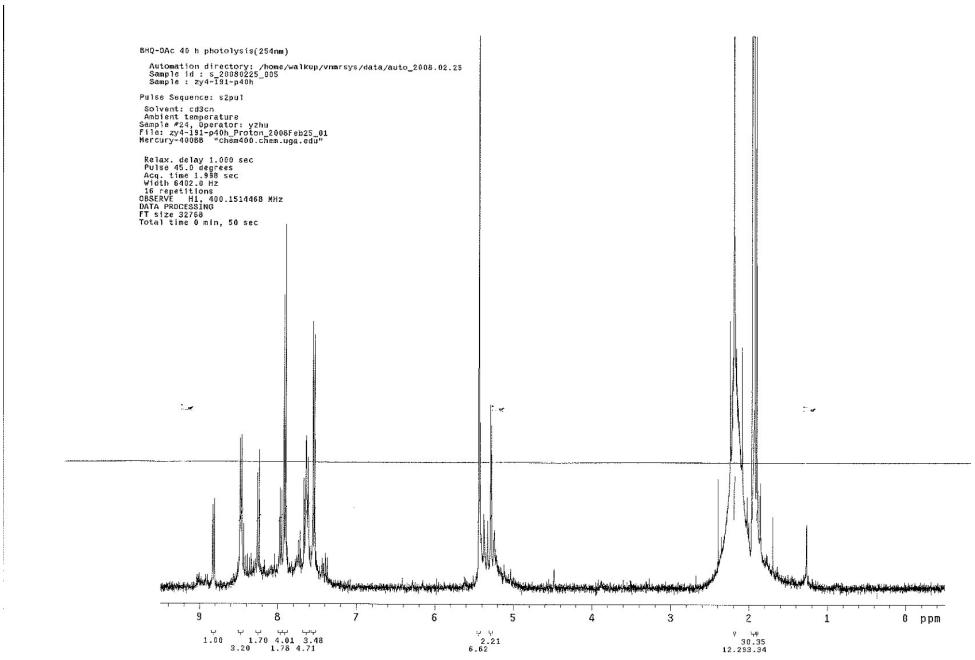


**Figure 34.** $^{1}$H NMR of BHQ-OAc after irradiation of 40 h in dry acetonitrile-$d_3$

***Time-resolved studies***

Successful applications of 2PE-mediated uncaging in biological studies require fast release to maintain tight spatially controlled release of bioactive molecules. Time-resolved studies were carried out to assess the kinetics of the BHQ caging group photolysis.

The Toscano group has executed time-resolved infrared (TRIR) experiments on the photolysis of BHQ-OAc.[145] The direct photolysis of BHQ-OAc by a 266-nm laser in argon-saturated acetonitrile-$d_3$ was analyzed by TRIR. The absorbance changes showed formation of a BHQ-OAc triplet excited state and incomplete recovery of the BHQ-OAc ground state. The incomplete recovery of the absorption bands indicates that some irreversible transformations (i.e., photoreaction to BHQ-OH and acetate) occur. Because oxygen is a triplet quencher, a similar experiment was executed in oxygen-saturated acetonitrile-$d_3$. The recovery of ground state was not complete, and based on the observation that the band changes recovered faster, the

conclusion that oxygen quenched the triplet excited states can be easily drawn. A solution of BHQ-OAc and the triplet sensitizer, xanthone, in argon-saturated acetonitrile was photolyzed using a 355-nm laser. Quenching of the xanthone excited state by BHQ-OAc was observed, and the recovery of BHQ-OAc ground state was complete. The results support the idea that the triplet excited state of BHQ-OAc is not on the productive pathway of the photolysis reaction.

To further investigate intermediates along the reaction pathway, the Phillips group in Hong Kong has conducted femtosecond transient absorption (TA), time-resolved fluorescence (TRF), nanosecond transient resonance raman, and time-resolved resonance raman (ns-$TR^3$) experiments on BHQ-OAc.[146] UV-Vis spectra were obtained after irradiation of BHQ-OAc in neat acetonitrile and an acetonitrile/water (60/40) mixture with 266-nm light. The photolysis of BHQ-OAc in acetonitrile/water (60/40) showed good UV result, which indicated a photo-transformation from BHQ-OAc to BHQ-OH with a quantum efficiency of 0.27 to 0.45. The UV spectrum of BHQ-OAc in neat acetonitrile after irradiation for 4 h was different from that in acetonitrile/water mixture. This result related well with the observations of photolysis experiment of BHQ-OAc in acetonitrile-$d_3$, and suggested a possible formation of some charged complex. The TA experiment of BHQ-OAc in neat acetonitrile after irradiation showed two bands, one at 350 nm and the other at 500 nm. The band at 350 nm was promptly formed and subsequently decayed on the tens of ps timescale, and the band at 500 nm was formed from the decay of the 350-nm band. The fluorescence emission spectra from TRF experiments showed a 400-nm band formed promptly and decayed on the tens of ps timescale. The 350-nm band was assigned to the singlet excited state and the 500-nm band to triplet excited state. The time constant for this ISC between the two states is 11 ps. The TA and TRF experiments on BHQ-OAc in mixed solvent after irradiation showed complicated results. Two bands were observed in

the TA experiments, one at 350 nm (decay) and the other at 500 nm (decay-growth-decay). The TRF experiments showed two bands, one at 390 nm (decay) and the other at 520 nm (growth-decay). According to the results from the TA and TRF experiments of BHQ-OAc in neat acetonitrile, the 350-nm band in TA and 390-nm band in TRF was assigned to the singlet excited state of phenol form of BHQ-OAc. The 520-nm band in TRF was assigned to singlet excited state of phenolate form of BHQ-OAc. The excited state deprotonation caused the decay of the 390-nm band and growth of the 520-nm band in TRF, and the time constant for this process is 4.8 ps. The 500-nm band in TA was then assigned to the triplet state of the phenolate form of BHQ-OAc. This assignment was confirmed by the comparison of the transient resonance raman spectra and density functional theory (DFT) calculations. This triplet intermediate formed with a time constant of 774 ps and decayed with a time constant of 6265 ps. The results of ns-TR$^3$ experiments and DFT calculations suggest that a triplet state zwitterion species formed from the decay of the triplet excited state of the phenolate form of BHQ-OAc (this zwitterion species formed on the 5-10 ns timescale, similar to the 6 ns triplet excited state decay time constant). These results from the Phillips group demonstrated that a triplet excited state of phenolate form of BHQ-OAc was formed during the photolysis process and this triplet state led to the release of bioactive molecules in the presence of water.

***Proposed mechanism of photolysis of BHQ-OAc***

Results of the Stern-Volmer quenching experiment and TRIR experiment correlate well with each other. The reaction proceeds through a singlet excited state; ISC to the triplet state competes with the productive pathway but does not lead to products. Results of the TA, TRF, nanosecond transient resonance raman, and ns-TR$^3$ experiments are in conflict with this conclusion. In these experiments, a very important absorption band of one intermediate was

assigned to a triplet excited state. The decay of this intermediate correlates with the rise of the product very well, and this intermediate is believed to be on the pathway leading to successful release of acetate. Thus these results support that the photolysis reaction proceeds through a triplet excited state.

It seems that this controversy can be explained as follows. (1) According to Stern-Volmer relation and assuming the quenching is diffusion-controlled, the quenching efficiency (quantum efficiency change) is related to the product of diffusion rate of the quencher, the concentration of the quencher, and the triplet state lifetime. Results of TRIR experiments and TA, TRF, nanosecond transient resonance raman, and ns-$TR^3$ experiments agree that the lifetime of triplet state of BHQ-OAc is several ns. The quenching of this short-lived triplet excited state by low concentrations of quenchers is not possible. This can explain the result of Stern-Volmer quenching experiment and the TRIR oxygen saturated photolysis experiment. (2) The photolysis wavelength of BHQ-OAc is 365 nm. The photolysis sensitizing experiment used 355-nm light to excite xanthone, and the excited xanthone transfers the energy to BHQ-OAc to form the triplet excited state of BHQ-OAc. The sensitized triplet state of BHQ-OAc might have a much lower energy than the triplet state of BHQ-OAc accessed through direct irradiation. The different triplet state might be the reason for not observing sensitized photolysis.

More mechanistic work is required to better understand the photolysis reaction of BHQ-caged compounds. With all the information available, the mechanism of photolysis of BHQ-OAc is proposed to proceed through a triplet excited state zwitterion that will undergo ISC to a ground state zwitterions, which will be trapped by water as shown in scheme 14.

**Scheme 14.** Proposed mechanism of photolysis of BHQ-OAc

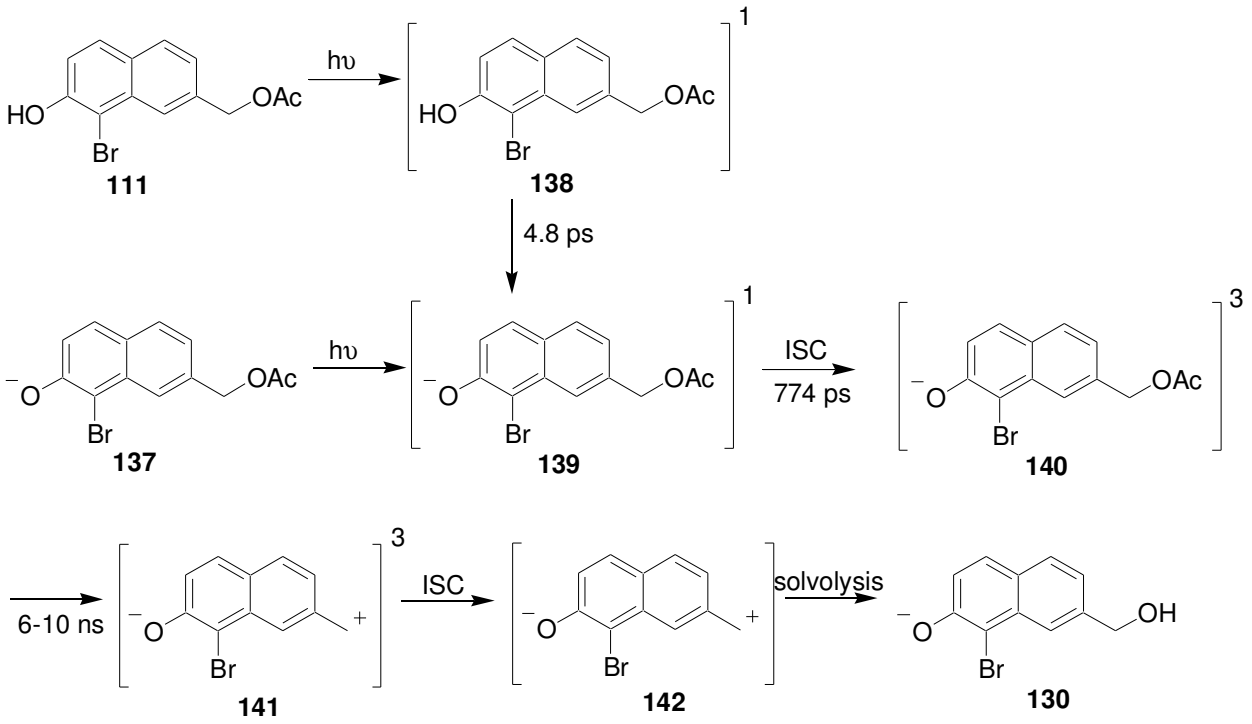


Both phenol form and phenolate form of BHQ-OAc are excited to their singlet excited states, respectively. Because the singlet excited state of quinoline is a superacid,[139] the phenol form is deprotonated with a time constant of 4.8 ps to generate the phenolate form **139**. The phenolate singlet excited state undergoes ISC with a time constant of 774 ps to the triplet excited state **140**. Time resolved experiments showed that the lifetime of the triplet phenolate **140** has a time constant of around 6 ns, and converted to a triplet zwitterion **141**, releasing acetate. The triplet zwitterion changes to the ground state zwitterion **142**, which is trapped by water to form BHQ-OH.

***Next generation of quinoline based cages and their photochemistry***

The Stern-Volmer and TRIR experiments suggest that the productive reaction intermediate is the singlet excited state. Other time-resolved experiments by the Phillips group declare that a triplet excited state is a key intermediate for successful uncaging. Design, synthesis, and

examination of photochemistry of new quinoline based caging group will benefit from mechanistic studies. Bromine is known for the heavy atom effect, through which it facilitates ISC and favors singlet excited state transfer to the triplet excited state. The presence of an electron withdrawing group at the 8-position is important because it lowers the $pK_a$ of the hydroxy by stabilizing the corresponding phenolate. The phenolate has a larger $\lambda_{max}$ and increased absorptivity than the phenolic form. At physiological pH the phenolate is favored. With these principals, two new 7-hydroxyquinoline derivatives, NHQ (**143**) and CyHQ (**144**) (Figure 35), were synthesized[147] to test the uncaging ability (Table 6).

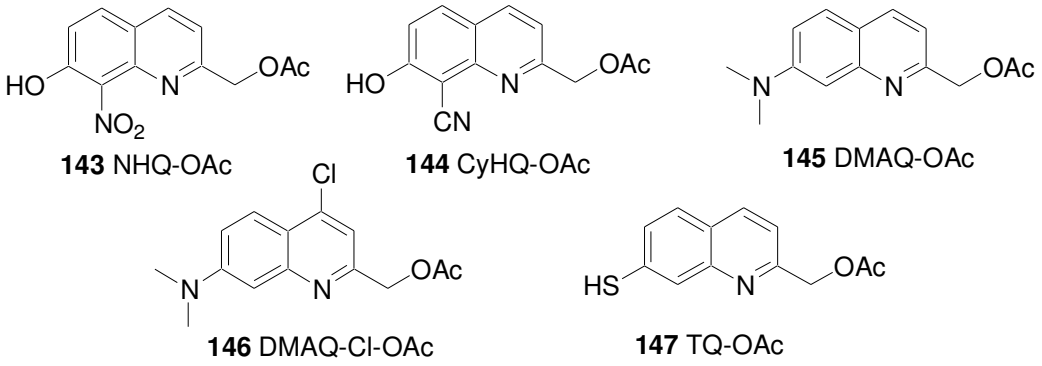


**Figure 35.** Next generation chromophores of quinoline derivatives

**Table 6.** Photochemical properties of 7- and 8- substituted quinolines[147]

| Compounds | $\lambda_{max}$ nm | $\varepsilon_{365\ nm}$ ($M^{-1}\cdot cm^{-1}$) | $Q_u$ | 1P sensitivity ($M^{-1}\cdot cm^{-1}$) | $\delta_u$ (GM) | $\tau_{dark}$ (h) | $\delta_a$ (GM) $\delta_u/Q_u$ |
|---|---|---|---|---|---|---|---|
| **111** | 369 | 2600 | 0.29 | 754 | 0.59 | 71 | 2 |
| **143** | 348 | 5400 | 0.0 | 0.0 | 0.0 | 282 | – |
| **144** | 363 | 7700 | 0.31 | 2387 | 0.31 | 388 | 1 |
| **145** | 368 | 4600 | 0.046 | 212 | 0.13 | 31 | 2.8 |
| **146** | 386 | 2800 | 0.084 | 235 | 0.43 | 34 | 5.1 |
| **147** | 369 | 5200 | 0.063 | 328 | 0.42 | 29 | 6.7 |

The data was measured in KMOPS buffer and the two photon cross section was measured at 740 nm.

Surprisingly, NHQ is not photolyzed to release acetate, yet it is stable under simulated physiological conditions. CyHQ, on the other hand, is sensitive to 1PE photolysis. The quantum

efficiency of CyHQ is similar to BHQ, but notably, CyHQ has a large extinction coefficient and enhanced fluorescence emission in contrast to BHQ. The extended conjugation provides better absorption, which leads to the increased sensitivity to 1PE uncaging. By changing bromine to a cyano group, presumably ISC to the triplet state is less favorable, but excited state decay through fluorescence has increased (Figure 36).

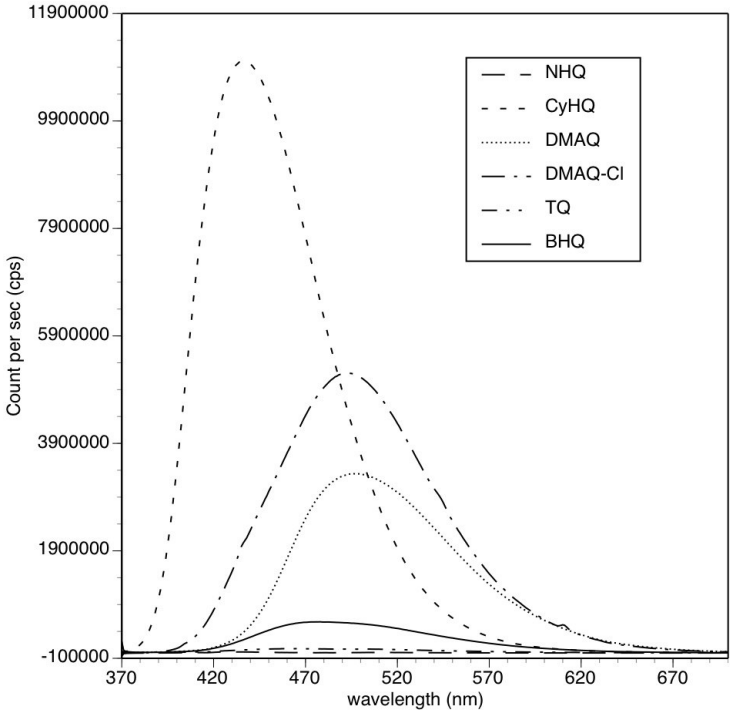


**Figure 36.** Fluorescence emission spectra of 15 $\mu$M solution of BHQ-OAc (**111**), NHQ-OAc (**143**), CyHQ-OAc (**144**), DMAQ-OAc (**145**), DMAQ-Cl-OAc (**146**), and TQ-OAc (**147**). The excitation wavelength is 365 nm.

The dimethylamino group on DMACM increases $\lambda_{max}$ of the coumarin chromophore.[69,70] DMAQ (**145**) and DMAQ-Cl (**146**) were designed to increase $\lambda_{max}$ on the quinoline chromophore. The thiol group is supposed to stablize the ion pair through conjugation, so TQ (**147**) was also targeted as possible caging group. These three quinoline derivative compounds were synthesized by Reddie[147] and examined for 1PE photochemistry. The quantum efficiencies of these compounds are not high; therefore, the sensitivities are not as large as BHQ. DMAQ and DMAQ-Cl are both fluorescent (Figure 36), which competes with the uncaging process, resulting

in a low quantum yield. The low quantum yield of TQ can be explained by the weaker electron donating ability of the sulfide comparing to phenolate. The 1PE quantum efficiencies of NHQ, CyHQ, DMAQ, DMAQ-Cl, and TQ are not impressive.

***Two-photon photolysis of second generation quinoline cages***

CyHQ, DMAQ, DMAQ-Cl, and TQ are sensitive to 1PE. To further assess their potentials as biological tools, 2PE photolysis experiments were conducted. CyHQ-OAc (**144**), DMAQ-OAc (**145**), DMAQ-Cl-OAc (**146**), and TQ-OAc (**147**) were dissolved in KMOPS buffer (100 uM). A Ti:Sapphire laser (mode locked, 300-350 mW) was used to photolyze the samples as previously described on page 49. Aliquots (25 μL) were photolyzed (5, 10, 20, and 40 min) and analyzed by HPLC. The results of the analyses fit to a single exponential decay equation (Figure 37). The two-photon uncaging action cross-section was calculated using equation (1) (Table 6).

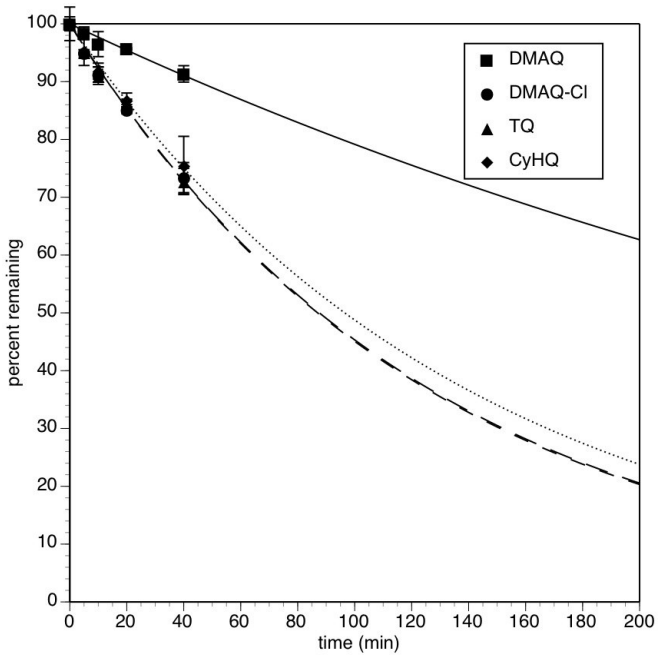


**Figure 37.** Time course of two-photon photolysis of 2nd generation quinoline based cages CyHQ-OAc (**144**), DMAQ-OAc (**145**), DMAQ-Cl-OAc (**146**), and TQ-OAc (**147**). The percent remaining was determined by HPLC and is the average of 3 runs. Lines are fits of a single exponential decay curve. Error bars represent the standard deviation of the measurement.

All of the new designed molecules have sufficient one-photon and two-photon sensitivity for uncaging except NHQ. CyHQ has a lower two-photon uncaging action cross-section in contrast to BHQ. But the high fluorescence might limit its use in biological applications. CyHQ is extremely stable under physiological conditions in the dark. NHQ does not show any ability to photorelease acetate. The UV spectrum of NHQ in KMOPS is very different from any other of hydroxyquinoline compounds (Figure 38). It only has one absorption peak at 350 nm. Upon irradiation with 365-nm light, the nitro group of NHQ is probably excited instead of the prospective quinoline ring, so that the desired chemistry does not take place from the excited nitro group. The UV spectra of NHQ-OAc and CyHQ-OAc also suggest that both of these two compounds exist as phenolate in KMOPS, while BHQ is a mixture of phenol and phenolate.

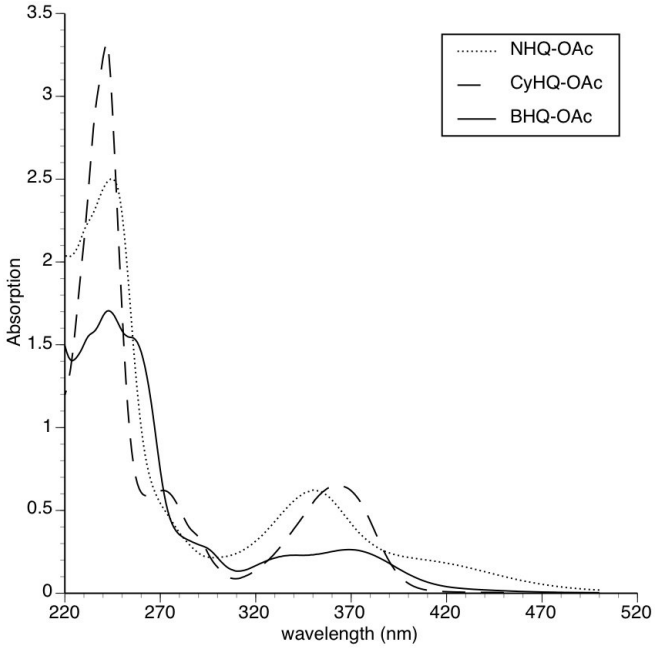


**Figure 38.** UV-Vis spectra of BHQ-OAc, NHQ-OAc, and CyHQ-OAc

The 2PE absorption cross-sections of DMAQ **145**, DMAQ-Cl **146**, and TQ **147** are better than that of BHQ **111** and CyHQ **144**, and these three compounds are stable in the dark under simulated physiological conditions ($\tau_{dark}$ =29-34 h).

The synthesis and photochemistry of these compounds support the proposed reaction mechanism and expand the pool of useful 2PE caging groups.

***Conclusions***

The BHQ chromophore can be used to protect carboxylates, phosphates, and diols via covalent bond, and efficiently release these three common functional groups found on bioactive molecules such as neurotransmitters, nucleic acids, and drugs, through both 1PE or 2PE at wavelengths that are not lethal to biological systems. The BHQ-caged compounds prepared are stable in the dark under simulated physiological conditions. Quantum efficiency alone is not a good criteria for evaluating caging groups. Sensitivity is a better factor for comparing chromophores. The 1PE sensitivity of caged compounds are measured by the product of the quantum efficiency and the molar absorptivity ($Q_u \times \varepsilon$).[123] The 1PE sensitivity of BHQ (780) is higher than DMNB (31),[135] Bhc (555),[15] and MNI (408).[39] CNB[18] and NPE[2] have high sensitivities, 714 and 2184, but the excitation wavelengths are below 270 nm, which are deleterious to biological and physiological systems. The two-photon uncaging cross-section of BHQ is greater than the 0.1 GM threshold for physiological use. The caged bioactive effectors (carboxylates and diols) can be recovered from photorelease in decent yield (60–70%) via both 1PE and 2PE. The kinetic TRIR study demonstrates that the photolysis timescale is sub-microsecond, which is faster than physiological signal transduction events (millisecond and slower). The physiological useful 2PE uncaging of BHQ-caged carboxylates and phosphates will enable tight three-dimensional localized release of bioactive substrates, and the sub-microsecond photolysis timescale is much shorter than the diffusion timescale (normally close to millisecond).[148] The localized concentration change requirement for a number of biological studies can be easily achieved.

The LC-MS analyses of the photoreaction in $^{18}O$-labeled water and normal water reveals that the reaction is not a simple ester hydrolysis; the label $^{18}O$ was found on the quinoline remnant, indicating that the bond cleavage occurred between benzylic carbon and oxygen. This result suggests that the mechanism is a $S_N1$ type solvent-assisted heterolysis at the benzylic carbon center. Results from photolysis experiment of BHQ-OAc in acetonitrile-$d_3$ support this conclusion. There is no desired photorelease of acetate without a nucleophilic solvent (*i.e.*, water).

The results of the Stern-Volmer quenching experiments and the triplet sensitized experiments agree that the productive photolysis pathway does not involve triplet excited state of BHQ. The increasing presence of two different triplet quenchers, sodium 2-naphthalene sulfonate and potassium sorbate, did not affect the 1PE quantum efficiency. The xanthone triplet excited state transfers its energy to BHQ, and the triplet excited state of BHQ is observed to completely recover back to the ground state, while the direct photolysis of BHQ showed incomplete recovery of the ground state. In the presence of oxygen as a triplet quencher, the triplet excited state of BHQ-OAc is efficiently quenched; the TRIR spectrums of BHQ-OAc photolysis showed that the same stable products form as in the absence of oxygen.

The results of TA, TRF, nanosecond transient resonance raman, and ns-TR$^3$ experiments do not support that a singlet excited state is the productive pathway. Important phenolate intermediates of the singlet excited state and the triplet excited state were observed and assigned. The singlet excited state undergoes ISC to the triplet excited state of phenolate BHQ-OAc, which is the key intermediate in the photolysis. This intermediate has a very short lifetime (6 ns). Thus, there is still disagreement whether the photolysis reaction proceeds through a singlet or a triplet excited state pathway.

A series of second generation of quinoline-based caging groups were synthesized. NHQ, CyHQ, DMAQ, DMAQ-Cl, and TQ were tested for 1PE and 2PE photolysis. NHQ is not photolyzed to release protected molecules. The other quinoline compounds have decent to good quantum efficiencies (0.046 to 0.31), and good sensitivities (212 to 2387 $M^{-1}\cdot cm^{-1}$) for 1PE photolysis; they are sensitive to 2PE ($\delta_u$ of 0.13 to 0.43 GM) and stable in the dark ($\tau_{dark}$ of 29 h to 388 h). The undesired fluorescence emission might be a limiting factor for applications in biological studies.

## Chapter 3

## Synthesis and Photochemistry of BHQ-ATP

### *Introduction*

ATP is a unique chemical energy carrier in most energy requiring processes. The solovolysis of ATP will release energy, and the process has been involved in active transports, in muscle contraction, endo- and exocytosis, cytoplasmic streaming, ciliary movements, conformational changes of proteins, and many other dynamic processes. It is not surprising that the first caged compound produced is NB-ATP by Kaplan.[2] Biologists and physiologists have used analogs of NB to cage ATP,[2 10 149] which are the only commercially available caged ATP;

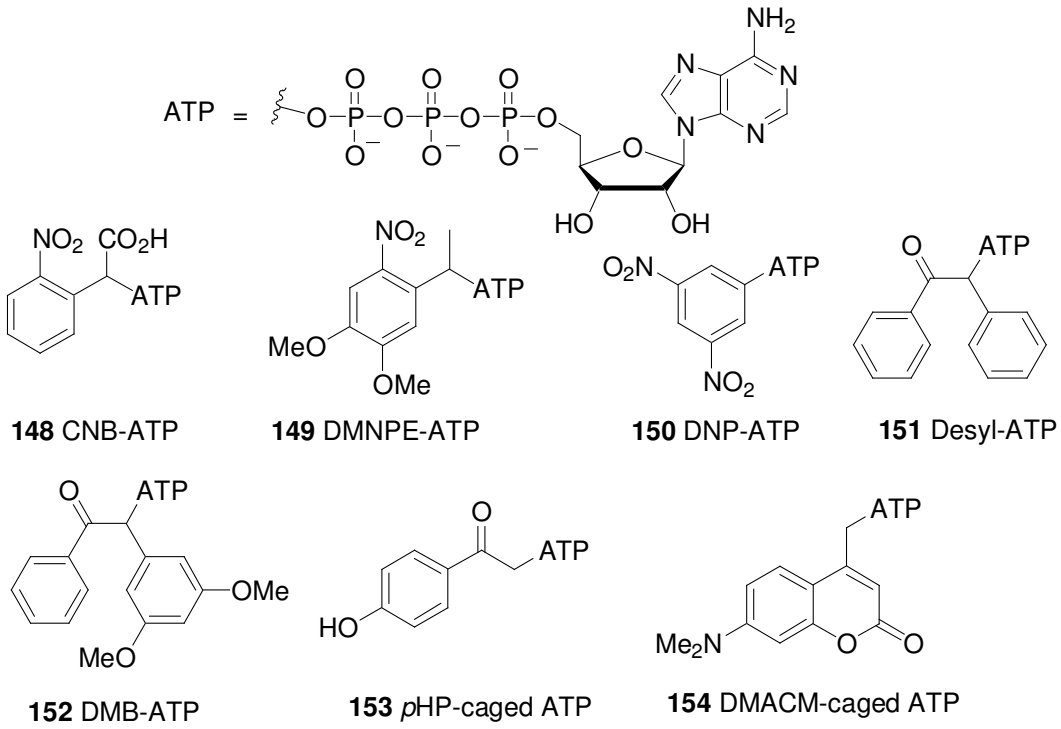


**Figure 39.** Structures of caged ATP

DNP-ATP;[45] Benzoin-ATP;[44] DMB-ATP;[46] *p*HP-ATP;[53] and DMACM-ATP[70] (Figure 39) for their studies. All of these molecules possess a covalent bond to the $P^3$ phosphate group of ATP to ensure that the biological activity of ATP is rendered inert. Photophysical and photochemical properties of these compounds are shown in Table 7.

**Table 7.** Photochemical properties of caged ATP compounds

| Caged ATP | $\lambda_{max}$ (nm) | $\varepsilon$ ($M^{-1}\cdot cm^{-1}$) | $\Phi_{ATP}$ | 1P sensitivity $\Phi \bullet \varepsilon$ | references |
|---|---|---|---|---|---|
| NB-ATP **1** | 260 | 26600 | ≤0.19 | <130 (347 nm) | 2 |
| NPE-ATP **2** | 260 | 26600 | 0.63 | 410 (347 nm) | 2, 10 |
| DMNPE-ATP **149** | 350 | 5100 | 0.07 | 350 (347 nm) | 150 |
| DNP-ATP **150** | — | — | ≤0.007 | Low | 45 |
| Desyl-ATP **151** | — | — | 0.3 | — | 44 |
| DMB-ATP **152** | 256 | 25600 | 0.3 | 50 (347 nm) | 45, 46, 47 |
| *p*HP-ATP **153** | 286 | 14600 | 0.3 | — | 44, 53 |
| DMACM-ATP **154** | 385 | 15300 | 0.086 | 645 (347 nm) | 75 |

The first synthetic caged compound, NB-ATP (**1**), was synthesized and its biological use as a controllable source of ATP was illustrated.[2] Incubated with renal Na,K-ATPase (a membrane protein that hydrolyzes ATP to drive the coupled extrusion and uptake of $Na^+$ and $K^+$ ions through the plasma membrane), NB-ATP was neither a substrate nor inhibitor of this enzyme. Upon irradiation, ATP was released and activated the pump.

Trentham and coworkers[46] used DMB-ATP (**152**) to study electrogenic ion transport by Na,K-ATPase. They chose DMB-ATP over NPE-ATP because DMB-ATP has an ATP release rate $>10^5$ $s^{-1}$,[47] while the ATP release rate of NPE-ATP is 118 $s^{-1}$.[151] The liberated ATP activated the pump for $Na^+$ transport. Transient currents in the system were recorded and analyzed to determine that the rate constants of enzyme phosphorylation and ADP-dependent dephosphorylation were 600 $s^{-1}$ and $1.5 \times 10^6$ $M^{-1}\cdot s^{-1}$.

DMACM-caged ATP (**154**) was synthesized to provide a better tool that has an efficient photorelease of ATP at long wavelengths and fast release of ATP ($1.6 \times 10^9$ $s^{-1}$).[70] In cultures of mouse astrocytes and in brain tissue slices from mice, the DMACM-caged ATP was irradiated, and the release of ATP evoked $Ca^{2+}$ ion waves.

Due to the lack of 2PE sensitivity of commercially available caged ATP, few biologists can take advantage of 2PE processes. Malicka and co-workers used DMNB-caged ATP and 2PE microscope to study muscle contraction,[152] which is believed to be caused by the rotation of the lever arm of myosin cross-bridges. Caged ATP was used to generate an ATP concentration jump in a fL volume, which enabled the observation of a small population of cross-bridges. Using 1PE to release ATP from caged-ATP, the number of observed cross-bridges was around 600. The rate of cross-bridge detachment and rebinding was determined, while the power stroke could not be resolved. It was suspected that the number of observed cross-bridges was too large because of the low 3-D selectivity of 1PE. With the help of two-photon microscopy, the number of observed cross-bridges was about 300, and the power stroke was observed to begin around 170 ms after the cross-bridge binds ATP.

A caged ATP with fast and efficient photorelease of ATP and good sensitivity to 2PE is in great need. Among all of the existing caged ATP compounds, none has been reported to have sensitivity to 2PE. Given that the Bhc caging group is known to be sensitive toward 2PE, one might conclude that the DMACM caging group will probably be sensitive to 2PE because of its similarity to Bhc. The DMACM caging group also has been reported for possible two-photon release of the biological active molecules.[124] Nevertheless, the high fluorescence levels and low water solubility of DMACM caged ATP are a limiting factor for its application in biological systems.

The BHQ caging group has been identified as a two-photon sensitive photolabile protecting group, and previous studies have revealed its fast kinetics of photolysis and its ability to protect and photorelease phosphates. The low fluorescence level, high water solubility, and the photochemical properties of BHQ make it a prospective photoremovable protecting group for ATP (Figure 40). Herein, the synthesis and photochemistry of a 2PE sensitive caged ATP will be discussed.

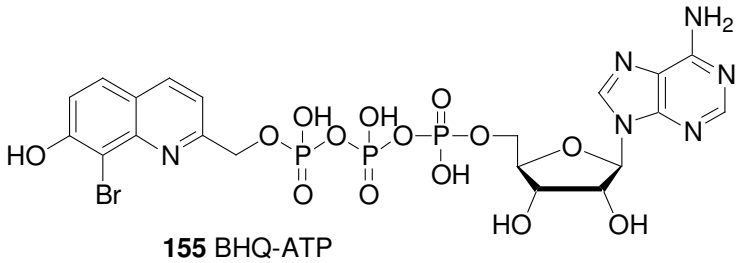


**155** BHQ-ATP

**Figure 40.** BHQ-ATP

***Synthesis of BHQ-ATP***

The synthesis of BHQ-ATP **155** started from BHQ **120** in seven steps (Scheme 15). BHQ was treated with triethyl amine and chloromethyl methyl ether in THF to protect the free hydroxy group. The next step is a selenium dioxide oxidation, which requires the free hydroxy on quinoline to be protected. The methoxymethyl (MOM) protecting group is ideal because it is stable to the oxidation conditions and it is removed a few steps later with the deprotection of the phosphate. Aldehyde **157** was prepared, and then reduced with sodium borohydride to alcohol **158**. Compound **158** was then converted to phosphate using phosphoramidite chemistry. Treating **158** with tetrazole, and di-*tert*-butyl-*N*,*N*-diethylphosphoramidite in THF generated BHQ-phosphite, which was oxidized with *tert*-butyl hydroperoxide to yield phosphate **159** in 79% for 2 steps. The MOM-protected BHQ-phosphate **159** was treated with TFA in dichloromethane and stirred overnight to yield BHQ-phosphate **160** in 85% yield. Both the MOM protecting group

and the two *tert*-butyl group on the phosphate were removed. BHQ-ATP **155** was synthesized from the coupling of BHQ-phosphate **160** and activated ADP under vigorously anhydrous conditions. The BHQ-phosphate and ADP were dried by sequential cycles of dissolution and evaporation in pyridine and DMF. Tri-*n*-octylamine and tri-*n*-butylamine were used to cap the hydroxy groups on the phosphates away from the expected reaction site. Tri-*n*-octylamine (1 eq) was used to transform BHQ-phosphate to its tri-octylammonium salt, and tri-*n*-butylamine (2 eq) was used to change ADP to its tri-butylammonium salt. The ADP salt was activated by treatment with carbonyldiimidazole to form ADP imidazolide in DMF and dried. The BHQ-phosphate salt was mixed with the activated ADP imidazolide in HMPA and stirred for two days.

**Scheme 15.** synthesis of BHQ-ATP[a]

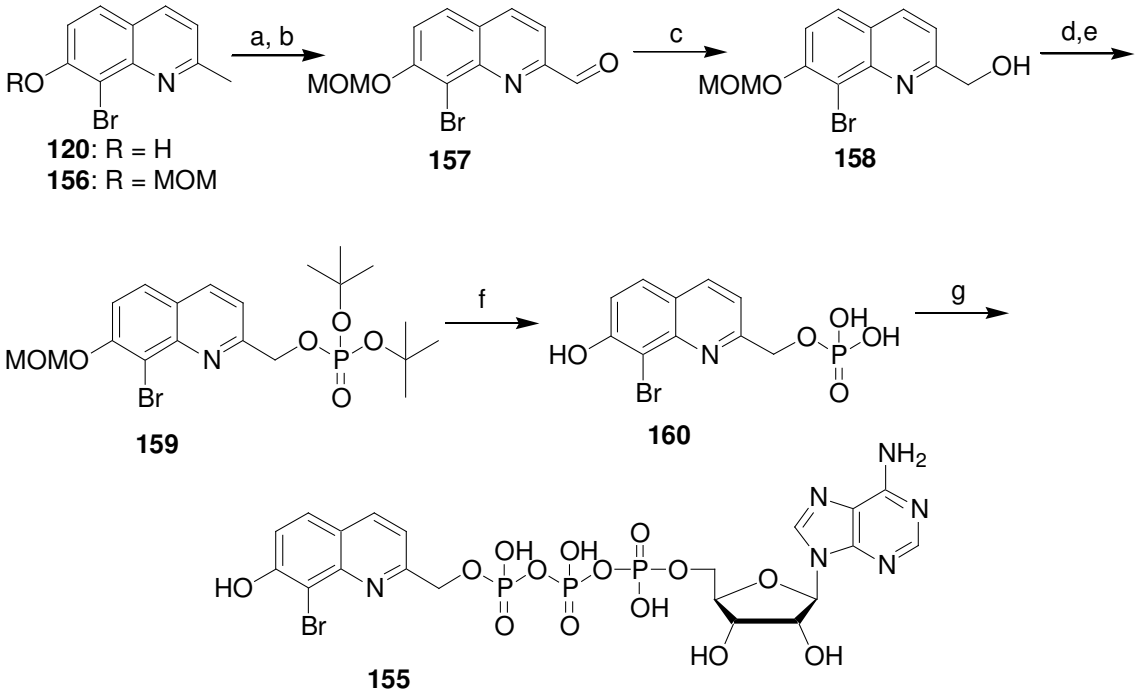


[a] Reagents and conditions: (a) MOMCl, $Et_3N$, THF, rt, 84%; (b) $SeO_2$, *p*-dioxane, 80°C, 4 h, 78%; (c) $NaBH_4$, EtOH, rt, 2 h, 94%; (d) $(t\text{-BuO})_2PNEt_2$, tetrazole, THF; (e) *t*-BuOOH, $Et_3N$, 4h, 79%; (f) TFA, $CH_2Cl_2$, rt, overnight, 82%; (g) ADP, $Im_2CO$, HMPA, rt

The purification of BHQ-ATP was performed with a DEAE cellulose column using a step gradient elution of aqueous ammonium bicarbonate. The ammonium salt of BHQ-ATP was acquired and further purified on a reverse phase C18 HPLC column using a methanol/water solvent system. The molecular structure was confirmed by $^{1}H$ NMR, $^{31}P$ NMR, and HRMS. Oddly, no $^{13}C$ NMR signal was observed. There are three possible reasons: (1) There are multiple conformations of BHQ-ATP, and the concentration of each conformation is very low so that no signal can be observed. (2) BHQ-ATP possesses a long relaxation time. There was no signal observed when we set the relaxation delay time up to one min. (3) The conformational changing dynamics of BHQ-ATP in $D_2O$ causes the problem. When the conformations change at a certain rate, a possible consequence is that no signal observation takes place.

***Photochemistry of BHQ-ATP***

The UV absorption spectra of BHQ-ATP in KMOPS buffer is similar to BHQ-OAc (Figure 41). It has two absorptive bands beyond 300 nm, one at 320 nm and the other at 370 nm. The 370-nm absorption band is arises from the phenolate form of the BHQ skeleton, and the

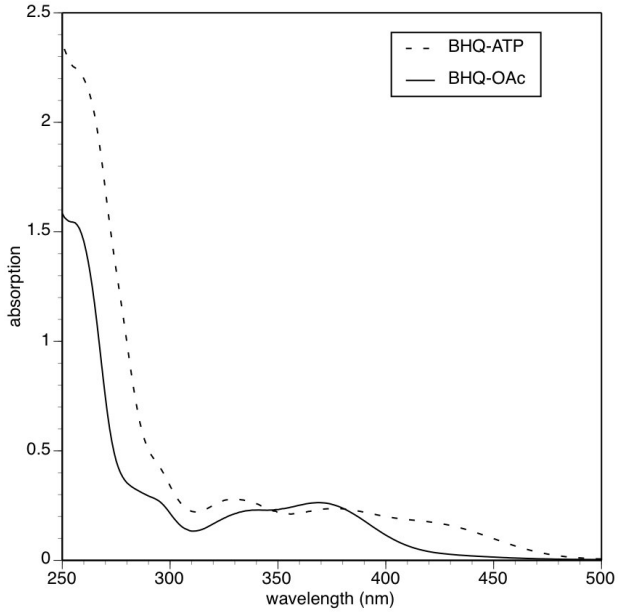


**Figure 41.** UV-Vis spectra of BHQ-ATP and BHQ-OAc

320-nm absorption band is from the phenol form. In contrast with the UV absorption spectrum of BHQ-OAc, the BHQ-ATP absorbed more at 320 nm than 370 nm, which indicates that in KMOPS buffer, the phenolic form of BHQ-ATP predominates over the phenolate form. The $\lambda_{max}$ of BHQ-ATP is 376 nm, and the extinction coefficient at this wavelength is 1300 $M^{-1} \cdot cm^{-1}$.

**Scheme 16.** Photolysis of BHQ-ATP

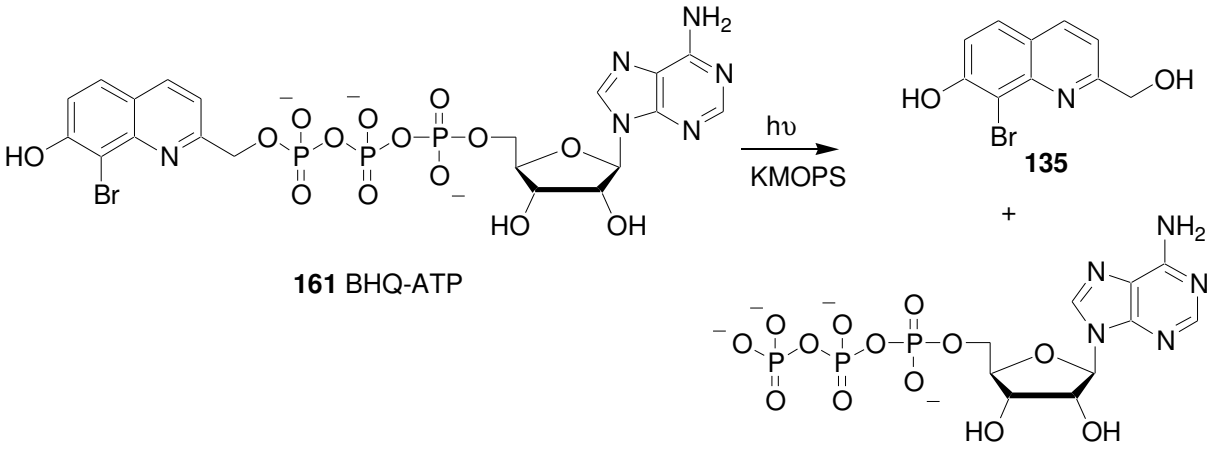


**161** BHQ-ATP

**162** ATP

Using the same method described previously in section 2.3, the quantum efficiency of BHQ-ATP decay and ATP recovery were determined by photolyzing a KMOPS solution of BHQ-ATP (100 μM) with light from a 365-nm lamp through a set of filters that narrowed the band of light to a tight 30-nm range around 365 nm. Aliquots (20 μL) were taken out from the photolysis cuvette after time interval of 0, 10, 20, 40, 60, and 90 s, and HPLC analyses of these samples with a reverse phase C18 column and 85% 25 mM $KH_2PO_4$ buffer (pH = 6.2)/15% methanol solvent system were carried out. The BHQ-ATP peak (retention time = 4.2 min) and ATP peak (retention time = 2.8 min) were recorded and analyzed. The decay of BHQ-ATP and the rise of ATP could be fit to single exponential curves (Figure 42).

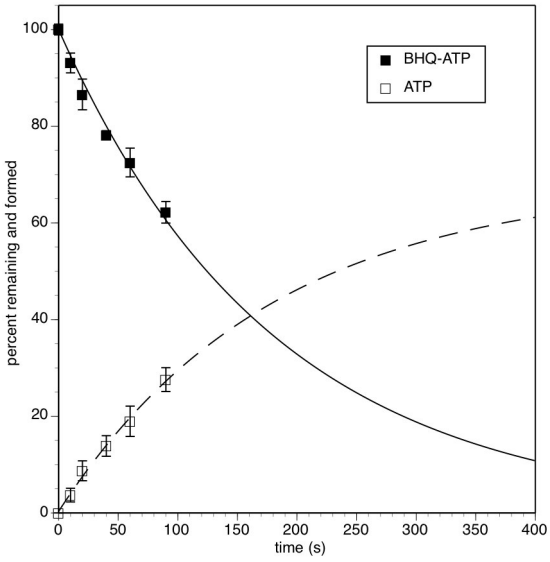


**Figure 42.** Time course of one-photon photolysis of BHQ-ATP (**161**). Also shown in the figure is the observation of ATP (**162**) generation. The percent remaining and formed were determined by HPLC and are the average of 3 runs. Lines are fits of a single exponential decay curve or rise to max. Error bars represent the standard deviation of the measurement.

The one-photon quantum efficiency was calculated with equation (2) and found to be 0.19, which is similar to the values measured for other BHQ caged compounds. The yield of ATP was about 70%. BHQ-ATP is extremely stable in the dark under simulated physiological conditions (KMOPS, pH = 7.2). The dark hydrolysis constant is about 1000 h. In a separate experiment, an NMR sample of BHQ-ATP in $D_2O$ was stable over the course of 2 weeks.

Knowing that BHQ-ATP can be photolyzed efficiently and possesses a decent yield of ATP upon irradiation with UV light, the two-photon photolysis of BHQ-ATP was also performed and monitored by HPLC to determine the two-photon uncaging action cross-section as described in section 2.3. BHQ-ATP (100 μM in KMOPS, pH = 7.2) was photolyzed with a Chameleon Ultra II laser at 740 nm in 25-uL aliquots. The irradiation time intervals of the pulsed laser were 0, 5, 10, 20, and 40 min. Three samples of each time interval were collected and analyzed by HPLC using the same method as in the one-photon photolysis. The decay of BHQ-

ATP and rise of ATP could be fit to single exponential curves (Figure 42). Using Tsien's method of determining two-photon uncaging action cross-section with a fluorescence reference solution, the two-photon uncaging action cross-section of BHQ-ATP was calculated to be 0.17 GM. The ATP is recovered in 40% yield. But we know that the HPLC traces do not have clean baseline, and the peaks do not have good symmetry, so confidence in this measurement is low.

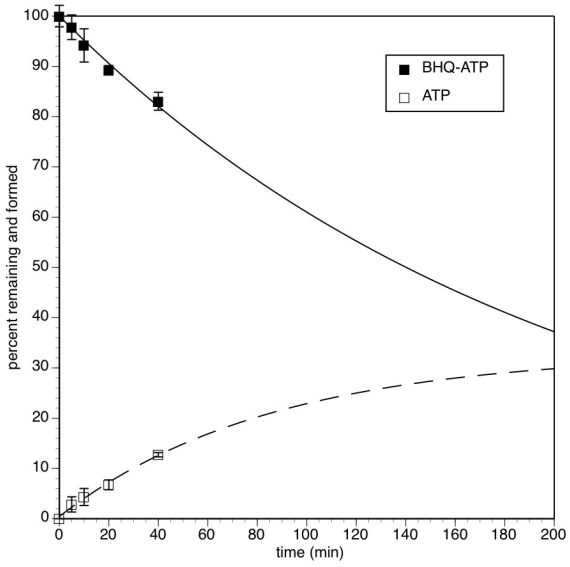


**Figure 43.** Time course of two-photon photolysis of BHQ-ATP (**161**). Also shown in the figure is the observation of ATP (**162**) generation. The percent remaining and formed were determined by HPLC and are the average of 3 runs. Lines are fits of a single exponential decay curve of rise to max. Error bars represent the standard deviation of the measurement.

***Conclusion***

BHQ-ATP can be synthesized from BHQ with all of the steps proceeding in high yield except for the last coupling reaction of BHQ-phosphate and ADP. The coupling step of the reaction route requires vigorously dry conditions and other by-products (mainly polyphosphates) are formed. The purification of BHQ-ATP can be achieved by passing the crude reaction mixture through a DEAE cellulose column, collecting fractions, and further purifying by HPLC.

Like other BHQ caged compounds, BHQ-ATP has good sensitivity to one-photon excitation (228 at 365 nm), and ATP can be recovered in 70% yield. BHQ-ATP also has a two-photon uncaging action cross-section of 0.17 GM, which is higher than the lower limit of 2PE sensitive compounds to be useful in biological studies. Upon irradiation with an IR laser, BHQ-ATP can be photolyzed efficiently and ATP concentration will be raised quickly in the focal volume of the laser. Possessing the good sensitivity to both one-photon and two-photon processes, decent recovery of ATP, and easy synthetic route, BHQ-ATP is going to be a useful tool for biological and physiological studies.

# Chapter 4

# Experimentals

## *General*

Compounds **112**,[135] **119**,[135] **125**,[136] **126**[137] and **111**[135] were prepared by known literature procedures. All other reagents and solvents were purchased from commercial sources and used without further purification with the following exceptions. Toluene and THF were dried by passing through activated alumina under nitrogen pressure (Solv-Tek, Berryville, VA). Pyridine and acetonitrile were refluxed with calcium hydride under nitrogen, and then distilled. DMF and HMPA were vacuum distilled over calcium hydride. $^{1}$H NMR, $^{13}$C NMR and $^{31}$P NMR spectra were recorded on Varian MercuryPlus 400 MHz and 500 MHz spectrometers. FTIR spectra were recorded on an Avatar 360 spectrophotometer (Thermo Nicolet). UV spectra were recorded on a Cary 300 Bio UV-Visible spectrophotometer (Varian). HPLC (analytical and preparative) was performed on a Varian ProStar HPLC system with an autosampler and diode array detector using Microsorb C-18 reverse phase columns and Dynamax C-18 reverse phase columns. Mass spectrometry was performed on a Sciex API-1 Plus quadrupole mass spectrometer with an electrospray ionization (ESI) source or a Bruker Autoflex MALDI-TOF. HRMS was performed on a Micromass QTOF-Ultima with ESI. KMOPS buffer consisted of 100 mM KCl and 10 mM MOPS titrated to pH 7.2 with KOH. Thin layer and column chromatography was performed on precoated silica gel 60 $F_{254}$ plates (Sorbent Technologies) and 230-400 mesh silica gel 60 (Sorbent Technologies), respectively. Melting points were determined on a Mel-Temp (Laboratory Devices, Inc.), and are uncorrected.

***TBDPS-HQ-benzoate* (113).**

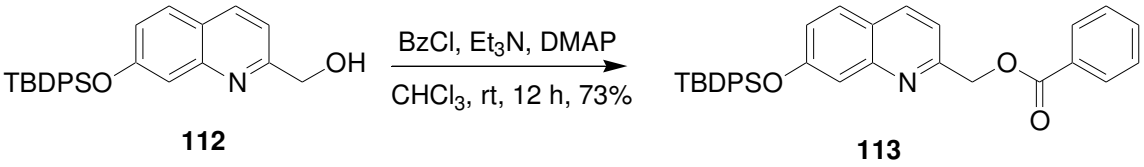


**112** **113**

Alcohol **112** (100 mg, 0.242 mmol) was dissolved in $CHCl_3$ (10 mL), and treated with $Et_3N$ (45 μL, 0.36 mmol) and DMAP (10 mg, 0.08 mmol) under nitrogen atmosphere. The mixture was stirred for 10 min, and benzoyl chloride (30 μL, 0.26 mmol) was added dropwise. The reaction mixture was stirred overnight. The mixture was diluted with $CHCl_3$, and washed with 15% citric acid, water, and brine. The organic layer was dried over anhydrous $Na_2SO_4$. The solvent was removed and the residue was purified by flash chromatography with EtOAc/hexane (1:9) to afford **113** as a white solid (92 mg, 0.18 mmol, 73% yield), mp = 85-89 °C.

**$^1$H NMR** ($CDCl_3$) δ 8.11 (2H, dd, *J* = 8.4, 1.2 Hz), 8.04 (1H, d, *J* = 8.4 Hz), 7.76 (4H, m), 7.57 (2H, d, *J* = 8.8 Hz), 7.41 (10H, m), 7.10 (1H, dd, *J* = 8.8, 2.4 Hz), 5.55 (2H, s), 1.13 (9H, s);

**$^{13}$C NMR** ($CDCl_3$) δ 166.27, 156.97, 156.52, 149.02, 136.59, 135.53, 134.83, 133.22, 132.36, 130.07, 129.85, 128.46, 127.91, 127.74, 123.06, 122.59, 117.28, 116.25, 67.91, 22.68, 14.16;

**FTIR** (neat) 3070, 2932, 2857, 2360, 1685, 1583, 1425, 1289, 1113, 933, 809, 702 $cm^{-1}$;

**HR-MS** (ESI) *m/z* calcd for $(C_{33}H_{31}NO_3Si+H)^+$ 518.2146, found 518.2130.

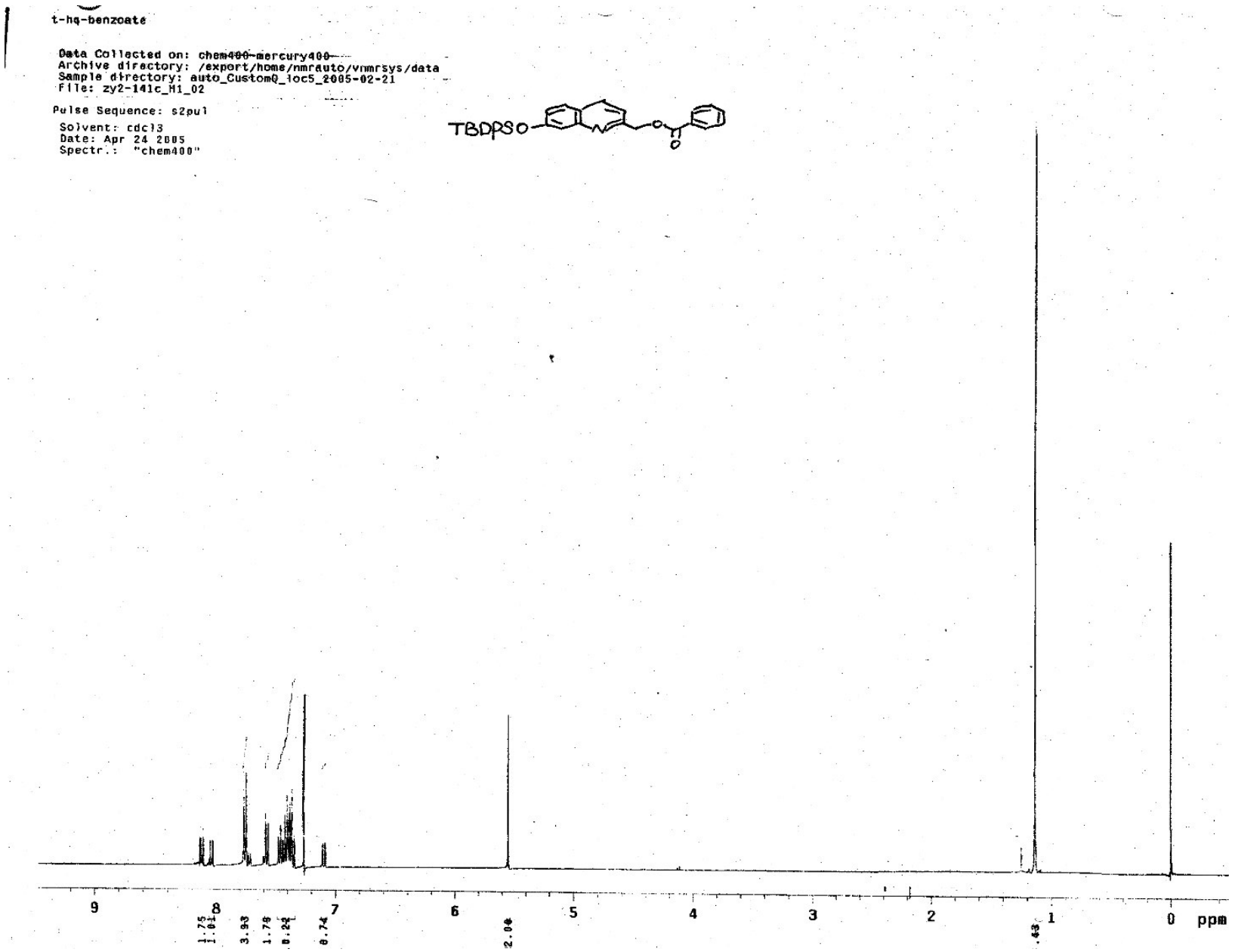
t-hq-benzoate
Data Collected on: chem400-mercury400
Archive directory: /export/home/nmrauto/vnmrsys/data
Sample directory: auto_CustomQ_ioc5_2005-02-21
File: zy2-141c_H1_02
Pulse Sequence: s2pul
Solvent: cdcl3
Date: Apr 24 2005
Spectr.: "chem400"
TBDPSO
9
8
7
6
5
4
3
2
1
0
ppm
1.75
1.01
3.93
1.78
8.21
8.74
2.00
9.43

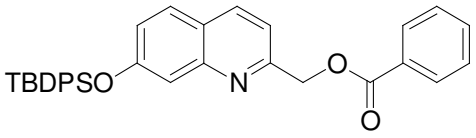
TBDPSO
N
O
O

**113**

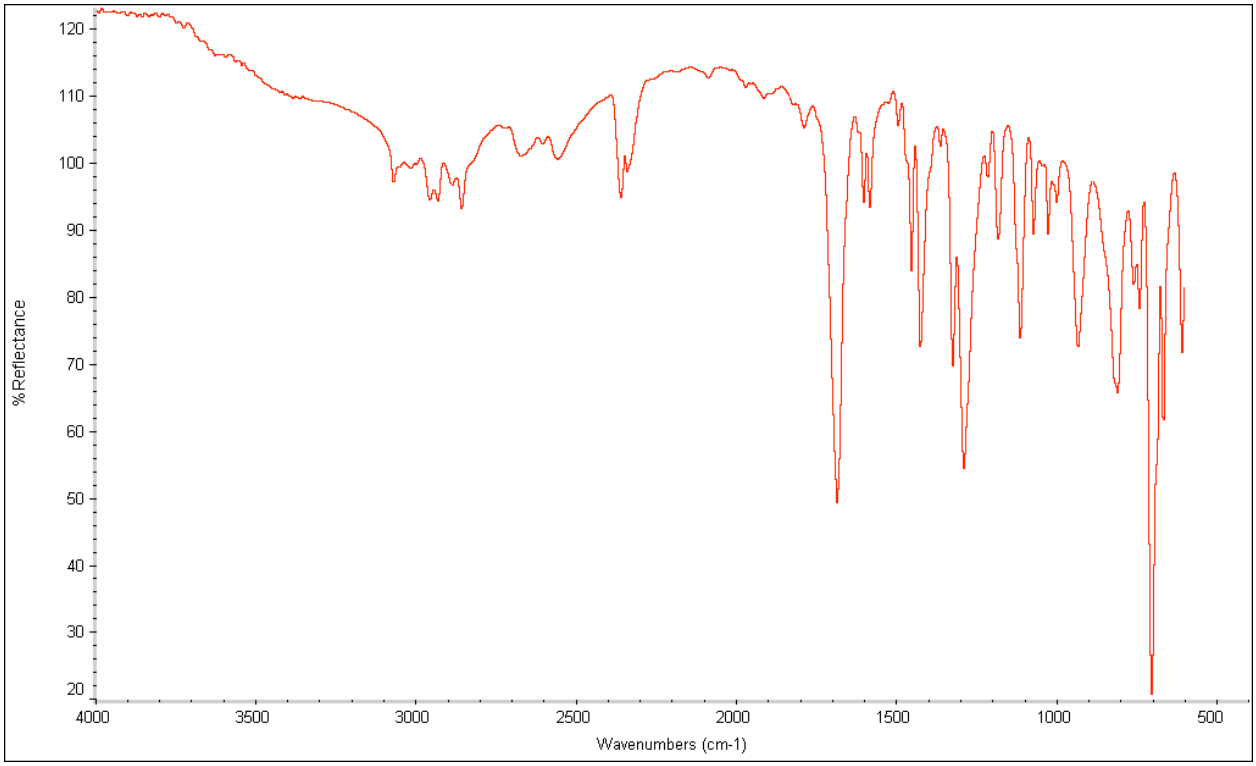
%Reflectance
120
110
100
90
80
70
60
50
40
30
20
4000
3500
3000
2500
2000
1500
1000
500
Wavenumbers (cm-1)

***TBDPS-BHQ-benzoate* (114).**

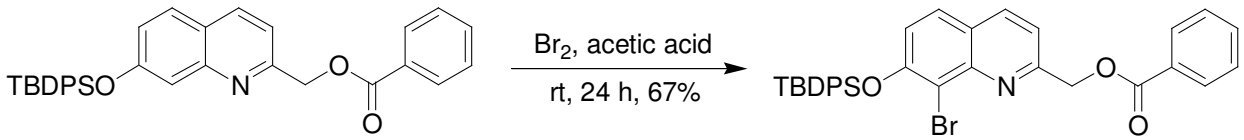


**113** **114**

Benzyl ester **113** (80.0 mg, 0.155 mmol) was dissolved in acetic acid (5 mL) in a round bottom flask and cooled in an ice bath. Bromine (140 mg, 20% in acetic acid solution, 0.175 mmol) was added dropwise with vigorous stirring. The reaction mixture was stirred for 24 h. The reaction solution was quenched with saturated aqueous $NaHCO_3$, and extracted with EtOAc. The organic layer was washed with water and brine, dried over anhydrous $Na_2SO_4$ and filtered. The solvent was evaporated and the remaining residue was purified by flash chromatography with EtOAc/hexane (1:9) to afford **114** as a white solid (62 mg, 0.10 mmol, 67% yield), mp = 80-84 °C.

**$^1$H NMR** ($CDCl_3$) δ 8.64 (1H, d, *J* = 8.8 Hz), 8.06 (2H, dd, *J* = 8.4, 1.2 Hz), 7.56 (6H, m), 7.41 (9H, m), 7.11 (1H, d, *J* = 8.8 Hz), 6.18 (2H, s), 1.14 (9H, s);

**$^{13}$C NMR** ($CDCl_3$) 166.15, 158.91, 157.64, 147.13, 136.99, 135.43, 134.88, 132.32, 131.63, 130.17, 129.58, 128.91, 127.85, 127.06, 123.94, 122.08, 118.18, 114.05, 69.17, 22.54, 14.16;

**FTIR** (neat) 3071, 2955, 2858, 1723, 1618, 1506, 1427, 1257, 1109, 862, 700 $cm^{-1}$;

**MS** (MALDI-TOF) *m/z* calcd for $(C_{33}H_{30}BrNO_3Si+H)^+$ 596.1 ($^{79}$Br) and 598.1 ($^{81}$Br), found 596.2 ($^{79}$Br) and 598.2 ($^{81}$Br).

t-bhq-benzoate
Data Collected on: chem400-mercury400
Archive directory: /export/home/nmrauto/vnmrsys/data
Sample directory: auto_CustomQ_loc1_2005-04-20
File: zy2-174a_H1_02
Pulse Sequence: s2pul
Solvent: cdcl3
Date: Apr 20 2005
Spectr.: "chem400"
ppm

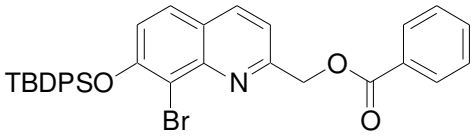
TBDPSO
N
O
Br
O

**114**

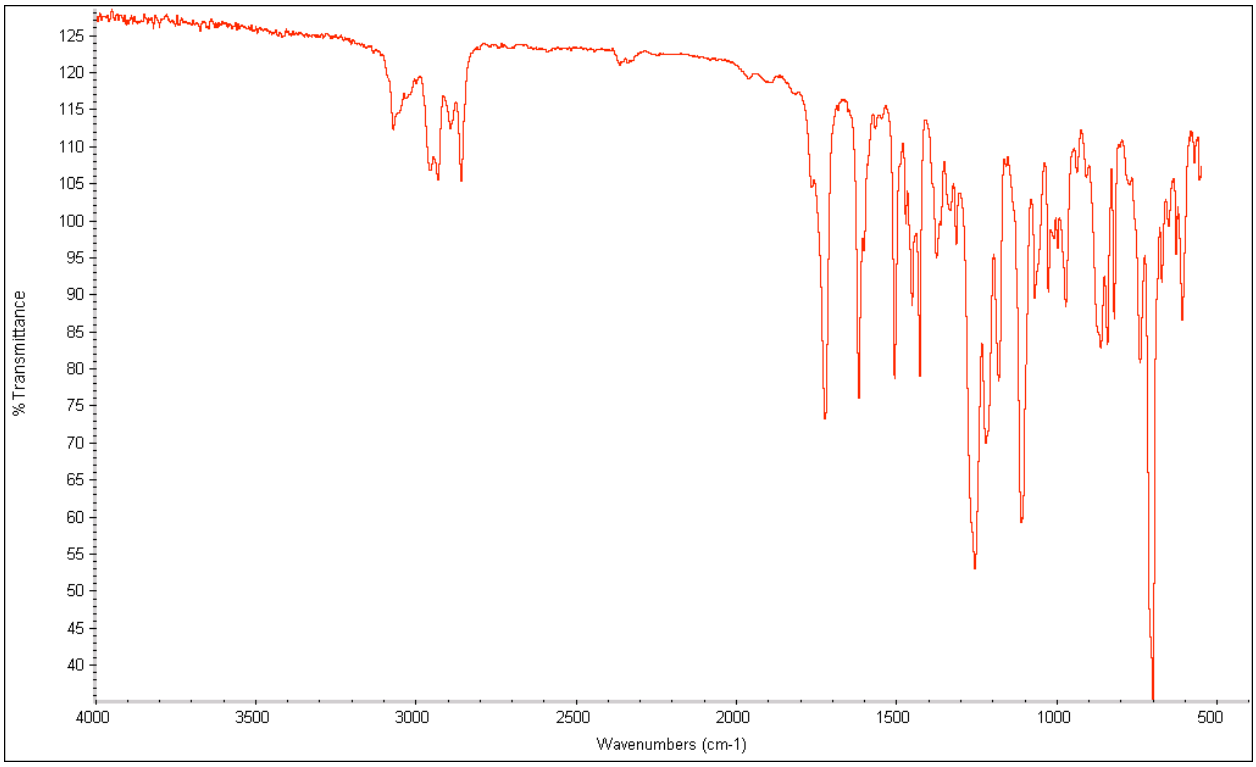
% Transmittance
125
120
115
110
105
100
95
90
85
80
75
70
65
60
55
50
45
40
4000
3500
3000
2500
2000
1500
1000
500
Wavenumbers (cm-1)

***BHQ-benzoate* (115).**

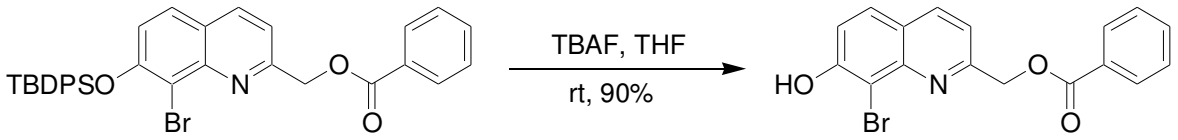


**114** **115**

Ester **114** (50 mg, 0.084 mmol) was dissolved in THF (5 mL). TBAF in THF (1 M, 90 µL, 0.09 mmol) was added dropwise. The reaction mixture was monitored by TLC. When complete, it was diluted with EtOAc, and washed with water and brine. The organic layer was dried over anhydrous $Na_2SO_4$. The solvent was evaporated and the remaining residue was purified by flash chromatography with EtOAc/hexane (3:7) to afford **115** as a pale yellow solid (27 mg, 0.075 mmol, 90% yield), mp = 180-202 °C dec.

**$^1$H NMR** ($CDCl_3$) δ 8.17 (2H, dd, *J* = 8.8, 1.6 Hz), 8.13 (1H, d, *J* = 8.8 Hz), 7.72 (1H, d, *J* = 9.2 Hz), 7.61 (1H, tt, *J* = 7.6, 1.6 Hz), 7.49 (3H, m), 7.33 (1H, d, *J* = 8.8 Hz), 5.72 (2H, s);

**$^{13}$C NMR** ($CDCl_3$) δ 166.25, 158.94, 155.80, 148.13, 137.43, 133.12, 130.19, 129.65, 128.86, 128.30, 122.19, 119.72, 116.68, 108.81, 66.96;

**FTIR** (neat) 2958, 1723, 1612, 1506, 1471, 1269, 1113, 842, 710 $cm^{-1}$;

**HR-MS** (ESI) *m/z* calcd for $(C_{17}H_{12}BrNO_3+H)^+$ 358.0073 ($^{79}$Br) and 360.0055 ($^{81}$Br), found 358.0074 ($^{79}$Br) and 360.0057 ($^{81}$Br).

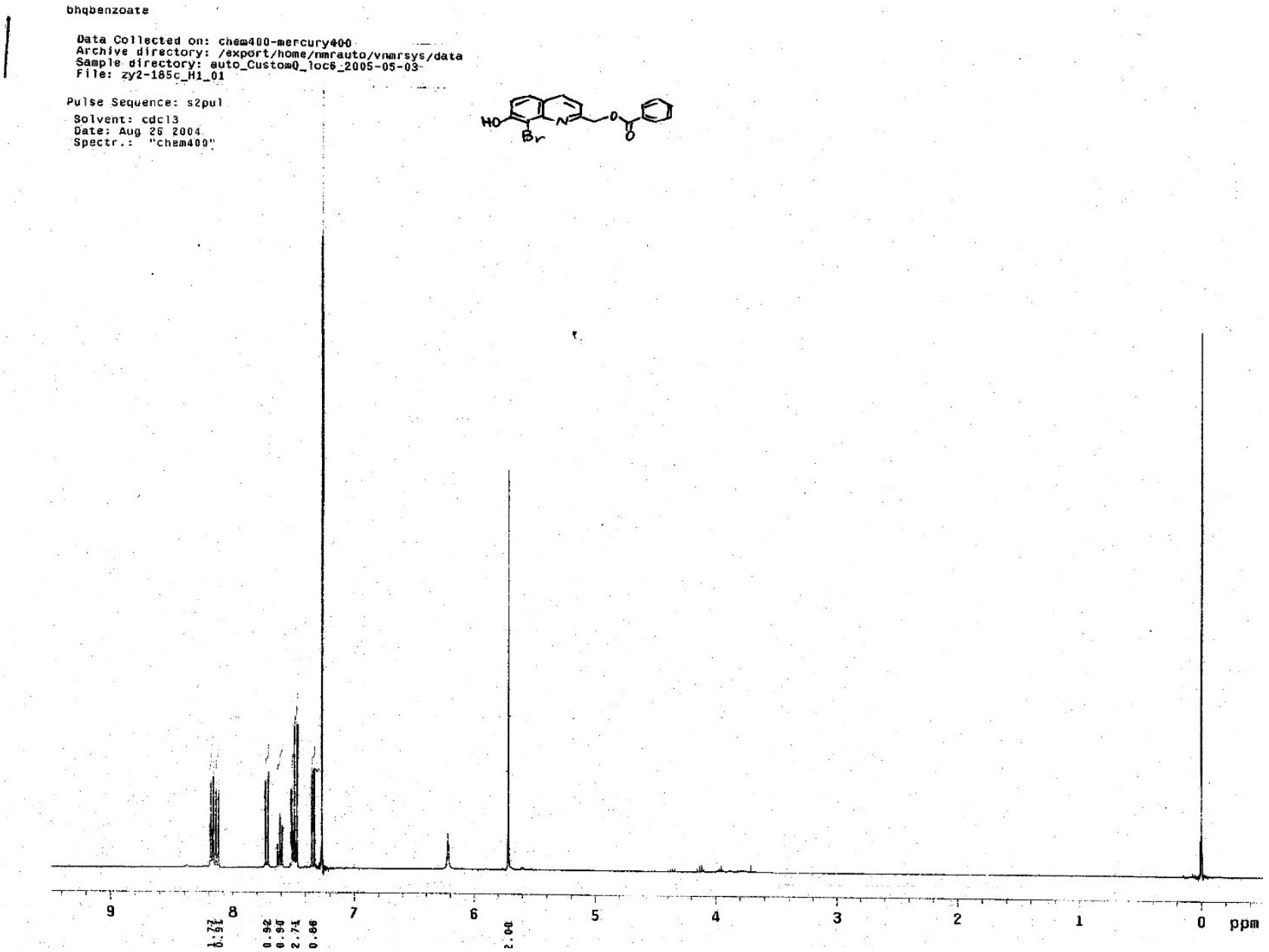
bhqbenzoate
Data Collected on: chem400-mercury400
Archive directory: /export/home/nmrauto/vnmrsys/data
Sample directory: auto_CustomQ_loc6_2005-05-03
File: zy2-185c_H1_01
Pulse Sequence: s2pul
Solvent: cdcl3
Date: Aug 26 2004
Spectr.: "chem400"
HO
Br
N
O
O
1.77
0.91
0.92
0.90
2.74
0.86
2.00
9
8
7
6
5
4
3
2
1
0
ppm

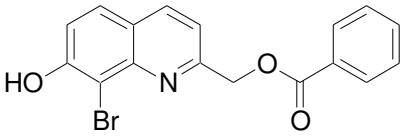
HO
N
O
Br
O

**115**

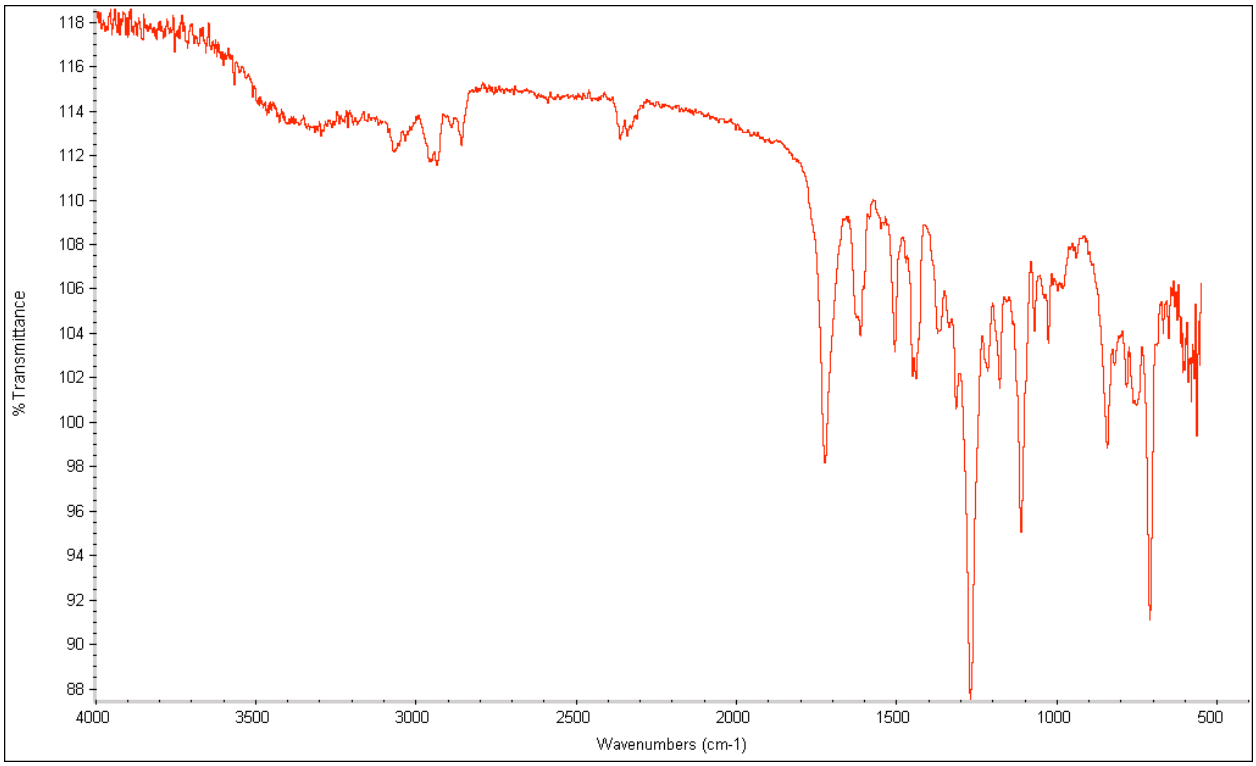
% Transmittance
118
116
114
112
110
108
106
104
102
100
98
96
94
92
90
88
4000
3500
3000
2500
2000
1500
1000
500
Wavenumbers (cm-1)

***TBDPS-HQ-piperonylate* (116).**

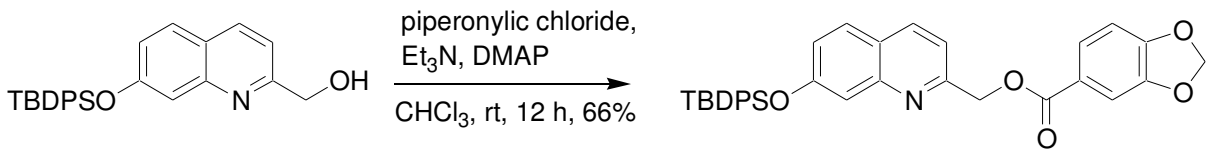


**112** **116**

Under nitrogen amosphere, alcohol **112** (100 mg, 0.242 mmol) was dissolved in $CHCl_3$ (10 mL), and treated with $Et_3N$ (45 μL, 0.36 mmol) and DMAP (10 mg, 0.08 mmol) for 10 min. Piperonylic chloride (50 mg, 0.27 mmol) was added and the resulting mixture was stirred overnight, then diluted with $CHCl_3$, and washed with 15% citric acid, water, and brine. The organic phase was dried over anhydrous $Na_2SO_4$. The solvent was removed by vacuo and the residue was purified by flash chromatography with EtOAc/hexane (1:9) to afford **116** as a white solid (90 mg, 0.16 mmol, 66% yield), mp = 90-95 °C.

**$^1$H NMR** ($CD_3OD$) δ 8.18 (1H, d, *J* = 8.0 Hz), 7.76 (4H, m), 7.71 (1H, d, *J* = 8.0 Hz), 7.66 (1H, dd, *J* = 8.4, 2.0 Hz), 7.40 (8H, m), 7.22 (1H, s), 7.21 (1H, d, *J* = 7.2 Hz), 6.87 (1H, d, *J* = 8.4 Hz), 6.03 (2H, s), 5.39 (2H, s), 1.12 (9H, s);

**$^{13}$C NMR** ($CD_3OD$) 165.48, 157.18, 156.92, 148.06, 137.39, 135.24, 131.84, 130.02, 128.88, 127.71, 125.33, 123.31, 123.23, 122.49, 117.24, 114.64, 108.85, 107.67, 102.10, 66.57, 25.50, 18.81;

**FTIR** (neat) 3072, 2932, 2858, 1719, 1619, 1506, 1442, 1257, 1113, 1076, 876, 842, 702 $cm^{-1}$;

**HR-MS** (ESI) *m/z* calcd for $(C_{34}H_{31}NO_5Si+H)^+$ 562.2044, found 562.2020.

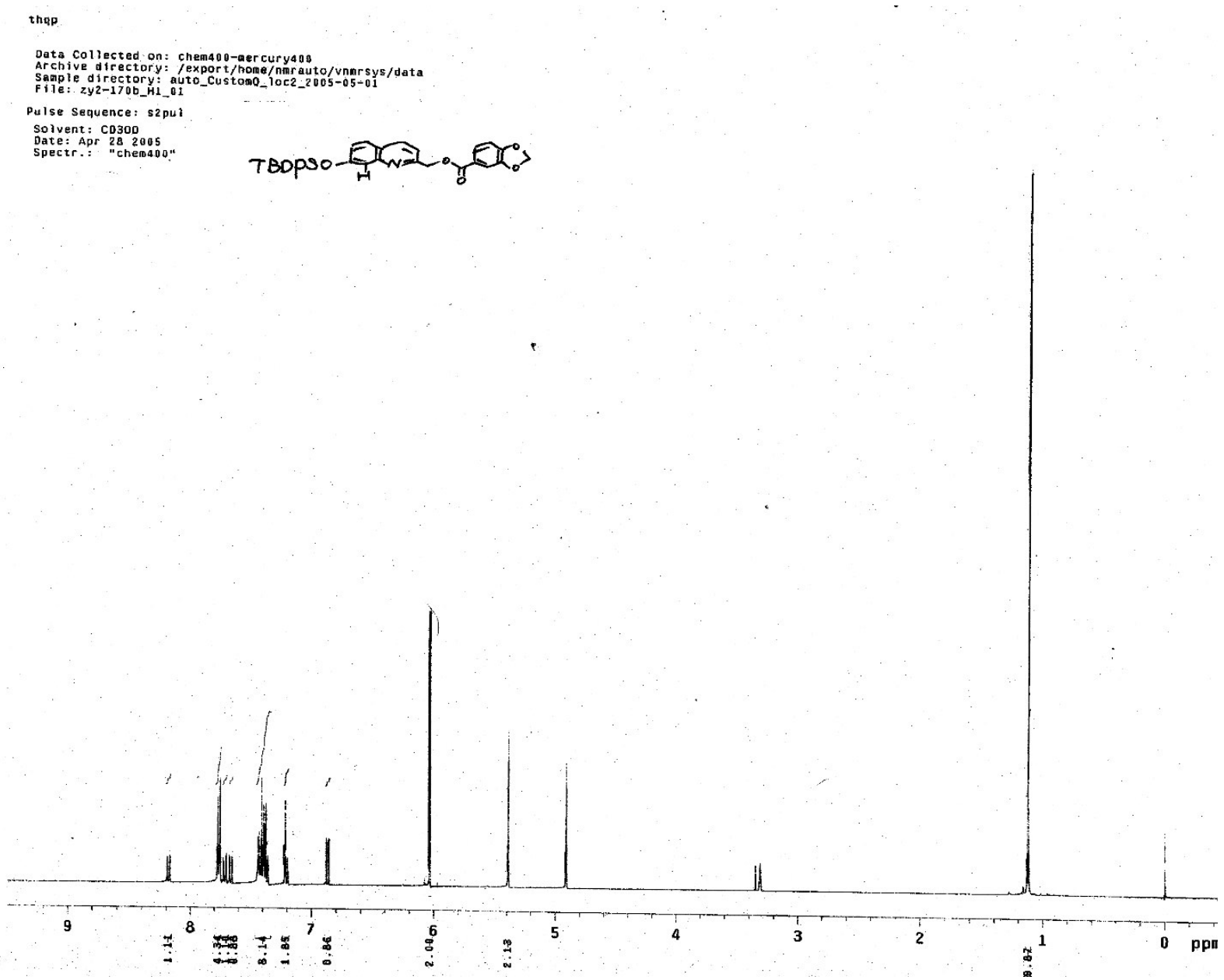
thqp
Data Collected on: chem400-mercury400
Archive directory: /export/home/nmrauto/vnmrsys/data
Sample directory: auto_CustomQ_loc2_2005-05-01
File: zy2-170b_H1_01
Pulse Sequence: s2pul
Solvent: CD3OD
Date: Apr 28 2005
Spectr.: "chem400"
TBDPSO
9
8
7
6
5
4
3
2
1
0
ppm

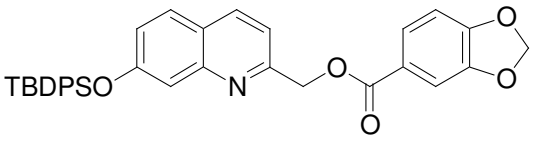
TBDPSO
N
O
O
O
O

**116**

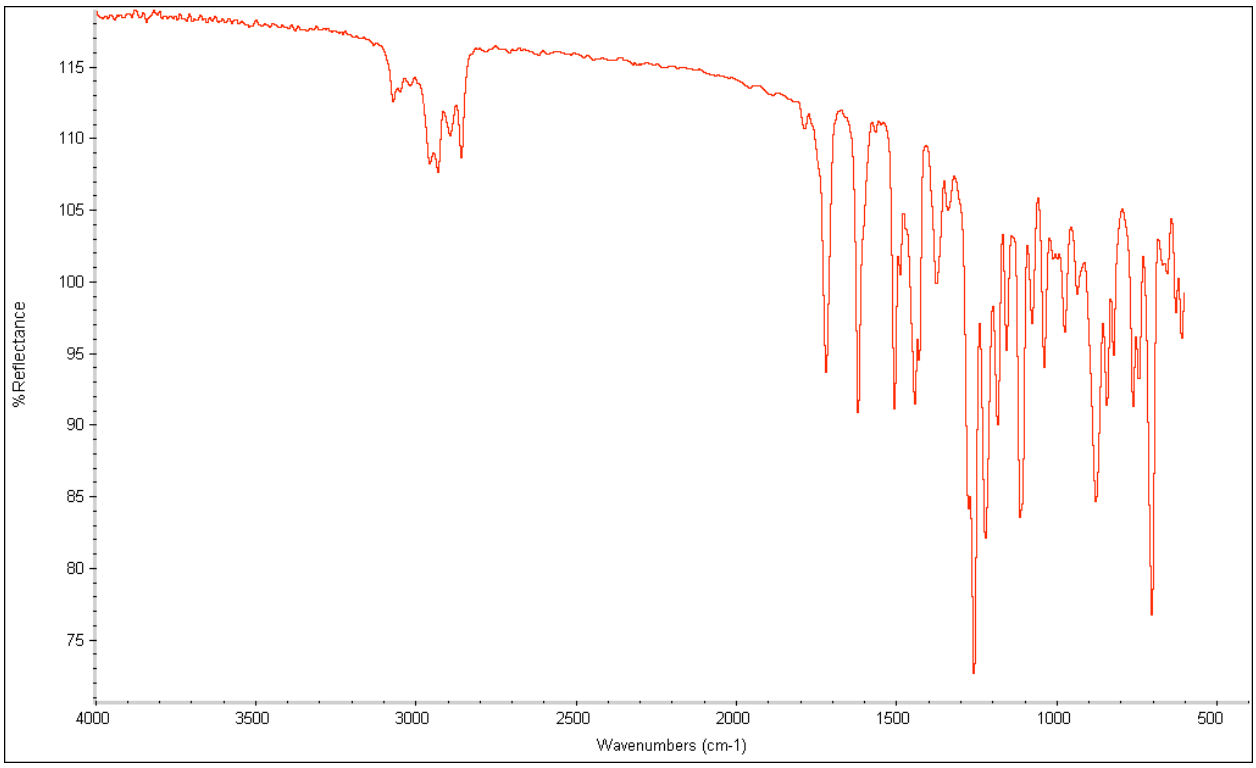
%Reflectance
115
110
105
100
95
90
85
80
75
4000
3500
3000
2500
2000
1500
1000
500
Wavenumbers (cm-1)

***HQ-piperonylate* (117).**

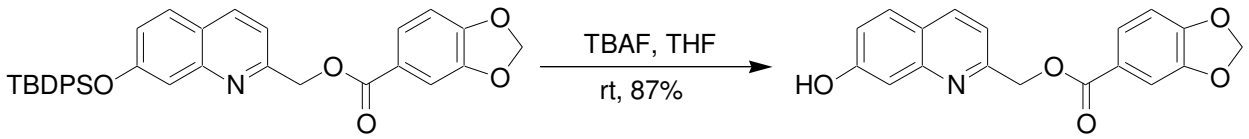


**116** **117**

Ester **116** (80.0 mg, 0.142 mmol) was dissolved in THF (5 mL), followed by addition of TBAF in THF (1 M, 150 μL, 0.15 mmol) dropwise. The reaction was monitored by TLC. When the reaction was complete, the reaction mixture was diluted with EtOAc and washed with water and brine. The organic layer was dried over anhydrous $Na_2SO_4$, and the solvent was evaporated. The residue was purified by flash chromatography with EtOAc/hexane (4:6) to afford **117** as a white solid (41.0 mg, 0.124 mmol, 87% yield), mp = 130-185 °C dec.

**$^1$H NMR** ($CD_3OD$) δ 8.25 (1H, d, *J* = 8.4 Hz), 7.79 (1H, d, *J* = 8.8 Hz), 7.73 (1H, dd, *J* = 8.0, 1.6 Hz), 7.51 (1H, d, *J* = 1.6 Hz), 7.43 (1H, d, *J* = 8.0 Hz), 7.29 (1H, d, *J* = 2.0 Hz), 7.18 (1H, dd, *J* = 8.8, 2.4 Hz), 6.92 (1H, d, *J* = 8.4 Hz), 6.06 (2H, s), 5.51 (2H, s);

**$^{13}$C NMR** ($CD_3OD$) 164.58, 157.67, 155.03, 154.49, 148.29, 143.52, 137.59, 128.75, 125.67, 123.77, 121.83, 120.49, 118.07, 117.68, 110.05, 109.40, 101.87, 66.41;

**FTIR** (neat) 2905, 2361, 1716, 1620, 1442, 1257, 1156, 1104, 1036, 842, 759 $cm^{-1}$;

**HR-MS** (ESI) *m/z* calcd for $(C_{18}H_{13}NO_5+H)^+$ 324.0866, found 324.0868.

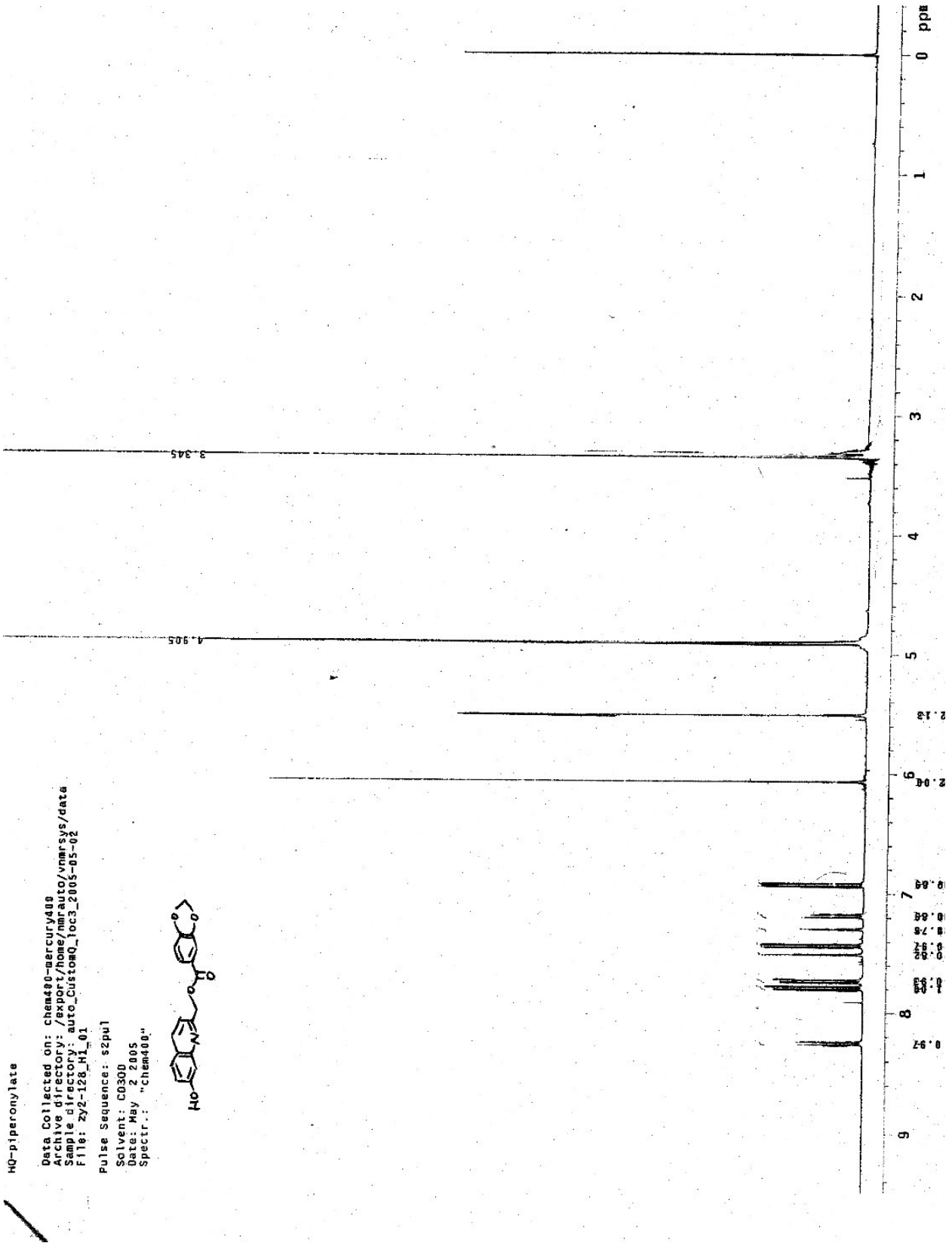
HQ-piperonylate
Data Collected on: chem400-mercury400
Archive directory: /export/home/nmrauto/vnmrsys/data
Sample directory: auto_CustomQ_toc3_2005-05-02
File: zy2-126_H1_01
Pulse Sequence: s2pul
Solvent: CD3OD
Date: May 2 2005
Spectr.: "chem400"
3.345
4.905
ppm

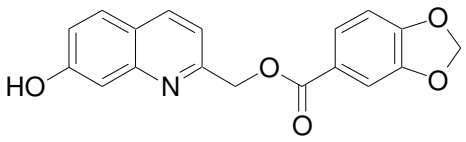
HO
N
O
O
O
O

**117**

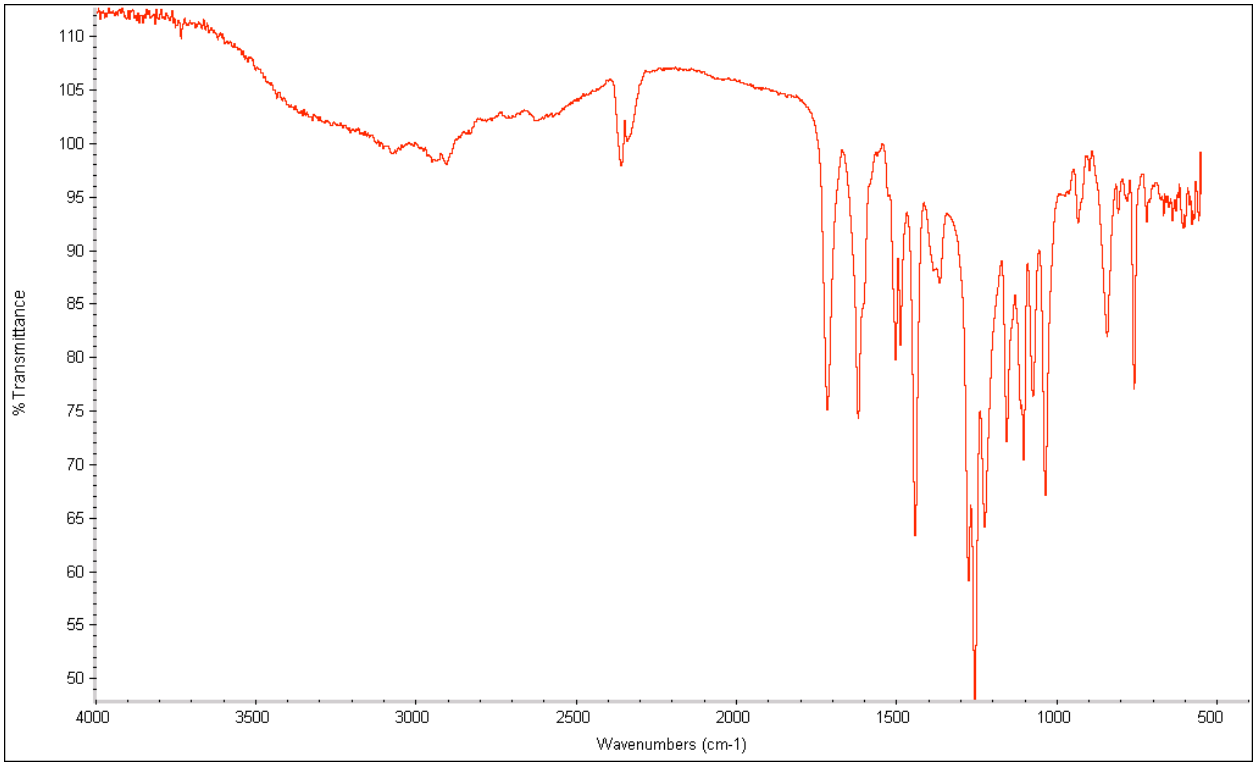
% Transmittance
110
105
100
95
90
85
80
75
70
65
60
55
50
4000
3500
3000
2500
2000
1500
1000
500
Wavenumbers (cm-1)

***BHQ-piperonylate* (118).**

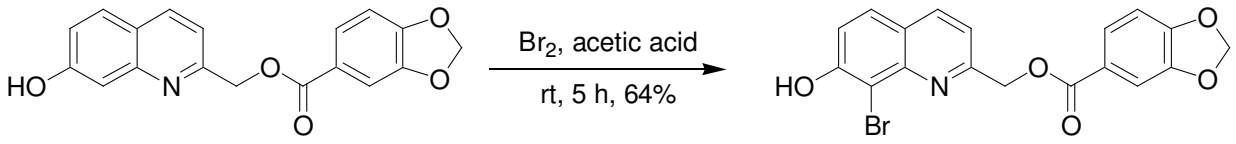


**117** **118**

Ester **117** (30 mg, 0.093 mmol) was dissolved in acetic acid (2 mL) and cooled in an ice bath. Bromine (100 mg, 20% in acetic acid, 0.125 mmol) was added dropwise with vigorous stirring. The mixture was stirred for 5 h. The reaction was quenched with saturated aqueous $NaHCO_3$, extracted with EtOAc, and washed with water and brine. The organic layer was dried over anhydrous $Na_2SO_4$ and the solvent was evaporated. The residue was purified by flash chromatography with EtOAc/hexane (4:6) to afford **118** as a white solid (24 mg, 0.06 mmol, 64% yield), mp = 186-194 °C dec.

**$^1$H NMR** ($CDCl_3$) δ 8.15 (1H, d, *J* = 8.4 Hz), 7.77 (1H, dd, *J* = 8.4, 1.6 Hz), 7.72 (1H, d, *J* = 8.8 Hz), 7.59 (1H, d, *J* = 2.0 Hz), 7.46 (1H, d, *J* = 8.4 Hz), 7.35 (1H, d, *J* = 8.4 Hz), 6.87 (1H, d, *J* = 8.4 Hz), 6.07 (2H, s), 5.69 (2H, s);

**$^{13}$C NMR** ($CDCl_3$) 165.67, 158.58, 158.03, 157.29, 148.49, 141.59, 137.52, 128.25, 125.77, 123.67, 122.43, 120.89, 117.87, 117.40, 109.68, 108.19, 101.90, 67.52;

**FTIR** (neat) 2909, 2359, 1716, 1622, 1504, 1444, 1259, 1229, 1157, 1037, 843, 760 $cm^{-1}$;

**HR-MS** (ESI) *m/z* calcd for $(C_{18}H_{12}BrNO_5+H)^+$ 401.9972 ($^{79}$Br) and 403.9954 ($^{81}$Br), found 401.9979 ($^{79}$Br) and 403.9960 ($^{81}$Br).

bhq-p
Data Collected on: chem400-mercury400
Archive directory: /export/home/nmrauto/vnmrsys/data
Sample directory: auto_Custom0_ioc6_2005-01-22
File: zy2-112c_H101
Pulse Sequence: s2pul
Solvent: cdcl3
Date: Jan 22 2005
Spectr... "chem400"
ppm

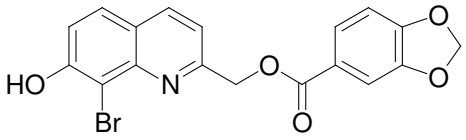
HO
N
Br
O
O
O
O

**118**

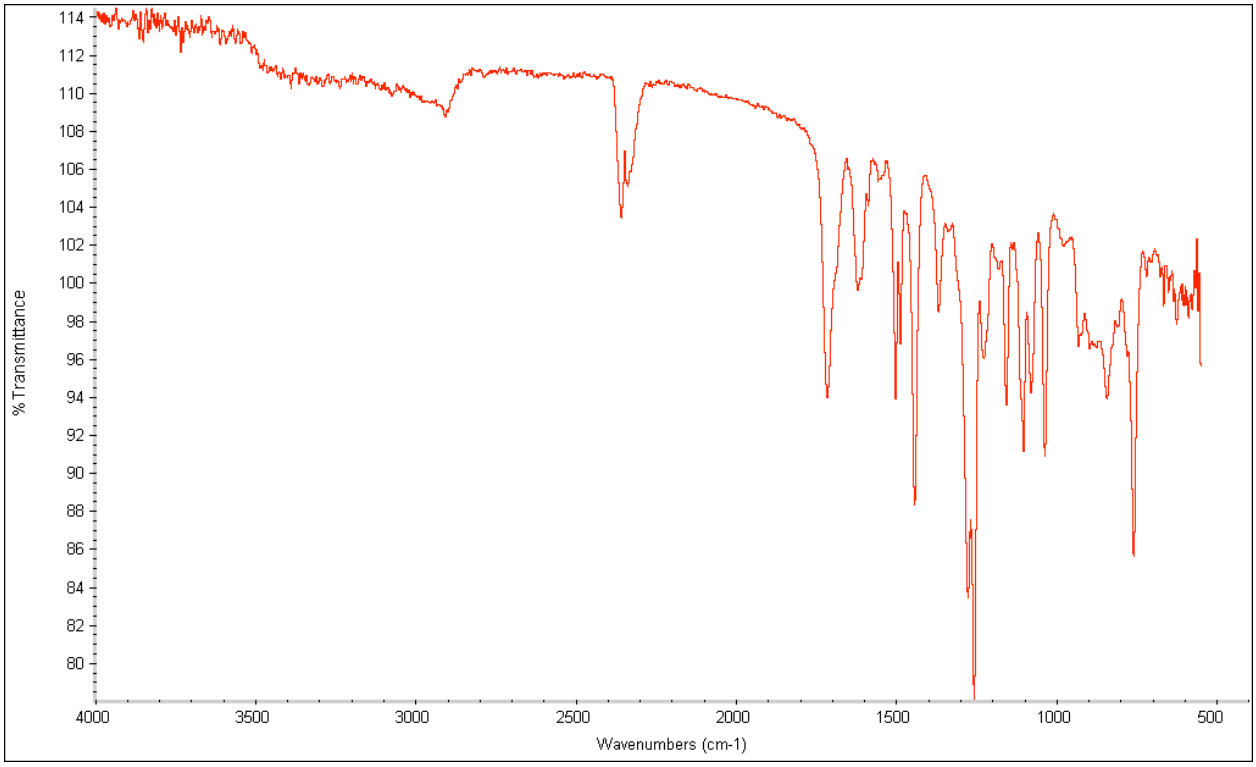
% Transmittance
114
112
110
108
106
104
102
100
98
96
94
92
90
88
86
84
82
80
4000
3500
3000
2500
2000
1500
1000
500
Wavenumbers (cm-1)

***8-bromo-7-hydroxyquinaldine* (120).**

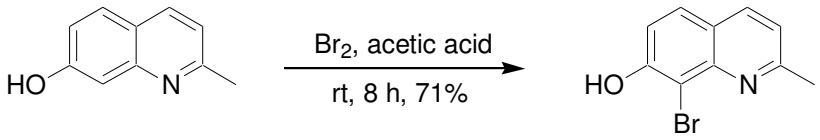


**119** **120**

7-hydroxyquinaldine (**119**, 1.00 g, 6.32 mmol) was dissolved in glacial acetic acid (15 mL) and cooled in an ice bath. Bromine (5.50 g, 20% acetic acid solution, 6.88 mmol) was added dropwise with vigorous stirring. The formation of a precipitate was observed. The reaction was stirred for 4 h, and then diluted with $CHCl_3$, neutralized with NaOH solution; and washed successively with saturated aqueous $NaHCO_3$, water, and brine. The organic layer was dried over anhydrous $Na_2SO_4$, filtered, and the solvent evaporated, leaving a brown oil, which was purified by flash chromatography with EtOAc/hexane (3:7) elution. Bromide **120** was acquired as a pale yellow solid (1.07 g, 4.49 mmol, 71% yield), mp = 175-180 °C dec.

**$^1$H NMR** ($CDCl_3$) δ 7.97 (1H, d, *J* = 8.4 Hz), 7.66 (1H, d, *J* = 8.4 Hz), 7.27 (1H, d, *J* = 9.2 Hz), 7.21 (1H, d, *J* = 8.0 Hz), 2.79 (3H, s);

**$^{13}$C NMR** ($CDCl_3$) 160.77, 153.89, 145.52, 136.39, 128.17, 122.57, 120.44, 116.79, 107.65, 25.69;

**FTIR** (neat) 3059, 2360, 1618, 1561, 1503, 1429, 1334, 1262, 984, 836 $cm^{-1}$;

**HR-MS** (ESI) *m/z* calcd for $(C_{10}H_8BrNO+H)^+$ 237.9862 ($^{79}$Br) and 239.9842 ($^{81}$Br), found 237.9856 ($^{79}$Br) and 239.9833 ($^{81}$Br).

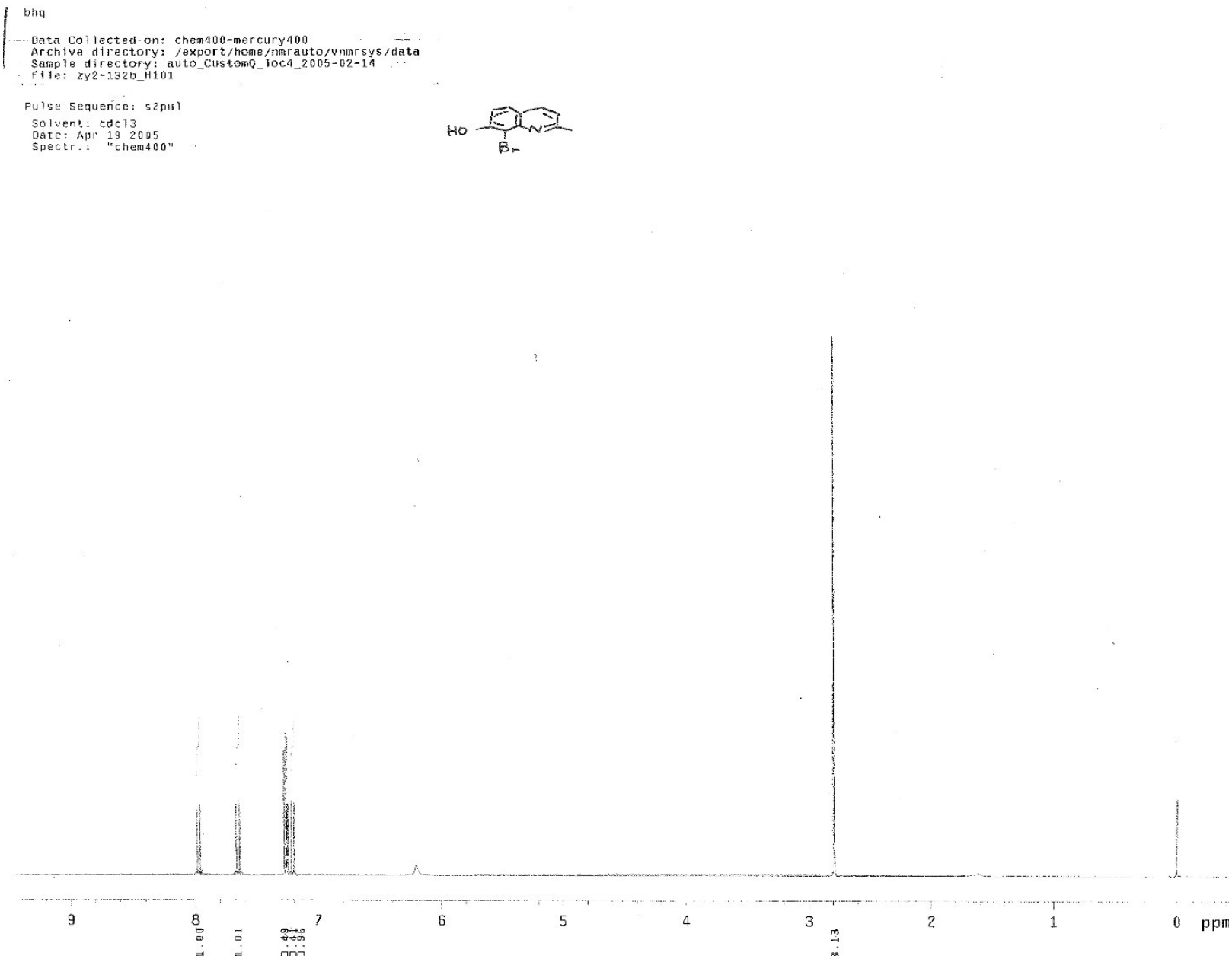
bhq
Data Collected-on: chem400-mercury400
Archive directory: /export/home/nmrauto/vnmrsys/data
Sample directory: auto_CustomQ_loc4_2005-02-14
File: zy2-132b_H101
Pulse Sequence: s2pul
Solvent: cdcl3
Date: Apr 19 2005
Spectr.: "chem400"
HO
Br
9
8
7
6
5
4
3
2
1
0
ppm
1.00
1.01
2.49
3.61
3.96
8.13

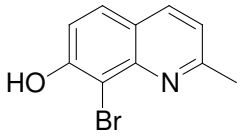
HO
N
Br

**120**

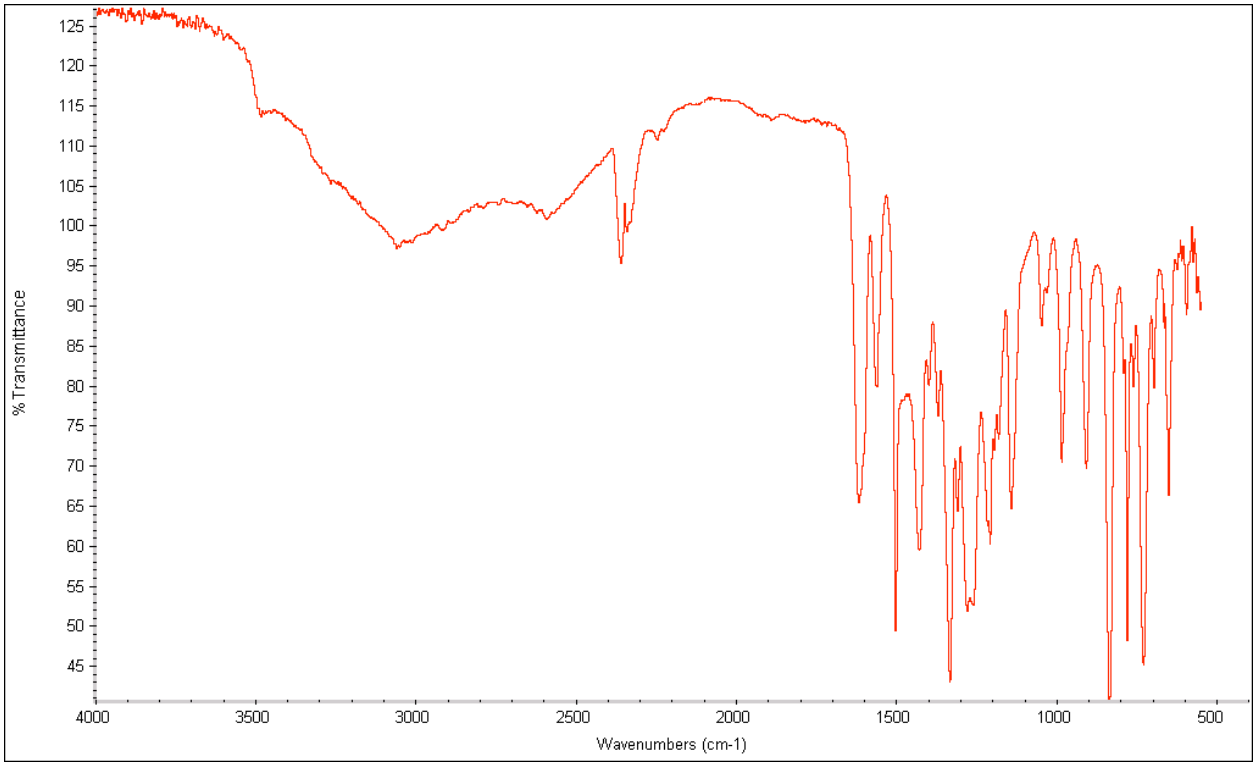
% Transmittance
125
120
115
110
105
100
95
90
85
80
75
70
65
60
55
50
45
4000
3500
3000
2500
2000
1500
1000
500
Wavenumbers (cm-1)

***7-acetyl-8-bromoquinaldine* (121).**

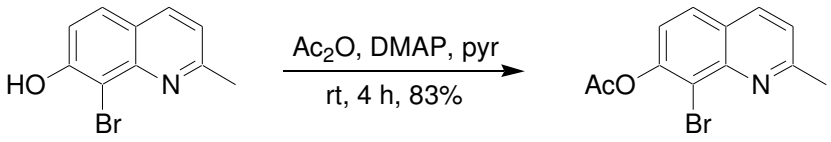


**120** **121**

Under a nitrogen atmosphere, 8-bromo-7-hydroxyquinaldine (**120**, 1.0 g, 4.2 mmol) was dissolved in pyridine (2 mL) and $CHCl_3$ (18 mL). DMAP (50 mg, 0.41 mmol) was added to the reaction, followed by slow addition of acetic anhydride (0.600 mL, 6.23 mmol). The reaction mixture was stirred for 4 h and then diluted with $CHCl_3$; successively washed with 15% citric acid, water, and brine; and dried over anhydrous $Na_2SO_4$. Filtration and evaporation of the solvent followed by purification by flash chromatography with EtOAc/hexane (2:8) provided **121** as a white solid (980 mg, 3.50 mmol, 83% yield), mp = 144-146 °C.

**$^1$H NMR** ($CDCl_3$) δ 8.05 (1H, d, *J* = 8.4 Hz), 7.76 (1H, d, *J* = 8.8 Hz), 7.34 (1H, d, *J* = 8.0 Hz), 7.29 (1H, d, *J* = 8.8 Hz), 2.83 (3H, s), 2.45 (3H, s);

**$^{13}$C NMR** ($CDCl_3$) 168.56, 161.06, 149.49, 145.78, 136.41, 127.73, 125.63, 122.61, 121.85, 117.12, 25.77, 20.97;

**FTIR** (neat) 2932, 1772, 1701, 1612, 1369, 1184, 1009, 841, 722 $cm^{-1}$;

**HR-MS** (ESI) *m/z* calcd for $(C_{12}H_{10}BrNO_2+H)^+$ 279.9968 ($^{79}$Br) and 281.9948 ($^{81}$Br), found 279.9975 ($^{79}$Br) and 281.9953 ($^{81}$Br).

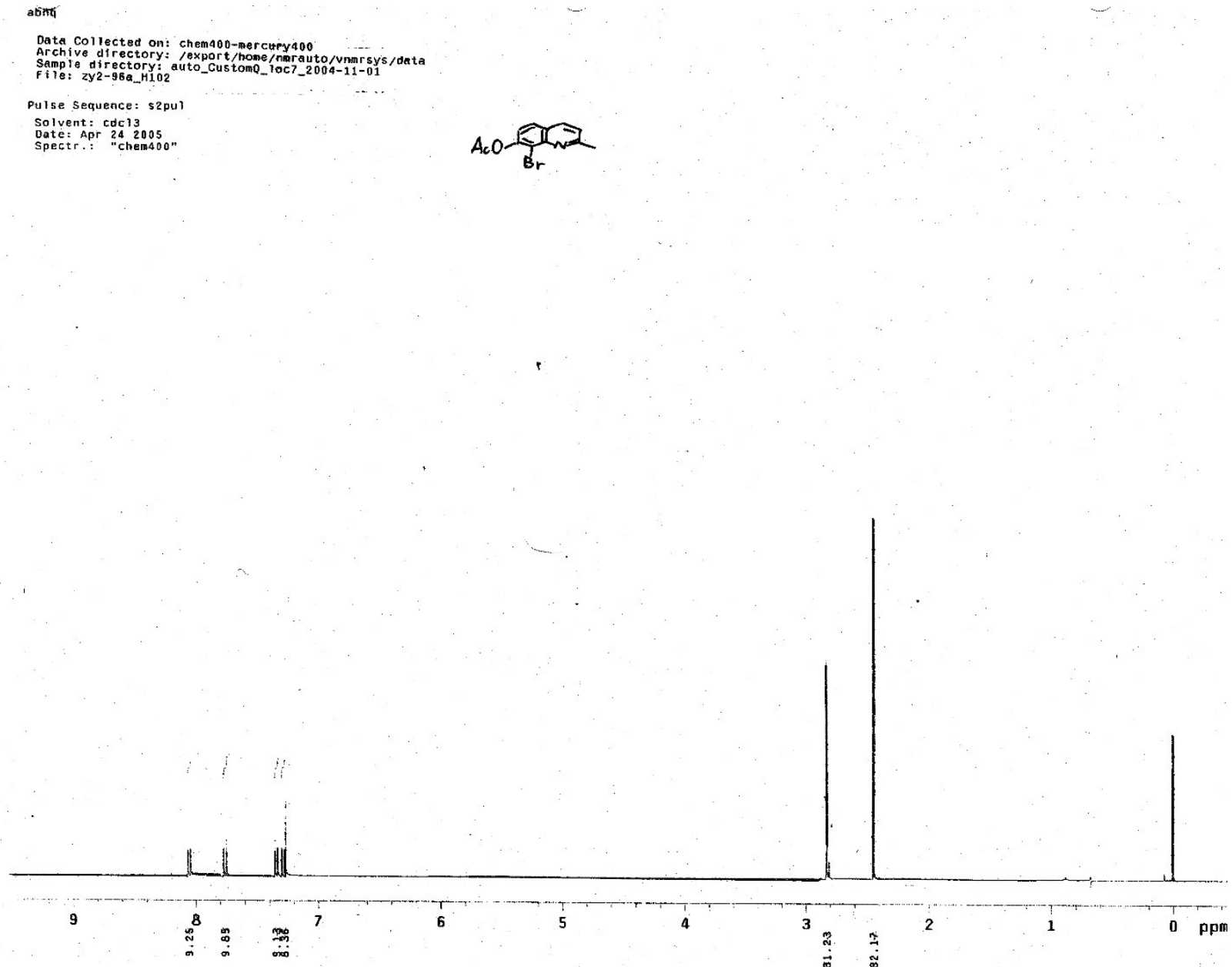
abnq
Data Collected on: chem400-mercury400
Archive directory: /export/home/nmrauto/vnmrsys/data
Sample directory: auto_CustomQ_loc7_2004-11-01
File: zy2-96a_H102
Pulse Sequence: s2pul
Solvent: cdcl3
Date: Apr 24 2005
Spectr.: "chem400"
AcO
Br
9.25
9.85
8.13
8.38
31.23
32.17
9
8
7
6
5
4
3
2
1
0
ppm

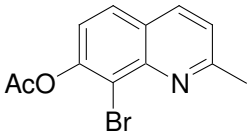
AcO
N
Br

**121**

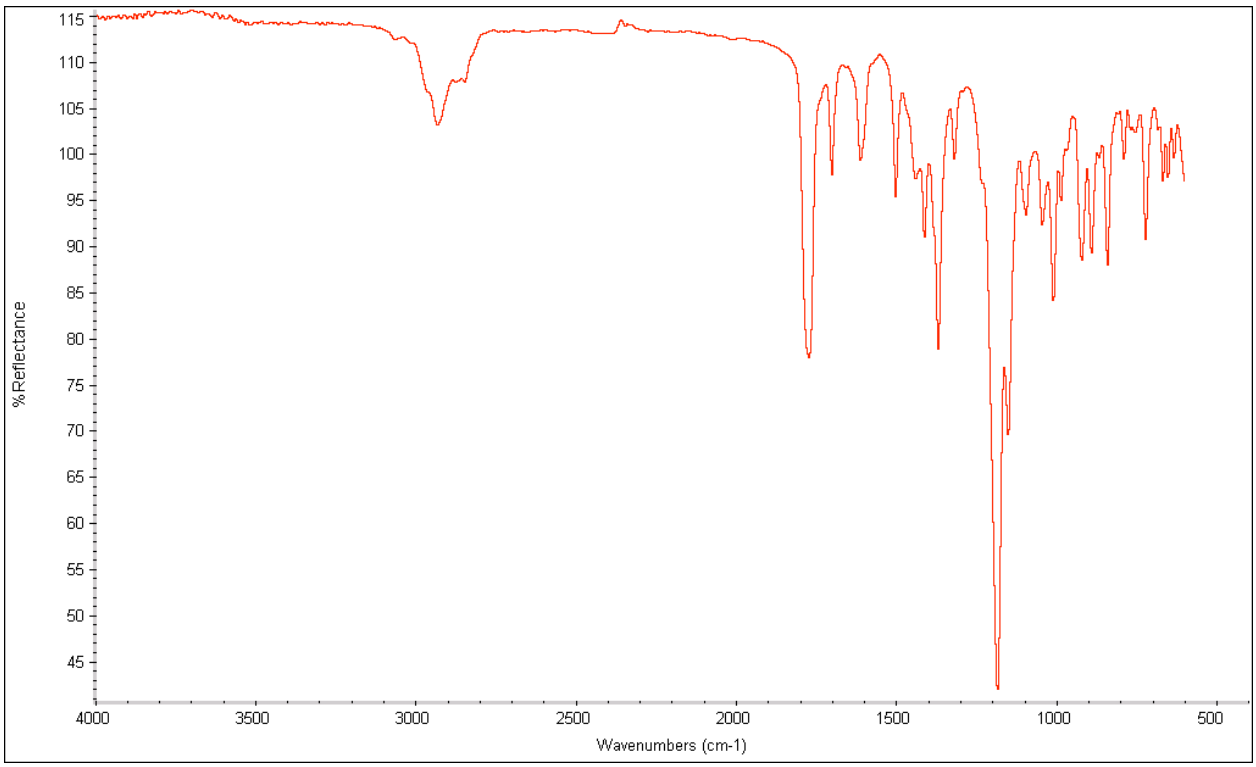
%Reflectance
115
110
105
100
95
90
85
80
75
70
65
60
55
50
45
4000
3500
3000
2500
2000
1500
1000
500
Wavenumbers (cm-1)

***7-acetyl-8-bromoquinolin-2-yl formaldehyde* (122).**

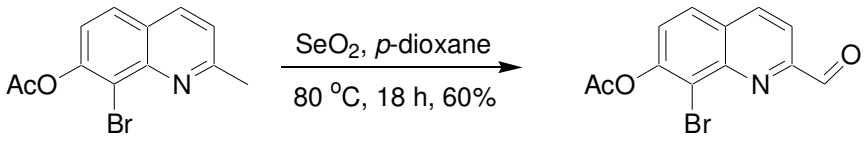


**121** **122**

A mixture of $SeO_2$ (375 mg, 3.38 mmol) and 1,4-dioxane (10 mL) was heated to 80 °C. 7-Acetyl-8-bromoquinaldine (**121**, 900 mg, 3.21 mmol) in 1,4-dioxane (5 mL) was added to the mixture. After heating at 80 °C for 18 h, the reaction was cooled and vacuum filtered. The filtrate was collected and concentrated, to afford a yellow solid. Purification by flash chromatography with EtOAc/hexane (3:7) gave **122** as a white solid (561 mg, 1.91 mmol, 60% yield), mp =190-196 °C dec.

**$^{1}$H NMR** ($CDCl_3$) δ 10.31 (1H, s), 8.36 (1H, d, *J* = 8.0 Hz), 8.09 (1H, d, *J* = 8.0 Hz), 7.91 (1H, d, *J* = 8.4 Hz), 7.50 (1H, d, *J* = 9.2 Hz), 2.48 (3H, s);

**$^{13}$C NMR** ($CDCl_3$) 193.34, 168.33, 153.39, 150.50, 146.01, 138.03, 129.28, 127.93, 125.51, 118.87, 117.85, 20.98;

**FTIR** (neat) 3054, 2848, 2360, 1751, 1708, 1369, 1194, 1157, 909, 851, 752 $cm^{-1}$;

**HR-MS** (ESI) *m/z* calcd for $(C_{12}H_8BrNO_3+Na)^+$ 315.9580 ($^{79}$Br) and 317.9561 ($^{81}$Br), found 315.9587 ($^{79}$Br) and 317.9559 ($^{81}$Br).

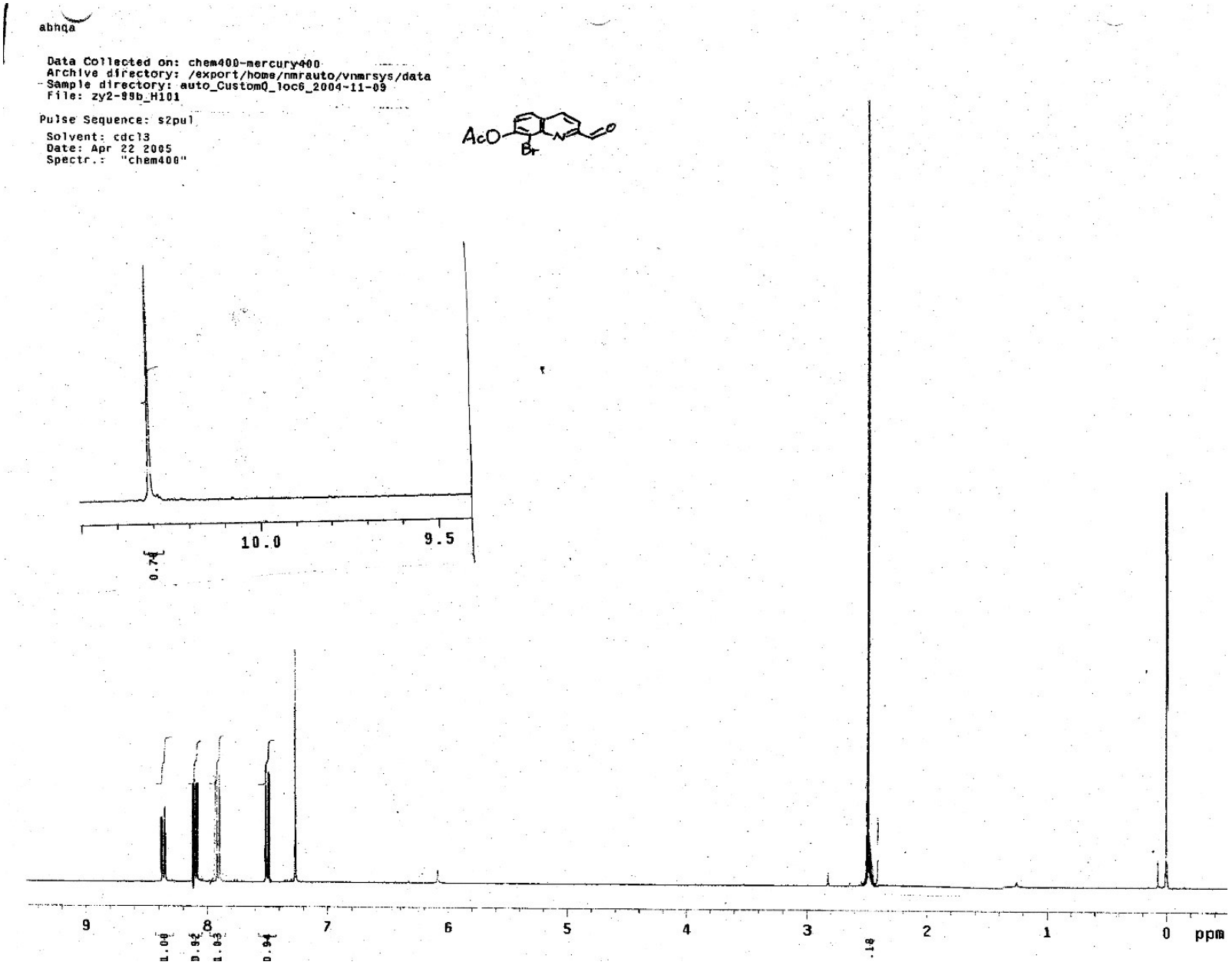
abhqa
Data Collected on: chem400-mercury400
Archive directory: /export/home/nmrauto/vnmrsys/data
Sample directory: auto_Custom0_loc6_2004-11-09
File: zy2-99b_H101
Pulse Sequence: s2pul
Solvent: cdcl3
Date: Apr 22 2005
Spectr.: "chem400"
AcO
Br
10.0
9.5
0.74
1.00
0.96
1.03
0.94
.18
9
8
7
6
5
4
3
2
1
0
ppm

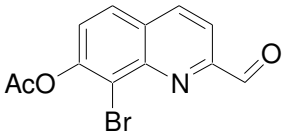
AcO
N
O
Br

**122**

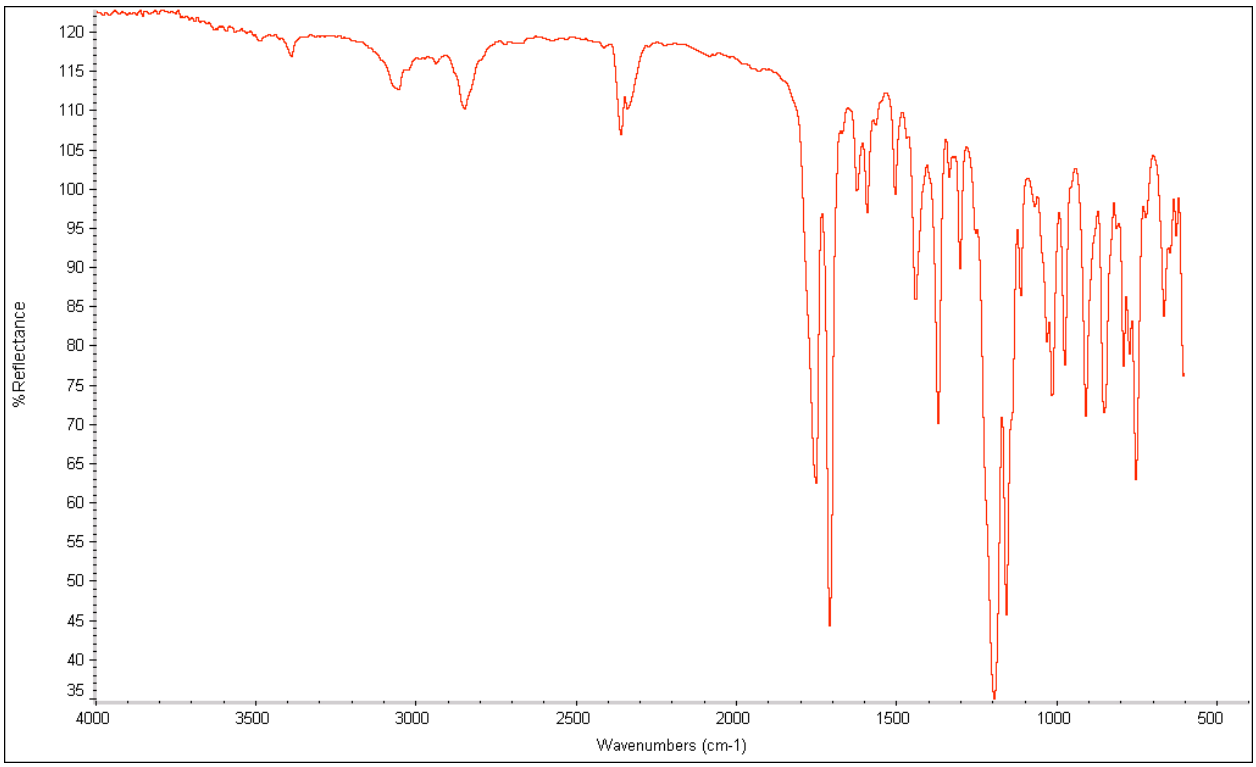
%Reflectance
120
115
110
105
100
95
90
85
80
75
70
65
60
55
50
45
40
35
4000
3500
3000
2500
2000
1500
1000
500
Wavenumbers (cm-1)

***7-acetyl-8-bromo-2-formylquinolinyltosylhydrazone* (123).**

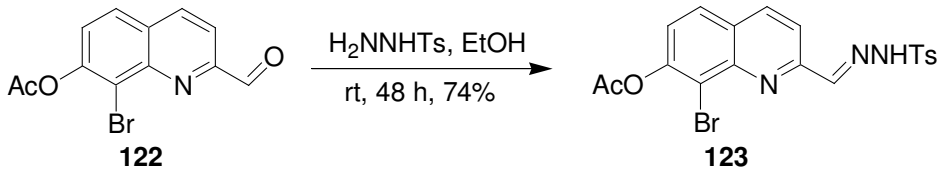


**122** **123**

*p*-Toluenesulfonylhydrazide (507 mg, 2.72 mmol) was added to a stirred solution of aldehyde **122** (400 mg, 1.36 mmol) in ethanol (5 mL). After 2 days, the resulting precipitate was collected by vacuum filtration, washed with a minimum amount of ethanol, and dried under vacuum to yield **123** as a white solid (466 mg, 1.01 mmol, 74% yield), mp = 180-190 °C dec.

**$^{1}$H NMR** (DMSO-$d_6$) δ 8.76 (1H, d, $J$ = 8.8 Hz), 8.19 (1H, d, $J$ = 8.8 Hz), 7.89 (1H, d, $J$ = 8.4 Hz), 7.83 (1H, s), 7.81 (2H, d, $J$ = 8.4 Hz), 7.74 (1H, d, $J$ = 8.4 Hz), 7.42 (2H, d, $J$ = 8.4 Hz), 2.47 (3H, s), 2.36 (3H, s);

**$^{13}$C NMR** (DMSO-$d_6$) 168.74, 152.80, 150.92, 144.52, 143.55, 140.08, 137.23, 136.51, 130.53, 129.22, 127.63, 127.09, 125.51, 123.74, 115.88, 21.50, 21.16;

**FTIR** (neat) 3178, 2360, 2339, 1764, 1599, 1502, 1434, 1356, 1162, 1079, 938, 895, 845 cm$^{-1}$;

**HR-MS** (ESI) *m/z* calcd for $(C_{19}H_{16}BrN_3O_4S+Na)^+$ 483.9937 ($^{79}$Br) and 485.9918 ($^{81}$Br), found 483.9936 ($^{79}$Br) and 485.9886 ($^{81}$Br).

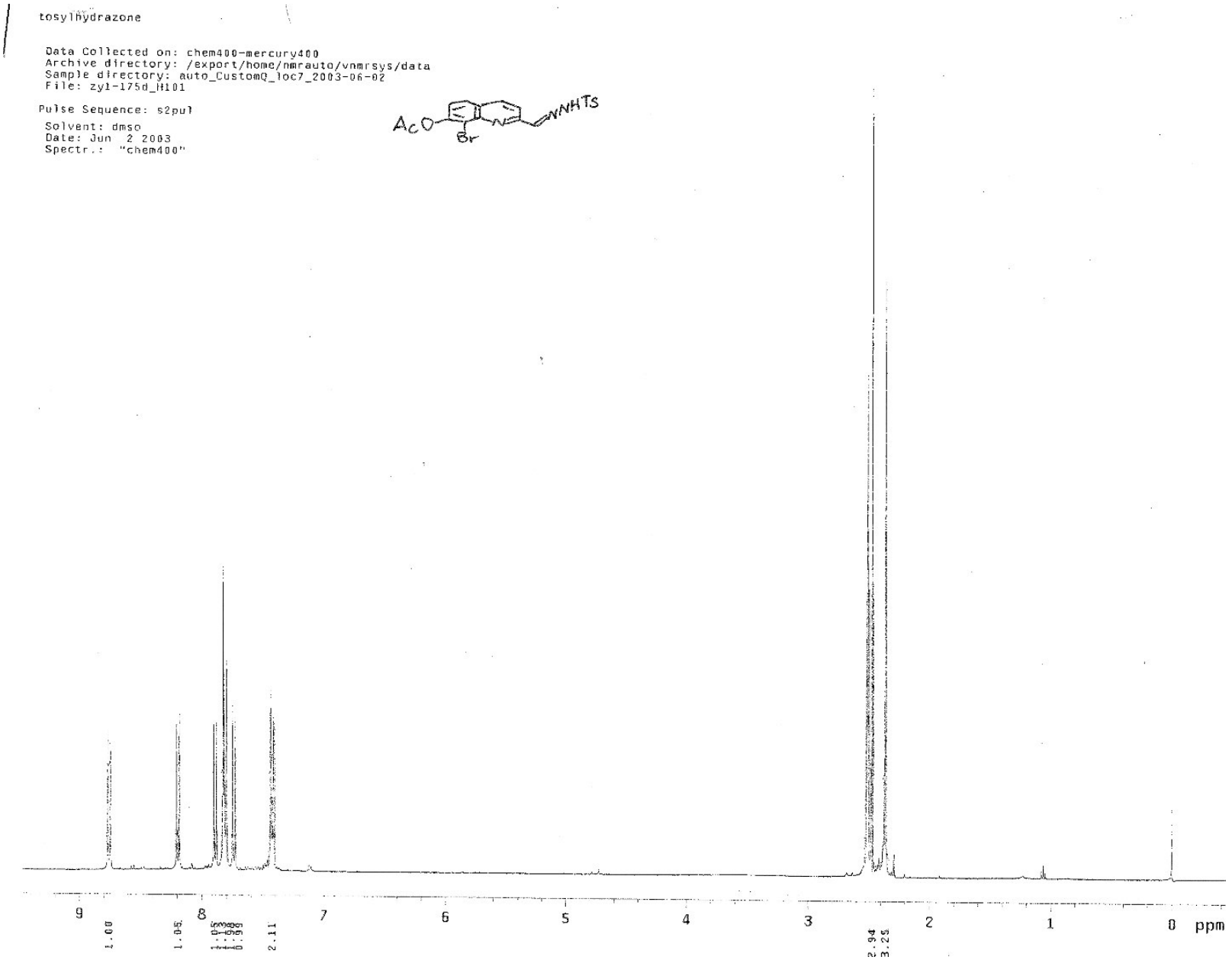
tosylhydrazone
Data Collected on: chem400-mercury400
Archive directory: /export/home/nmrauto/vnmrsys/data
Sample directory: auto_CustomQ_loc7_2003-06-02
File: zy1-175d_H101
Pulse Sequence: s2pul
Solvent: dmso
Date: Jun 2 2003
Spectr.: "chem400"
AcO
Br
NNHTs
9
8
7
6
5
4
3
2
1
0
ppm
1.00
1.05
2.11
2.94
3.25

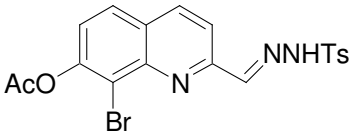
AcO
N
NNHTs
Br

**123**

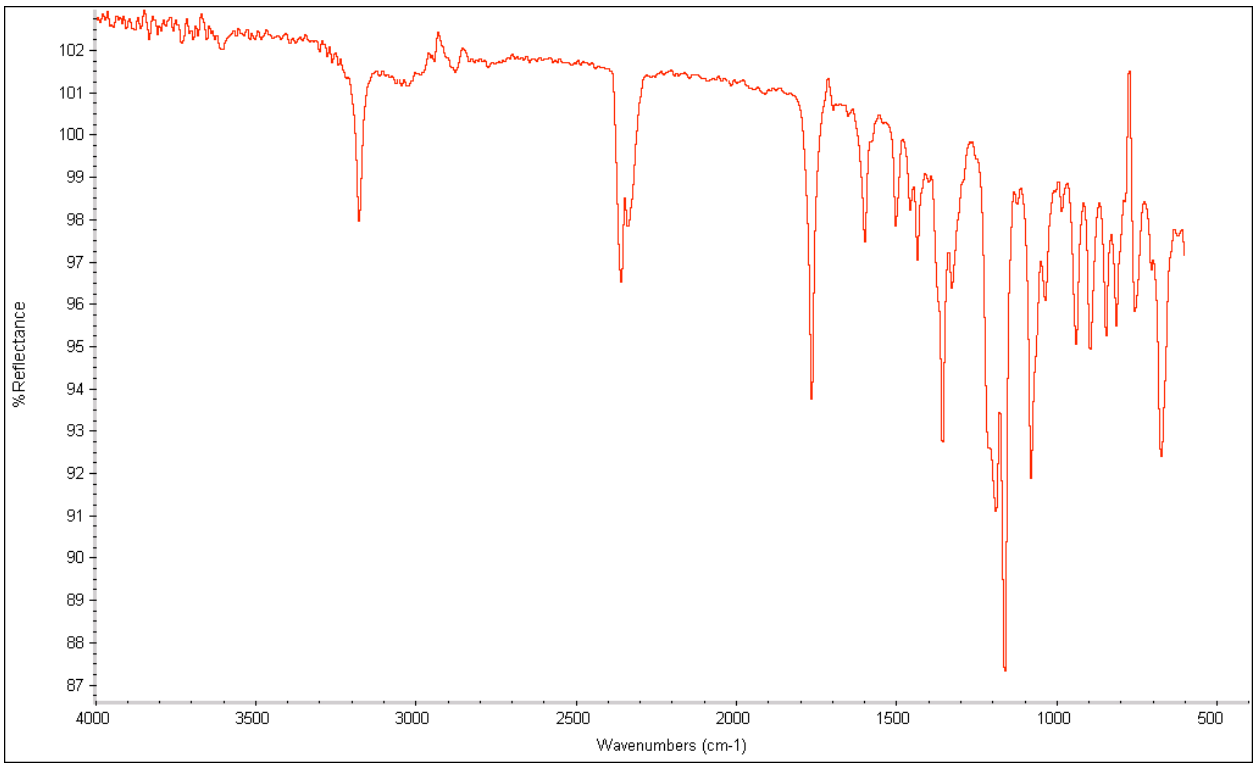
%Reflectance
102
101
100
99
98
97
96
95
94
93
92
91
90
89
88
87
4000
3500
3000
2500
2000
1500
1000
500
Wavenumbers (cm-1)

***8-bromo-7-hydroxyquinolin-2-ylmethyl dimethylphosphate* (124).**

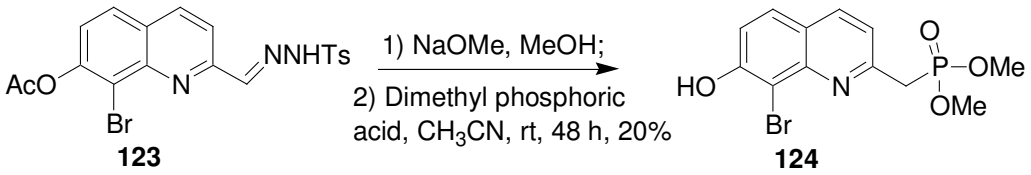


NaOMe (80 mg, 1.48 mmol) was added to a mixture of compound **123** (300 mg, 0.65 mmol) in MeOH (5 mL). The MeOH was removed by rotary evaporation. The resulting residue was taken up in dry $CH_3CN$ (15 mL) and dimethylphosphate (492 mg, 3.9 mmol) was added dropwise. The reaction was stirred for 2 days. The solvent was evaporated and the residue was purified by flash chromatography using EtOAc/hexane (4:6) to afford **124** (47 mg, 0.13 mmol, 20% yield) as a pale yellow oil.

**$^1$H NMR** ($CDCl_3$) δ 8.02 (1H, d, *J* = 8.4 Hz), 7.75 (1H, d, *J* = 8.8 Hz), 7.34 (1H, d, *J* = 8.4 Hz), 7.24 (1H, d, *J* = 8.4 Hz), 5.37 (2H, d, *J* = 8.0 Hz), 3.80 (6H, d, *J* = 10.8 Hz);

**$^{13}$C NMR** ($CDCl_3$) 160.87, 154.59, 144.32, 134.51, 128.47, 121.97, 120.84, 116.74, 104.76, 71.77, 49.56;

**FTIR** (neat) 2929, 2832, 2359, 1614, 1505, 1438, 1332, 1217, 1189, 1108, 1070, 986, 909, 844 $cm^{-1}$;

**HR-MS** (ESI) *m/z* calcd for $(C_{12}H_{13}BrNO_5P+H)^+$ 361.9788 ($^{79}$Br) and 363.9768 ($^{81}$Br), found 361.9808 ($^{79}$Br) and 363.9782 ($^{81}$Br).

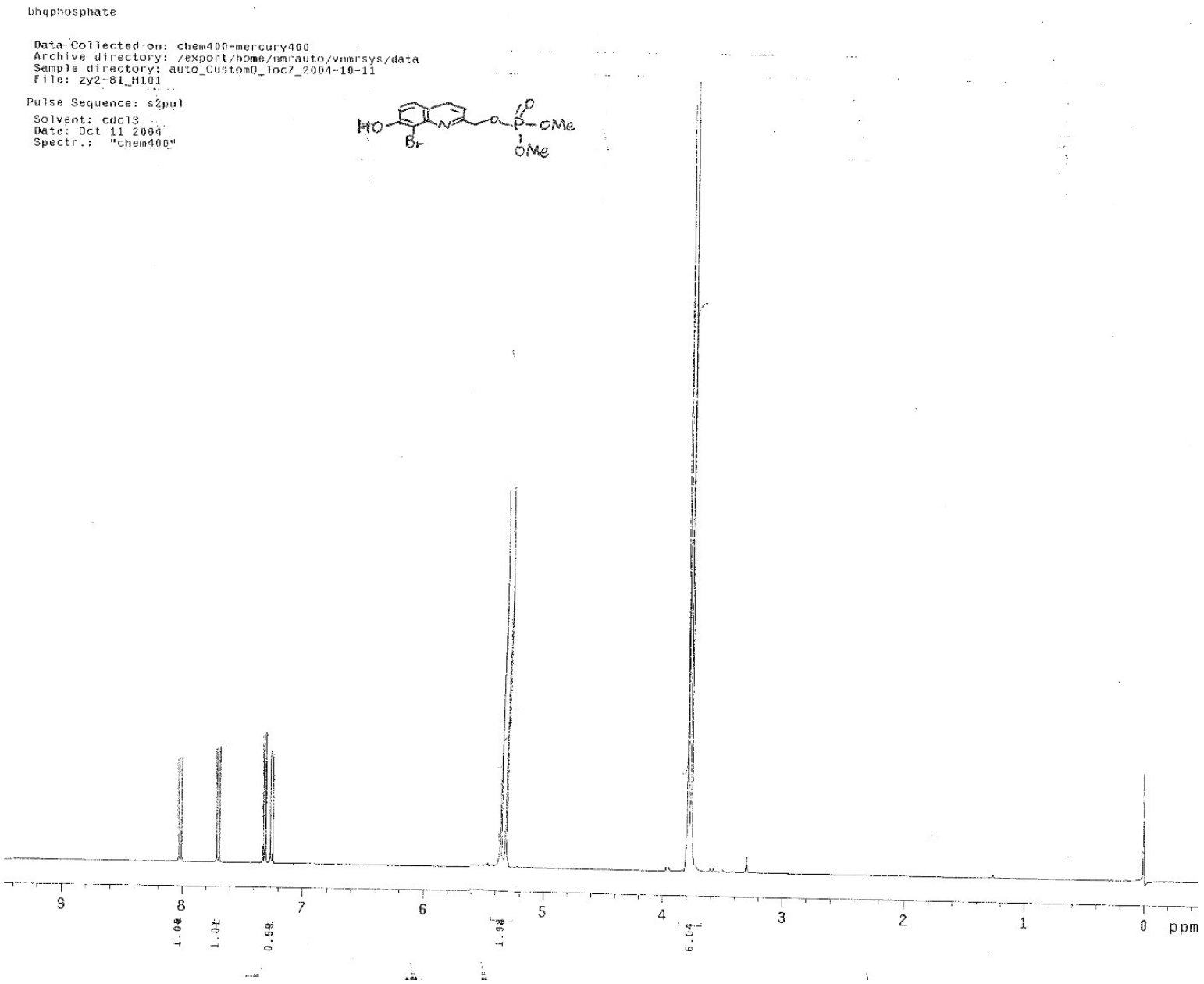
bhqphosphate
Data Collected on: chem400-mercury400
Archive directory: /export/home/nmrauto/vnmrsys/data
Sample directory: auto_Custom0_loc7_2004-10-11
File: zy2-81_H101
Pulse Sequence: s2pul
Solvent: cdcl3
Date: Oct 11 2004
Spectr.: "chem400"
HO
Br
N
O
P
OMe
OMe
9
8
7
6
5
4
3
2
1
0
ppm
1.00
1.02
0.99
1.98
6.04

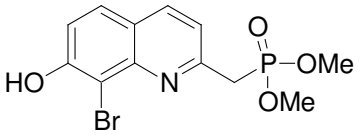
HO
N
Br
O
P
OMe
OMe

**124**

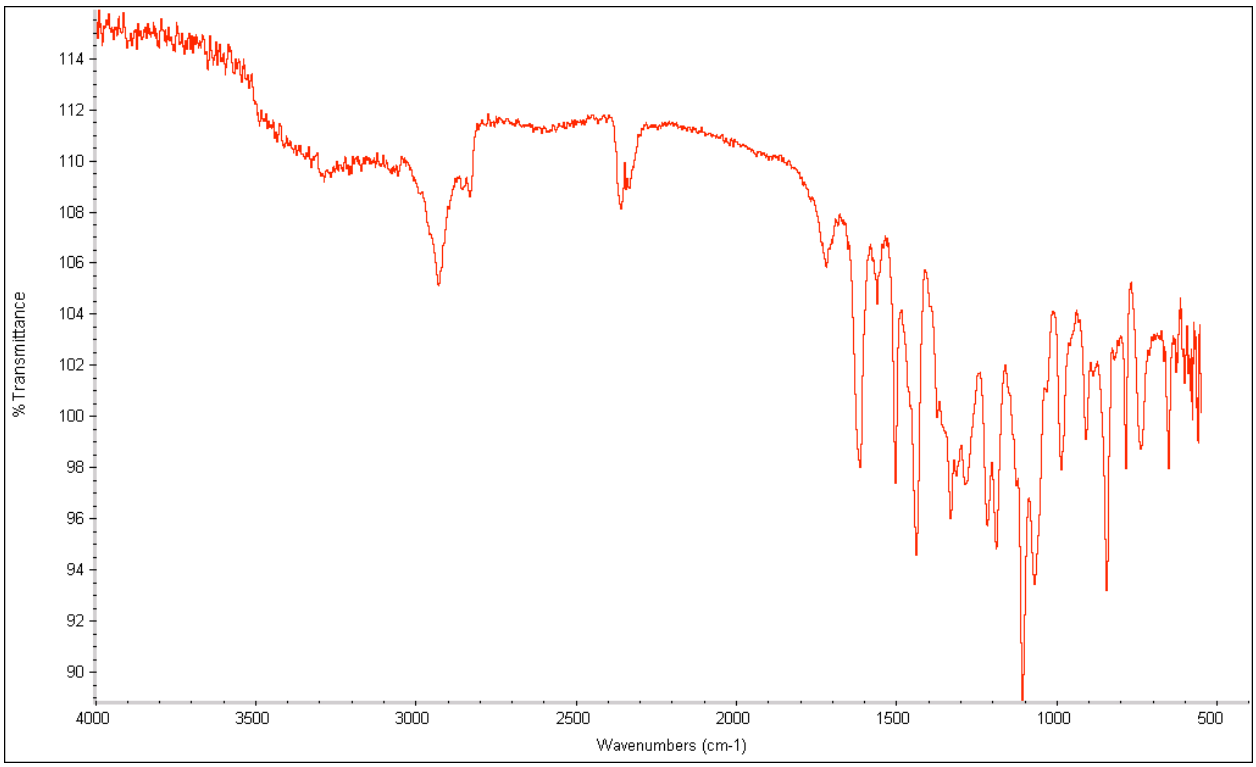
% Transmittance
114
112
110
108
106
104
102
100
98
96
94
92
90
4000
3500
3000
2500
2000
1500
1000
500
Wavenumbers (cm-1)

***BHQ-glycerol(OPh)* (127).**

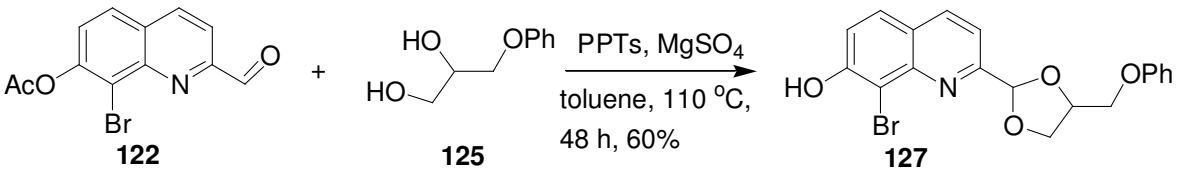


7-Acetyl-8-bromoquinolin-2-yl formaldehyde (**122**, 50 mg, 0.17 mmol), 1-phenoxypropane-2,3-diol (**125**, 86 mg, 0.51 mmol), and pyridinium *p*-toluenesulfonate (85 mg, 0.34 mmol) were dissolved in toluene (25 mL), and anhydrous $MgSO_4$ (50 mg) was added as a drying agent. The reaction mixture was refluxed for 48 h and then cooled to rt. After vacuum filtration, the filtrate was concentrated, and the resulting residue was purified by flash chromatography using EtOAc/hexane (3:7) to yield **127** as a white solid (41 mg, 0.10 mmol, 60% yield), mp = 210 °C dec., as a mixture of diastereomers (1:1):

**$^1$H NMR** ($CDCl_3$) δ [8.16 (d, *J* = 8.4 Hz), 8.15 (d, *J* = 8.4 Hz) (1H)], [7.72 (d, *J* = 9.2 Hz), 7.72 (d, *J* = 9.2 Hz) (1H)], [7.64 (dd, *J* = 8.0, 1.2 Hz), 7.59 (dd, *J* = 8.4, 1.2 Hz) (1H)], 7.31 (3H, m), 6.97 (3H, m), [6.24 (s), 6.12 (s) (1H)], [4.86 (m), 4.72 (m) (1H)], 4.55 (0.5H, m), [4.32 (d, *J* = 6.0 Hz), 4.31 (d, *J* = 6.0 Hz) (1H)], 4.26 (1H, m), 4.15 (1.5H, m);

**$^{13}$C NMR** ($CDCl_3$) (158.48, 158.37), 157.98, 154.18, 145.24, 137.39, 129.58, 128.22, (124.64, 124.52), (121.31, 121.25), (116.86, 116.74), 114.56, 108.29, (104.95, 104.89), (104.52, 104.46), 75.09, (68.41, 68.32), 68.07;

**FTIR** (neat) 2924, 1599, 1496, 1442, 1374, 1241, 1102, 907, 842, 728 $cm^{-1}$;

**HR-MS** (ESI) *m/z* calcd for $(C_{19}H_{16}BrNO_4+H)^+$ 402.0335 ($^{79}$Br) and 404.0317 ($^{81}$Br), found 402.0350 ($^{79}$Br) and 404.0330 ($^{81}$Br).

bhqdf01(p)
Data Collected on: chem400-mercury400
Archive directory: /export/home/nmrauto/vnmrsys/data
Sample directory: auto_CustomQ_loc19_2005-02-21
File: zy2-143d_H1_01
Pulse Sequence: s2pul
Solvent: cdcl3
Date: Apr 25 2005
Spectr.: "chem400"
HO
Br
O
O
Ph
ppm

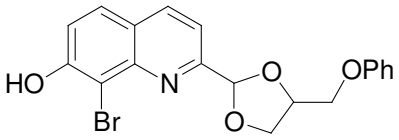
HO
N
O
OPh
Br
O

**127**

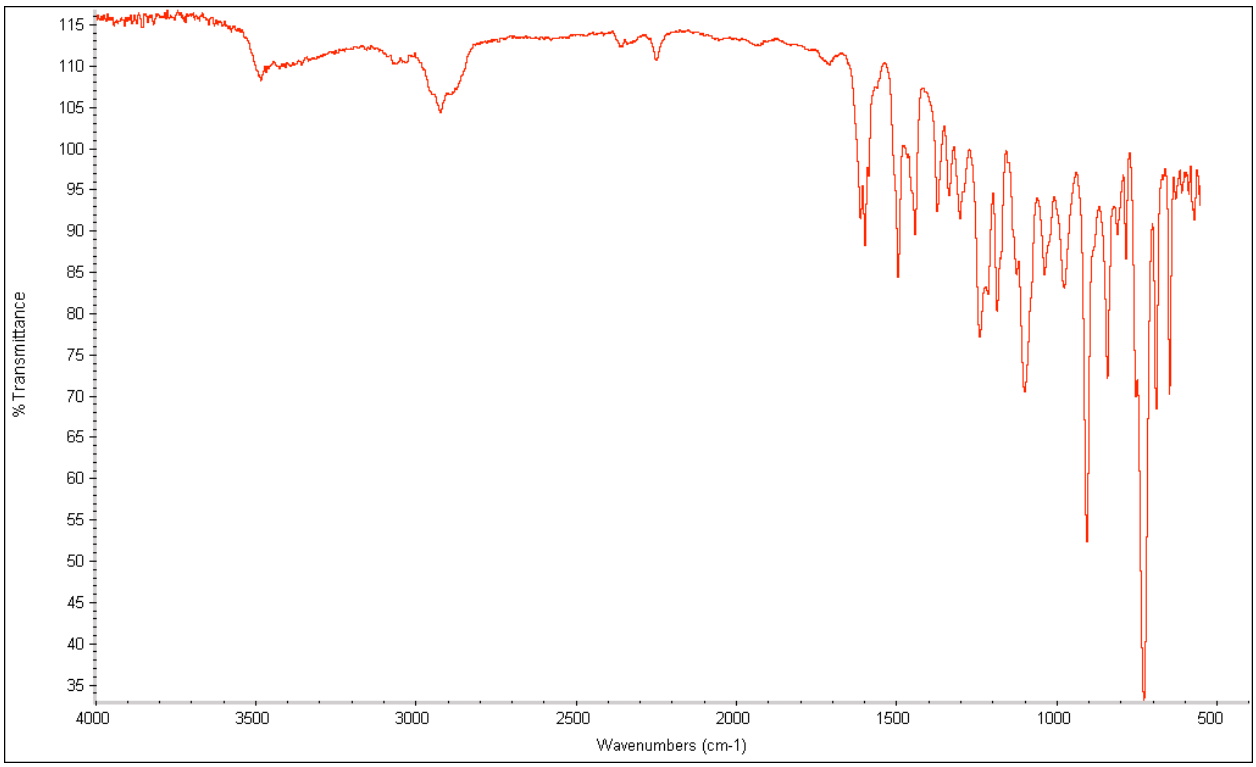
% Transmittance
115
110
105
100
95
90
85
80
75
70
65
60
55
50
45
40
35
4000
3500
3000
2500
2000
1500
1000
500
Wavenumbers (cm-1)

***BHQ-glycerol(SPh)* (128).**

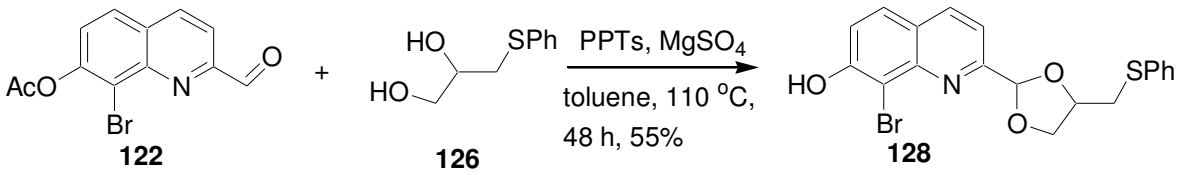


7-Acetyl-8-bromoquinolin-2-yl formaldehyde (**122**, 50 mg, 0.17 mmol), 1-phenthioxypropane-2,3-diol (**126**, 94 mg, 0.51 mmol), pyridinium *p*-toluenesulfonate (85 mg, 0.34 mmol), and anhydrous $MgSO_4$ (50 mg) were mixed in toluene (25 mL). Using the same reaction and workup procedure as the synthesis of compound **127**, compound **128** was acquired as a pale yellow solid (39 mg, 0.093 mmol, 55% yield), mp = 205 °C dec., as a pair of diastereomers (3:2):

**$^1$H NMR** ($CDCl_3$) δ [8.15 (d, *J* = 8.4 Hz), 8.13 (d, *J* = 8.0 Hz) (1H)], [7.72 (d, *J* = 9.2 Hz), 7.71 (d, *J* = 9.2 Hz) (1H)], [7.59 (d, *J* = 8.8 Hz), 7.51 (d, *J* = 8.4 Hz) (1H)], 7.42 (1.5H, m), 7.33 (4H, m), 7.23 (0.5H, m), [6.19 (s), 6.05 (s) (1H)], [4.62 (m), 4.50 (m) (1H)], [4.45 (m), 4.24 (m) (1H)], [4.13 (m), 3.94 (m) (1H)], [3.45 (m), 3.42 (m) (1H)], [3.20 (m), 3.10 (m) (1H)];

**$^{13}$C NMR** ($CDCl_3$) 158.05, 154.19, 145.26, 137.41, (130.08, 129.91), 129.16, 128.23, (126.81, 126.71), 124.61, 118.38, (116.82, 116.65), 105.29, 104.91, 104.26, (75.95, 75.70), 70.57, 70.08;

**FTIR** (neat) 2925, 2359, 1613, 1508, 1439, 1374, 1337, 1304, 1187, 1092, 908, 842, 734 $cm^{-1}$;

**HR-MS** (ESI) *m/z* calcd for $(C_{19}H_{16}BrNO_3S+H)^+$ 418.0107 ($^{79}$Br) and 420.0088 ($^{81}$Br), found 418.0121 ($^{79}$Br) and 420.0103 ($^{81}$Br).

Data Collected on: chem400-mercury400
Archive directory: /export/home/nmrauto/vnmrsys/data
Sample directory: auto_CustomQ_1dc9_2005-04-25
File: zy2-bhqdiol_H1_02
Pulse Sequence: s2pul
Solvent: cdcl3
Date: Apr 25 2005
Spectr.: "chem400"
ZY2-164
OH
Br
Ph
Si
7.261
0.000
ppm

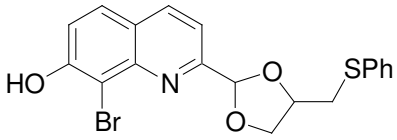
HO
N
O
O
SPh
Br

**128**

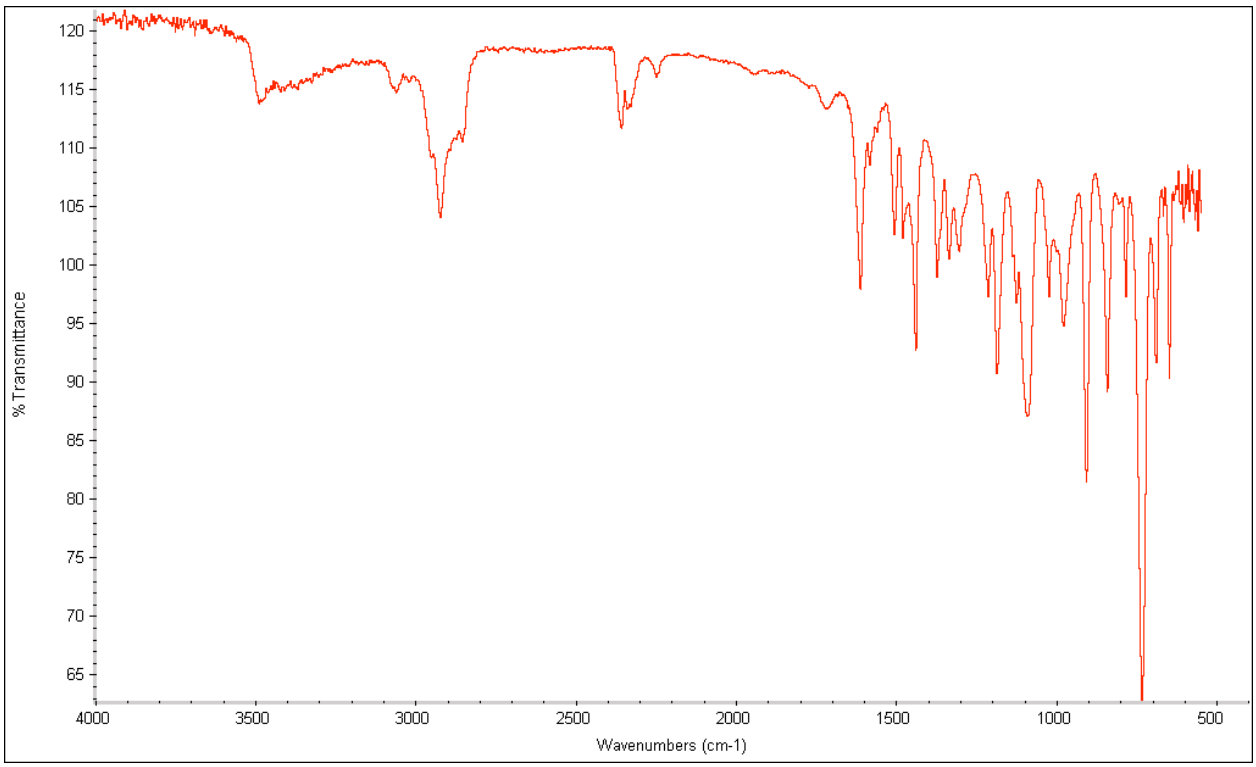
% Transmittance
120
115
110
105
100
95
90
85
80
75
70
65
4000
3500
3000
2500
2000
1500
1000
500
Wavenumbers (cm-1)

***MOM-BHQ* (156)**

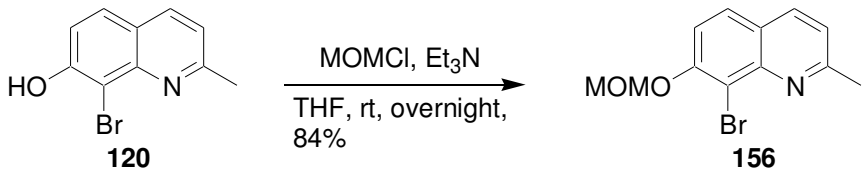


BHQ **120** (1.83 g, 7.38 mmol) was dissolved in THF (30 mL). Triethylamine (2.00 mL, 14.2 mmol) was added to the solution. After 2 min of stirring, chloromethyl methyl ether (1.00 mL, 13.2 mmol) was added dropwise and the reaction was stirred overnight. The solvents were evaporated, and the residue dissolved with chloroform (100 mL). The chloroform solution was washed with water and brine, and dried over anhydrous $Na_2SO_4$. The solvent was evaporated and the residue was purified by flash chromatography with EtOAC/hexane (1:9) to yield **156** (1.74g, 6.17 mmol, 84% yield).

**$^1$H NMR** ($CDCl_3$) δ 7.98 (1H, d, *J* = 8.0 Hz), 7.70 (1H, d, *J* = 9.2 Hz), 7.43 (1H, d, *J* = 9.2 Hz), 7.24 (1H, d, *J* = 8.0 Hz), 5.40 (2H, s), 3.58 (3H, s), 2.80 (3H, s);

**$^{13}$C NMR** ($CDCl_3$) δ 161.08, 155.11, 146.30, 136.48, 127.97, 123.64, 121.32, 116.57, 112.14, 95.63, 56.84, 26.05;

**FTIR** (neat) 2906, 2844, 1614, 1508, 1322, 1248, 1154, 1056, 993, 920, 831 $cm^{-1}$;

**HR-MS** (ESI) *m/z* calcd for $(C_{12}H_{12}BrNO_2+H)^+$ 282.0130 ($^{79}$Br) and 284.0109 ($^{81}$Br), found 282.0132 ($^{79}$Br) and 284.0107 ($^{81}$Br).

MOM-BHQ

File: zy4-079a_Proton_2006Oct20_01

Pulse Sequence: s2pul

Solvent: cdcl3
Ambient temperature
Sample #28, Operator: yzhu
File: zy4-079a_Proton_2006Oct20_01
INOVA-500 "LinuxWS1"

Relax. delay 1.000 sec
Pulse 45.0 degrees
Acq. time 2.000 sec
Width 4001.6 Hz
16 repetitions
OBSERVE H1, 400.1493174 MHz
DATA PROCESSING
FT size 16384
Total time 0 min, 48 sec

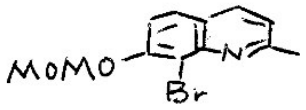


| INDEX | FREQUENCY | PPM | HEIGHT |
|---|---|---|---|
| 1 | 2161.020 | 5.401 | 106.6 |
| 2 | 1431.725 | 3.578 | 157.0 |
| 3 | 1122.519 | 2.805 | 148.5 |

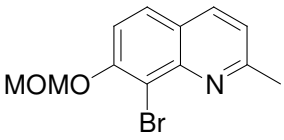
MOMO
N
Br

**156**

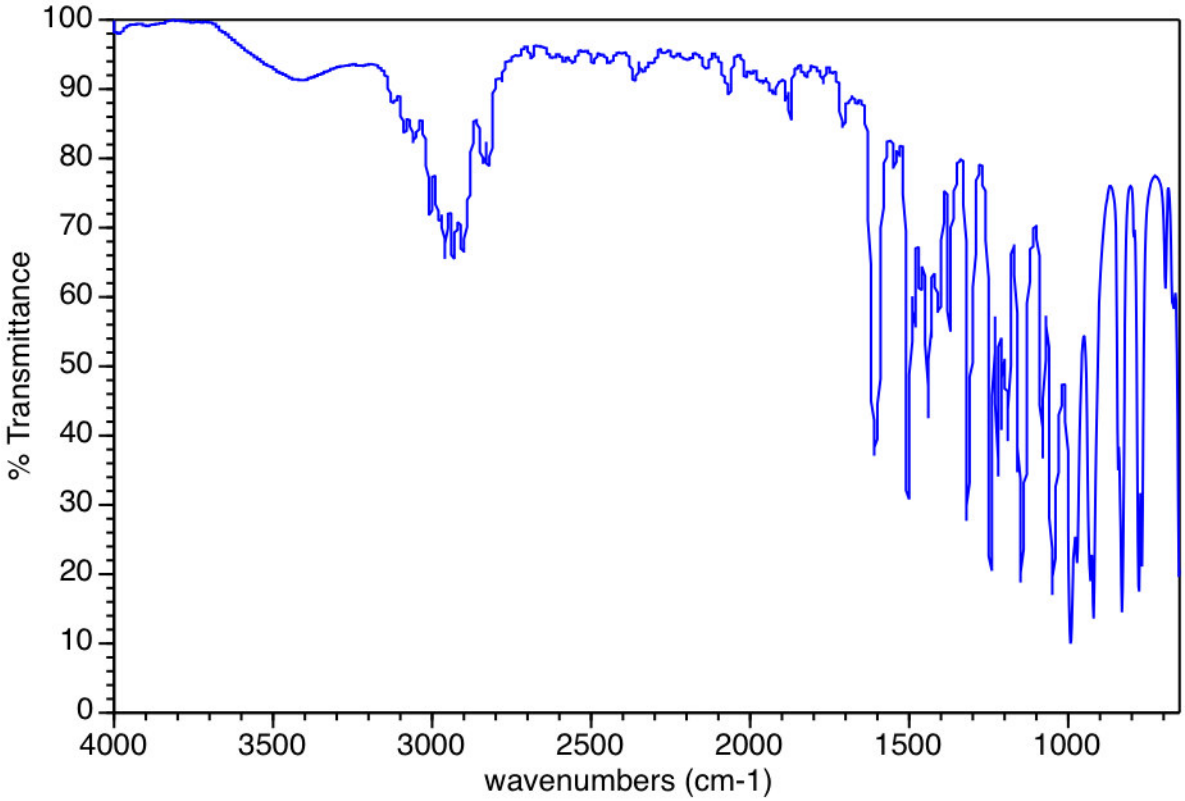
% Transmittance
100
90
80
70
60
50
40
30
20
10
0
4000
3500
3000
2500
2000
1500
1000
wavenumbers (cm-1)

***MOM-BHQ aldehyde* (157)**

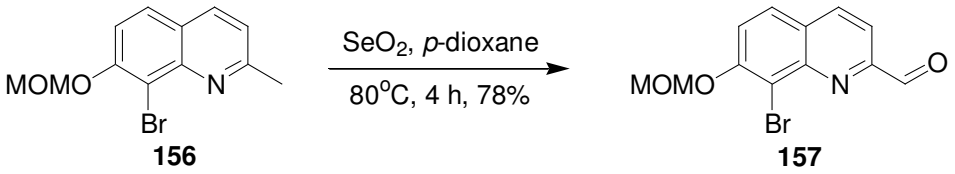


MOM-protected BHQ **156** (250 mg, 0.887 mmol) was dissolved in *p*-dioxane (5 mL). Selenium dioxide (100 mg, 0.901 mmol) was added to the solution, and the mixture was heated at 80 $^{o}$C for 4 h with stirring. The reaction mixture was vacuum filtered and the filtrate was concentrated. The remaining residue was purified by flash chromatography using EtOAc/hexane (1:3) to provide **157** (205 mg, 0.693 mmol, 78% yield).

**$^{1}$H NMR** ($CDCl_3$) δ 10.30 (1H, s), 8.27 (1H, d, *J* = 8.4 Hz), 7.97 (1H, d, *J* = 8.4 Hz), 7.84 (1H, d, *J* = 9.2 Hz), 7.66 (1H, d, *J* = 9.6 Hz), 5.45 (2H, s), 3.60 (3H, s);

**$^{13}$C NMR** ($CDCl_3$) δ 193.86, 156.05, 153.58, 146.49, 137.98, 128.20, 127.16, 119.94, 116.47, 113.29, 95.60, 56.97;

**FTIR** (neat) 2933, 2834, 1708, 1615, 1442, 1261, 1156, 1038, 920, 839 $cm^{-1}$;

**HR-MS** (ESI) *m/z* calcd for $(C_{12}H_{10}BrNO_3+H)^+$ 295.9922 ($^{79}$Br) and 297.9902 ($^{81}$Br), found 295.9925 ($^{79}$Br) and 297.9895 ($^{81}$Br).

MOM-BHQ-CHO

File: zy4-197a_Proton_2008Feb04_01

Pulse Sequence: s2pul

Solvent: cdcl3
Ambient temperature
Sample #4, Operator: yzhu
File: zy4-197a_Proton_2008Feb04_01
INOVA-500 "LinuxWS1"

Relax. delay 1.000 sec
Pulse 45.0 degrees
Acq. time 1.998 sec
Width 6402.0 Hz
16 repetitions
OBSERVE H1, 400.1493115 MHz
DATA PROCESSING
FT size 32768
Total time 0 min, 48 sec

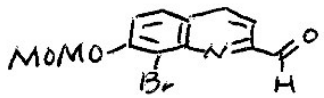


| INDEX | FREQUENCY | PPM | HEIGHT |
|---|---|---|---|
| 1 | 4120.068 | 10.296 | 54.1 |
| 2 | 3314.342 | 8.283 | 30.4 |
| 3 | 3306.136 | 8.262 | 35.2 |
| 4 | 3193.991 | 7.982 | 49.3 |
| 5 | 3185.785 | 7.961 | 43.7 |
| 6 | 3141.240 | 7.850 | 37.6 |
| 7 | 3131.862 | 7.827 | 49.9 |
| 8 | 3067.779 | 7.667 | 50.9 |
| 9 | 3058.401 | 7.643 | 41.2 |
| 10 | 2181.167 | 5.451 | 200.9 |
| 11 | 1439.523 | 3.597 | 321.3 |

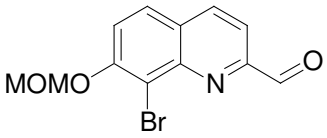
MOMO
N
O
Br

**157**

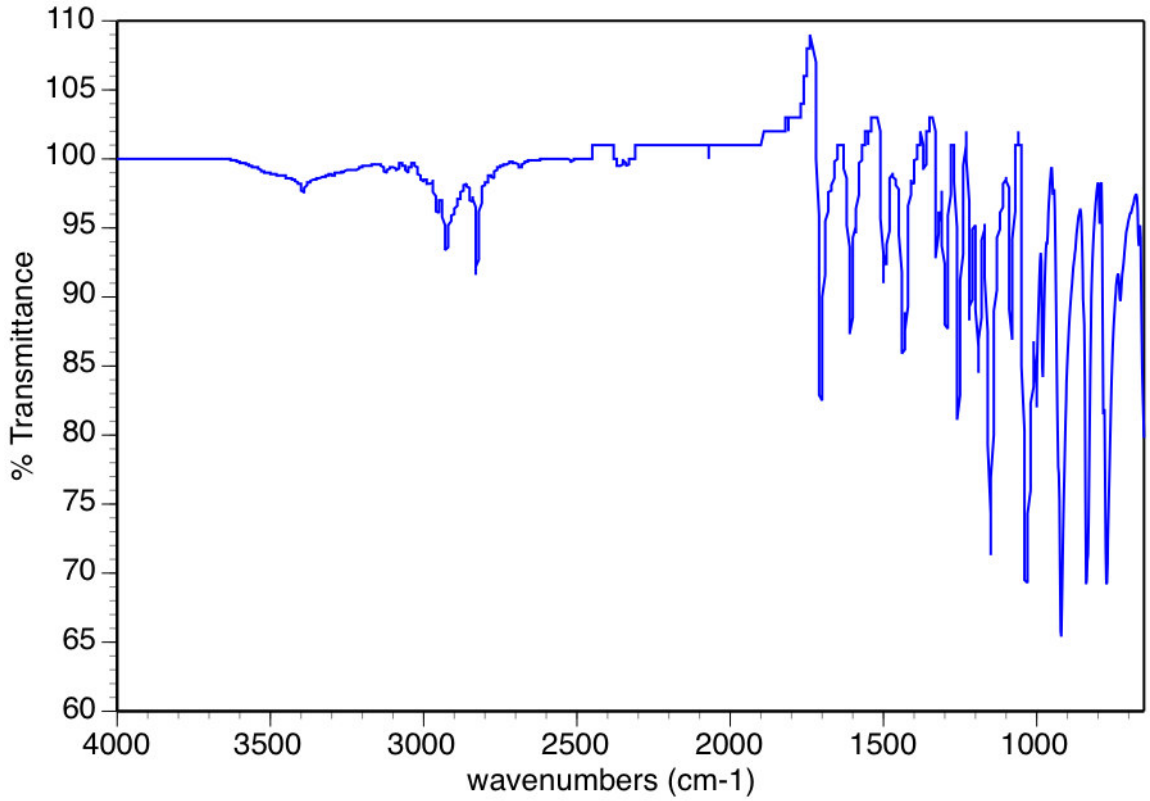
% Transmittance
110
105
100
95
90
85
80
75
70
65
60
4000
3500
3000
2500
2000
1500
1000
wavenumbers (cm-1)

***MOM-BHQ alcohol* (158)**

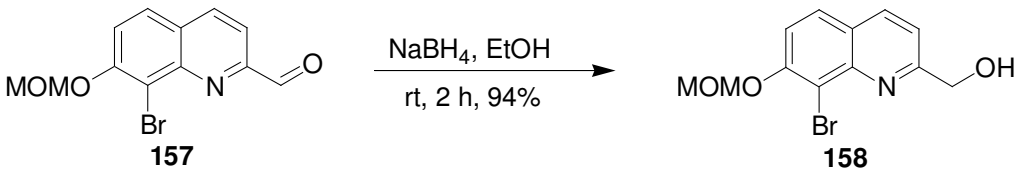


MOM-protected BHQ aldehyde **157** (150 mg, 0.51 mmol) was mixed with ethanol, then sodium borohydride (15 mg, 0.41 mmol) was added in small portions to the mixture. When the reaction was complete as determined by TLC, it was concentrated, and the remaining residue was diluted with chloroform. The mixture was then washed successively with water and brine, dried over anhydrous $Na_2SO_4$, and evaporated to provide **158** (140 mg, 0.47 mmol, 92%).

**$^1$H NMR** ($CDCl_3$) δ 8.08 (1H, d, *J* = 8.4 Hz), 7.76 (1H, d, *J* = 8.8 Hz), 7.50 (1H, d, *J* = 8.8 Hz), 7.22 (1H, d, *J* = 8.4 Hz), 5.42 (2H, s), 4.94 (2H, s), 3.58 (3H, s);

**$^{13}$C NMR** ($CDCl_3$) δ 160.45, 155.58, 144.96, 137.24, 128.05, 124.54, 117.39, 117.11, 112.12, 95.58, 64.26, 56.88;

**FTIR** (neat) 3294, 2935, 1618, 1514, 1256, 1197, 1152, 1055, 989, 916, 835 $cm^{-1}$;

**HR-MS** (ESI) *m/z* calcd for $(C_{12}H_{12}BrNO_3+H)^+$ 298.0079 ($^{79}$Br) and 300.0058 ($^{81}$Br), found 298.0075 ($^{79}$Br) and 300.0056 ($^{81}$Br).

MOM-BHQ-OH

File: zy4-198a_Proton_2008Feb04_01

Pulse Sequence: s2pul

Solvent: cdcl3
Ambient temperature
Sample #5, Operator: yzhu
File: zy4-198a_Proton_2008Feb04_01
INOVA-500 "LinuxWS1"

Relax. delay 1.000 sec
Pulse 45.0 degrees
Acq. time 1.998 sec
Width 6402.0 Hz
16 repetitions
OBSERVE H1, 400.1493158 MHz
DATA PROCESSING
FT size 32768
Total time 0 min, 48 sec

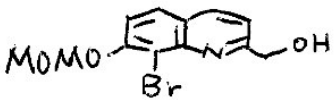


| INDEX | FREQUENCY | PPM | HEIGHT |
|---|---|---|---|
| 1 | 3238.927 | 8.094 | 33.8 |
| 2 | 3230.331 | 8.073 | 34.7 |
| 3 | 3107.635 | 7.766 | 30.8 |
| 4 | 3098.648 | 7.744 | 36.7 |
| 5 | 3004.868 | 7.509 | 35.0 |
| 6 | 2995.881 | 7.487 | 29.6 |
| 7 | 2891.550 | 7.226 | 32.3 |
| 8 | 2882.954 | 7.205 | 30.0 |
| 9 | 2168.272 | 5.419 | 160.4 |
| 10 | 1976.023 | 4.938 | 95.1 |
| 11 | 1434.053 | 3.584 | 245.7 |
| 12 | 0.000 | 0.000 | 28.5 |

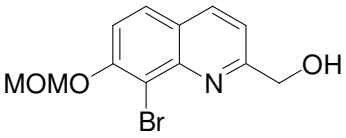
MOMO
N
OH
Br

**158**

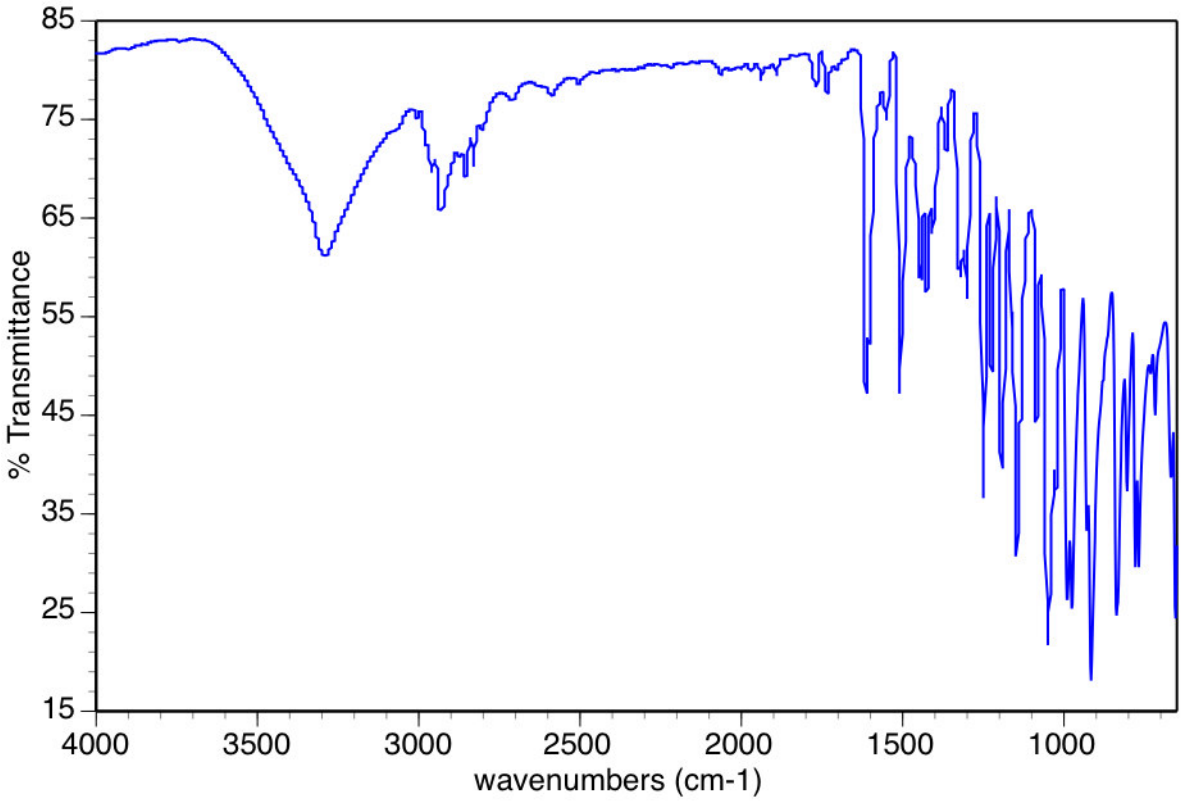
% Transmittance
85
75
65
55
45
35
25
15
4000
3500
3000
2500
2000
1500
1000
wavenumbers (cm-1)

***MOM-BHQ di-t-butyl phosphate* (159)**

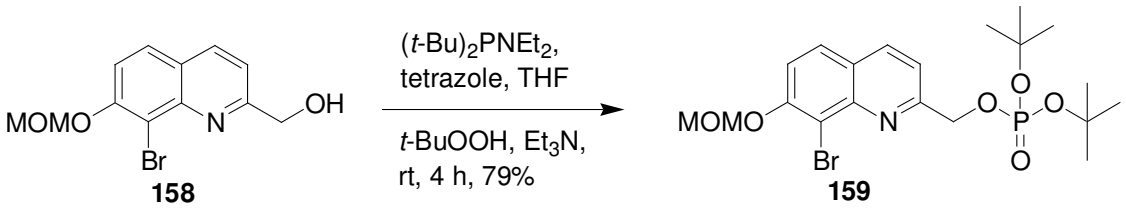


MOM-protected BHQ alcohol **158** (450 mg, 1.51 mmol) was dissolved in THF (10 mL). Tetrazole (0.45 M solution in acetonitrile, 13.5 mL, 6.08 mmol) was added to the solution, and the mixture was stirred in a –20 $^{o}$C bath for 5 min. Di-*tert*-butyl *N*,*N*-diethylphosphoramidite (0.630 mL, 2.26 mmol) was added dropwise. After 10 min of stirring at –20 $^{o}$C, the reaction mixture was allowed to warm to 0 $^{o}$C and stirred for 1 h. The mixture was treated with triethylamine (2.12 mL, 15.1 mmol) followed by addition of *tert*-butylhydroperoxide (70% in water, 1.00 mL, 7.30 mmol) at 0 $^{o}$C and the mixture was allowed to warm to room temperature. After an additional 4 h of reaction time, the excess oxidant was destroyed by addition of concentrated sodium thiosulfate solution. The mixture was concentrated, diluted with chloroform, and washed with water and brine. The organic layer was dried over $Na_2SO_4$, and concentrated. The remaining residue was purified by flash chromatography using EtOAc/Hexane (4:6) to yield **159** (550 mg, 1.12 mmol, 79% yield).

**$^{1}$H NMR** ($CDCl_3$) δ 8.15 (1H, d, *J* = 8.4 Hz), 7.76 (1H, d, *J* = 8.8 Hz), 7.67 (1H, d, *J* = 8.4 Hz), 7.50 (1H, d, *J* = 8.8 Hz), 5.41 (2H, s), 5.33 (2H, d, *J* = 6.8 Hz), 3.58 (3H, s);

**$^{13}$C NMR** ($CDCl_3$) δ 159.37, 155.40, 145.83, 137.29, 128.15, 124.66, 118.13, 117.39, 112.19, 95.60, 83.06, 69.67, 56.87, 30.15;

**$^{31}$P NMR** ($CDCl_3$) δ -7.00

**FTIR** (neat) 2985, 1618, 1512, 1375, 1261, 1158, 1046, 991, 941 $cm^{-1}$;

**HR-MS** (ESI) *m/z* calcd for $(C_{20}H_{29}BrNO_6P+H)^+$ 490.0994 ($^{79}Br$) and 492.0974 ($^{81}Br$), found 490.0997 ($^{79}Br$) and 492.0978 ($^{81}Br$).

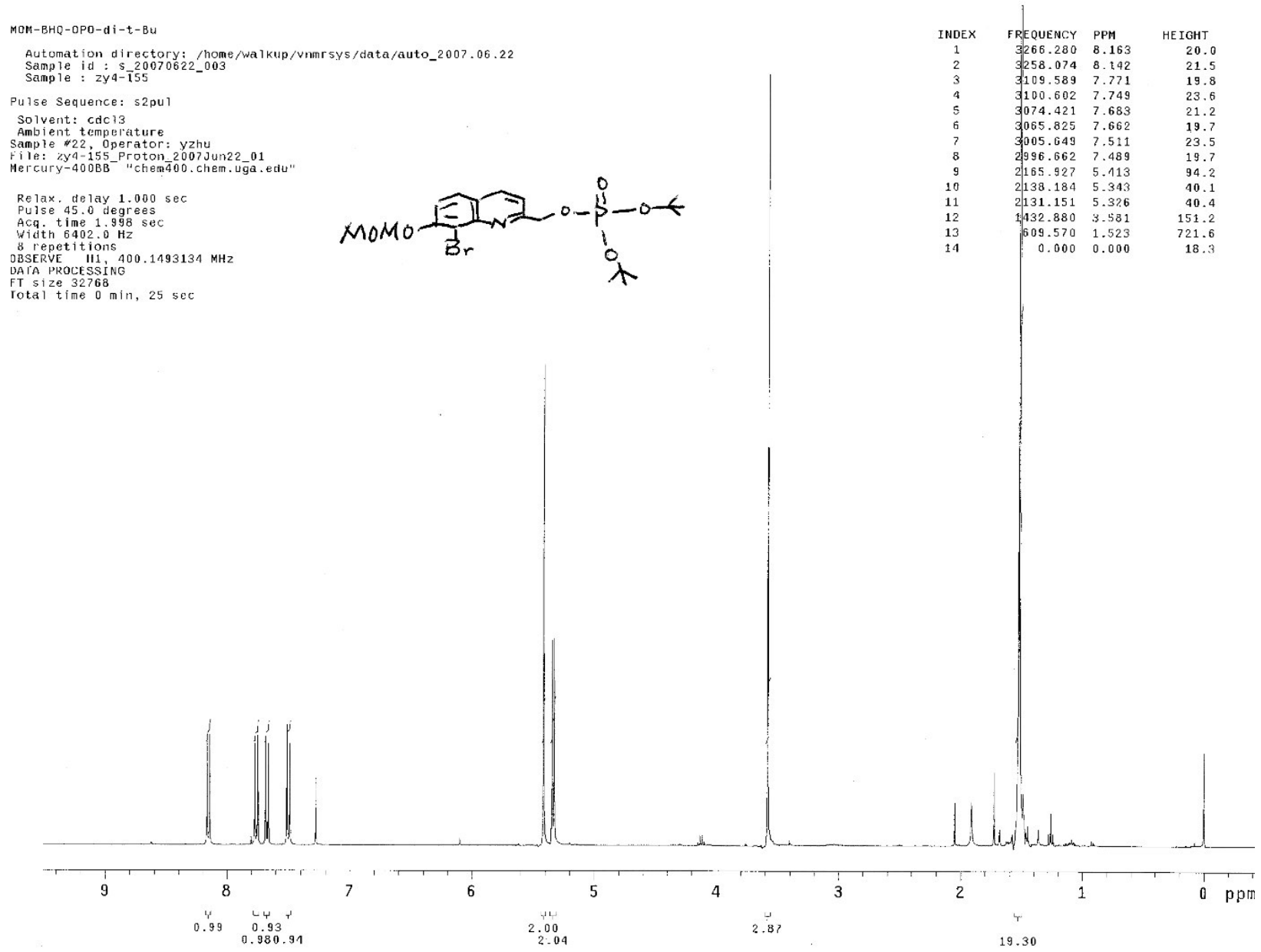
MOM-BHQ-OPO-di-t-Bu
Automation directory: /home/walkup/vnmrsys/data/auto_2007.06.22
Sample id : s_20070622_003
Sample : zy4-155
Pulse Sequence: s2pul
Solvent: cdcl3
Ambient temperature
Sample #22, Operator: yzhu
File: zy4-155_Proton_2007Jun22_01
Mercury-400BB "chem400.chem.uga.edu"
Relax. delay 1.000 sec
Pulse 45.0 degrees
Acq. time 1.998 sec
Width 6402.0 Hz
8 repetitions
OBSERVE H1, 400.1493134 MHz
DATA PROCESSING
FT size 32768
Total time 0 min, 25 sec
MOMO
Br
INDEX FREQUENCY PPM HEIGHT
1 3266.280 8.163 20.0
2 3258.074 8.142 21.5
3 3109.589 7.771 19.8
4 3100.602 7.749 23.6
5 3074.421 7.683 21.2
6 3065.825 7.662 19.7
7 3005.649 7.511 23.5
8 2996.662 7.489 19.7
9 2165.927 5.413 94.2
10 2138.184 5.343 40.1
11 2131.151 5.326 40.4
12 1432.880 3.581 151.2
13 609.570 1.523 721.6
14 0.000 0.000 18.3
9
8
7
6
5
4
3
2
1
0 ppm
0.99
0.93
0.98
0.94
2.00
2.04
2.87
19.30

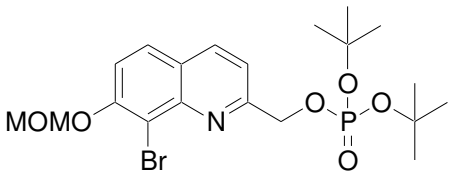
MOMO
N
O
O
P
O
O
Br

**159**

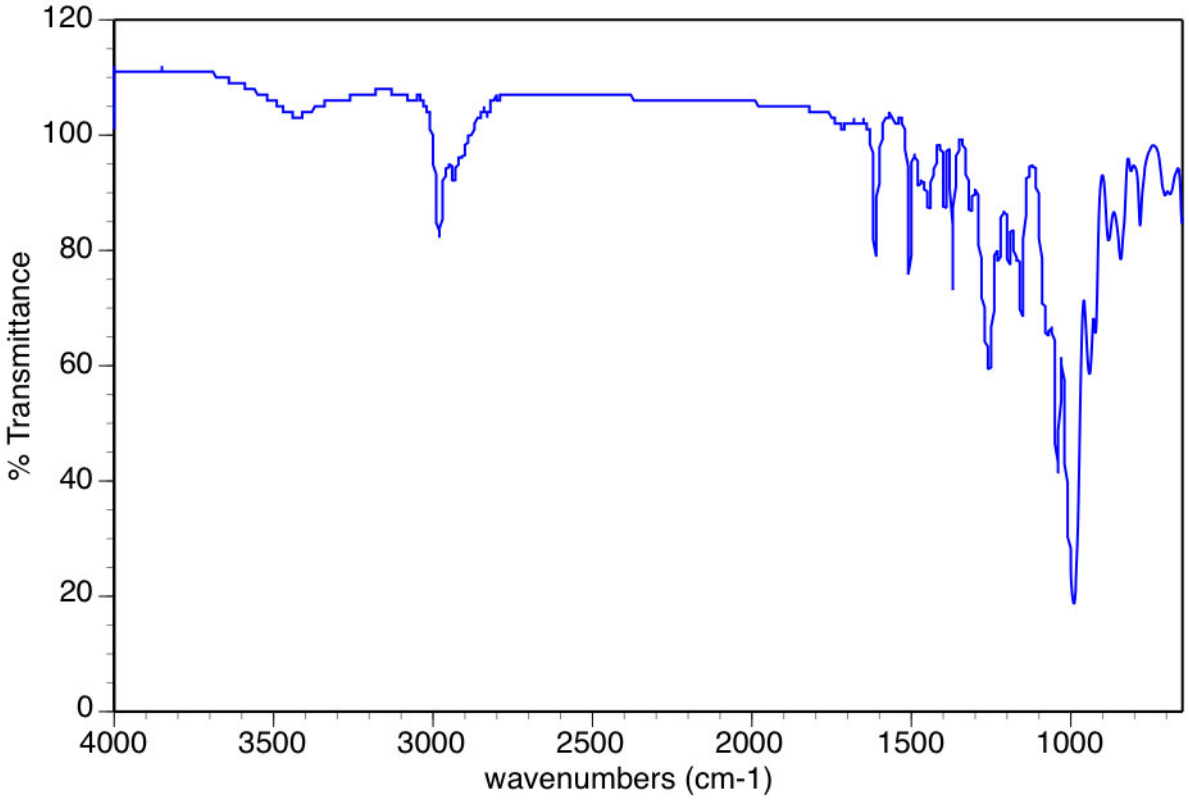
120
100
80
60
40
20
0
% Transmittance
4000
3500
3000
2500
2000
1500
1000
wavenumbers (cm-1)

***BHQ phosphate (free)*** **(160)**

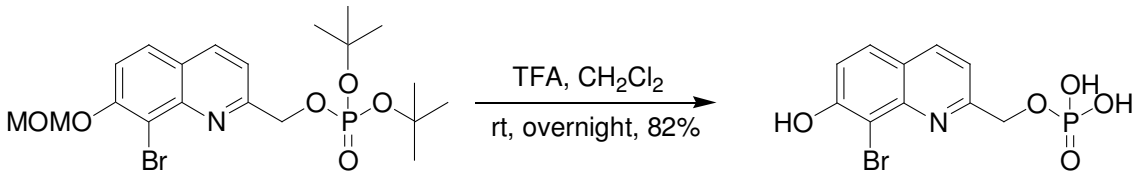


**159** **160**

MOM-protected BHQ di-*tert*-butyl phosphate **159** (550 mg, 1.12 mmol) was dissolved in anhydrous dichloromethane (7 mL). Trifluoroacetic acid (0.5 mL, 6.62 mmol) was added and the resulting mixture was stirred overnight. The precipitate formed was filtered, washed with hexane (10 mL × 3) and then dried under vacuum to provide **160** (308 mg, 0.922 mmol, 82% yield).

**$^{1}$H NMR** (DMSO-$d_6$) δ 8.35 (1H, d, $J$ = 8.4 Hz), 7.86 (1H, d, $J$ = 9.2 Hz), 7.51 (1H, d, $J$ = 8.4 Hz), 7.35 (1H, d, $J$ = 9.2 Hz), 5.10 (2H, d, $J$ = 8.4 Hz);

**$^{13}$C NMR** (DMSO-$d_6$) δ 159.78, 156.93, 146.03, 138.22, 128.85, 123.67, 119.91, 117.89, 105.78, 69.23;

**$^{31}$P NMR** (DMSO-$d_6$) δ 2.17

**FTIR** (neat) 2555, 1637, 1558, 1447, 1336, 1185, 1108, 1014, 936, 866, 843 $cm^{-1}$;

**HR-MS** (ESI) *m/z* calcd for $(C_{10}H_9BrNO_5P+H)^+$ 333.9480 ($^{79}$Br) and 335.9459 ($^{81}$Br), found 333.9486 ($^{79}$Br) and 335.9472 ($^{81}$Br).

BHQ-OPi

Automation directory: /home/walkupl/vnmrsys/data/auto_2008.04.16
Sample id : s_20080416_007
Sample : zy4-BHQ-OPi

Pulse Sequence: s2pul
Solvent: dmso
Ambient temperature
Operator: yzhu
File: zy4-BHQ-OPi_Proton_20080416_01
Mercury-400BB "chem400.chem.uga.edu"

Relax. delay 1.000 sec
Pulse 45.0 degrees
Acq. time 1.998 sec
Width 6402.0 Hz
16 repetitions
OBSERVE H1, 400.1512165 MHz
DATA PROCESSING
FT size 32768
Total time 0 min, 50 sec

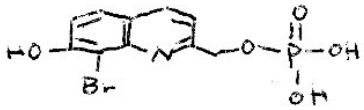

| INDEX | FREQUENCY | PPM | HEIGHT |
|---|---|---|---|
| 1 | 3346.383 | 8.363 | 42.9 |
| 2 | 3338.178 | 8.342 | 43.0 |
| 3 | 3147.882 | 7.867 | 42.3 |
| 4 | 3138.895 | 7.844 | 45.7 |
| 5 | 3008.385 | 7.518 | 46.4 |
| 6 | 2999.788 | 7.497 | 44.3 |
| 7 | 2946.255 | 7.363 | 47.4 |
| 8 | 2937.268 | 7.340 | 44.6 |
| 9 | 2046.749 | 5.115 | 75.3 |
| 10 | 2038.543 | 5.094 | 75.6 |
| 11 | 1004.618 | 2.511 | 82.9 |
| 12 | 1003.055 | 2.507 | 104.7 |
| 13 | 1001.492 | 2.503 | 73.5 |
| 14 | 0.000 | 0.000 | 69.5 |

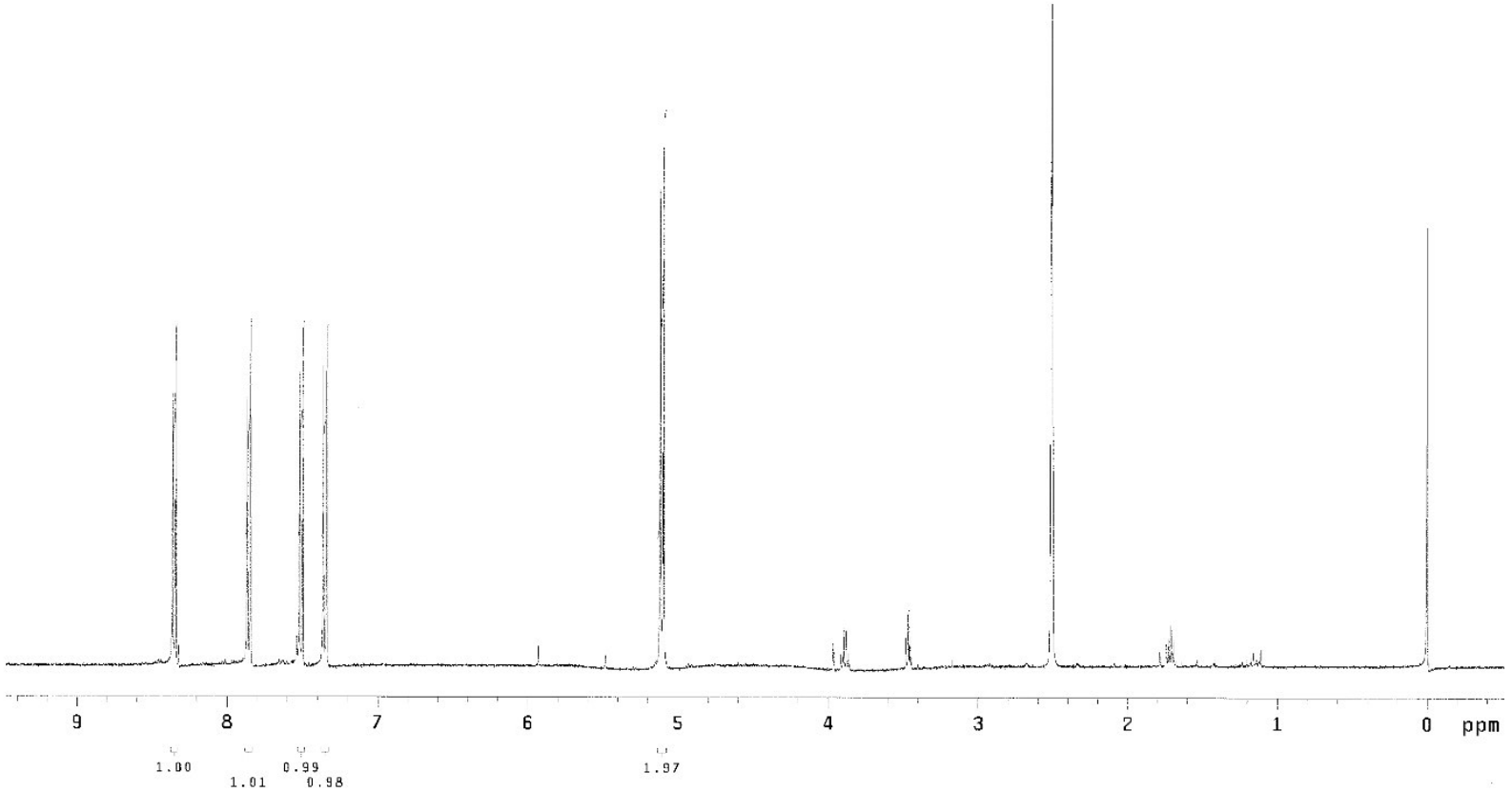

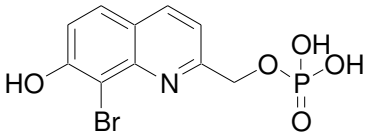
HO
N
Br
O
P
OH
OH
O

**160**

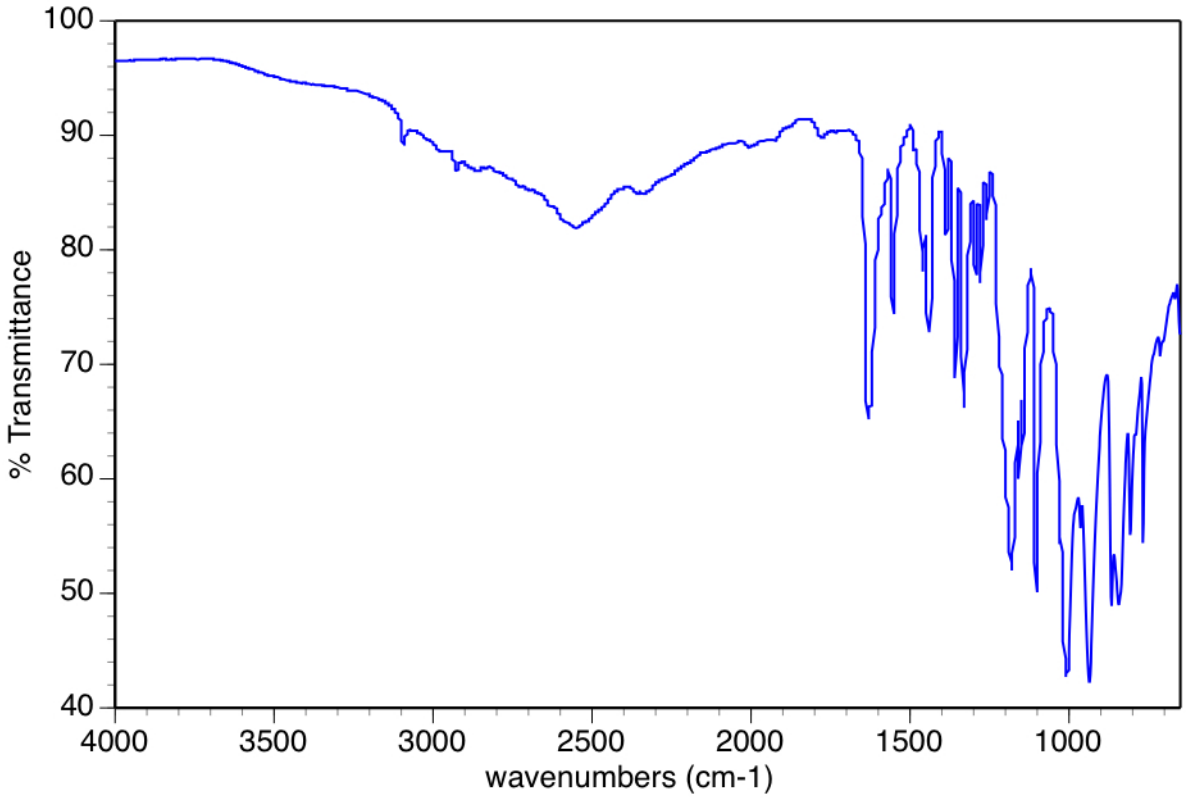
100
90
80
70
60
50
40
% Transmittance
4000
3500
3000
2500
2000
1500
1000
wavenumbers (cm-1)

***BHQ-ATP* (155)**

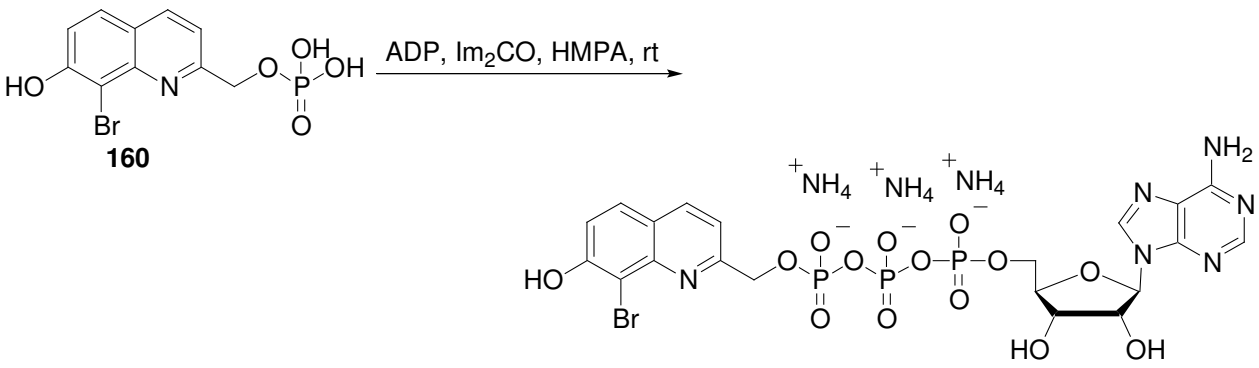


ADP (511 mg, 1.20 mmol) was dissolved in water, tri-*n*-butylamine (106 mg, 0.570 mL, 2.39 mmol) was added to the solution. The mixture was evaporated and the remaining residue was further dried by sequential cycles of dissolution and evaporation of dry pyridine (2 mL × 2) and dry DMF (2 mL × 2). The dried residue was redissolved in dry DMF (2 mL), carbonyldiimidazole (800 mg, 4.93 mmol) was added. The resulting mixture was stirred overnight under nitrogen at ambient temperature. The solvent was then evaporated. Meanwhile, BHQ phosphate **160** was mixed with tri-*n*-octylamine (131 mg, 0.370 mL, 0.837 mmol) in water, followed by solvent evaporation. The remaining residue was dried by cycles of dissolution and evaporation of dry pyridine (2 mL × 2) and dry DMF (2 mL × 2). The resulting gummy residue was redissolved in dry DMF (2 mL) and added to the above ADP imidazole mixture. The DMF was evaporated and anhydrous HMPA (3 mL) added to the residue. The mixture was stirred for 2 days under a nitrogen atmosphere. The reaction was quenched with water (15 mL) and washed with chloroform (10 mL × 4) and hexane (10 mL). The aqueous layer was poured to a DEAE-cellulose column (bicarbonate form, 50 mL dry volume). The column was eluted successively with water (100 mL), and a stepping gradient of ammonium bicarbonate solution (0.05–0.30 M, 0.05 M increments, 500 mL of each concentration). The fractions with only one component were

combined and purified by HPLC (15% MeOH, 85% water, 3.3 min retention time). The pure fractions were combined and evaporated to dryness to yield **94** (90 mg, 0.11 mmole, 9.4 % yield). HPLC (85% 25 mM $KH_2PO_4$ buffer/15% methanol) chromatogram of BHQ-ATP in KMOPS is shown in Figure 43.

**$^1$H NMR** ($D_2O$) δ 7.91 (1H, s), 7.86 (1H, d, *J* = 8.0 Hz), 7.61 (1H, s), 7.32 (1H, d, *J* = 8.8 Hz), 7.20 (1H, d, *J* = 8.4 Hz), 6.89 (1H, d, *J* = 9.2 Hz), 5.68 (1H, d, *J* = 3.6 Hz), 5.01 (2H, d, *J* = 6.4 Hz), 4.29-4.23 (4H, m), 4.15-4.12 (1H, m);

**$^{31}$P NMR** ($D_2O$) δ -10.24 (d, *J* = 22 Hz), -10.34 (d, *J* = 21 Hz), -22.04 (t, *J* = 48 Hz);

**FTIR** (neat) 3042, 2338, 1623, 1438, 1218, 1067, 916 $cm^{-1}$;

**HR-MS** (ESI) *m/z* calcd for $(C_{20}H_{22}BrN_6O_{14}P_3\text{-}H)^+$ 740.9517 ($^{79}$Br) and 742.9501 ($^{81}$Br), found 740.9515 ($^{79}$Br) and 742.9499 ($^{81}$Br).

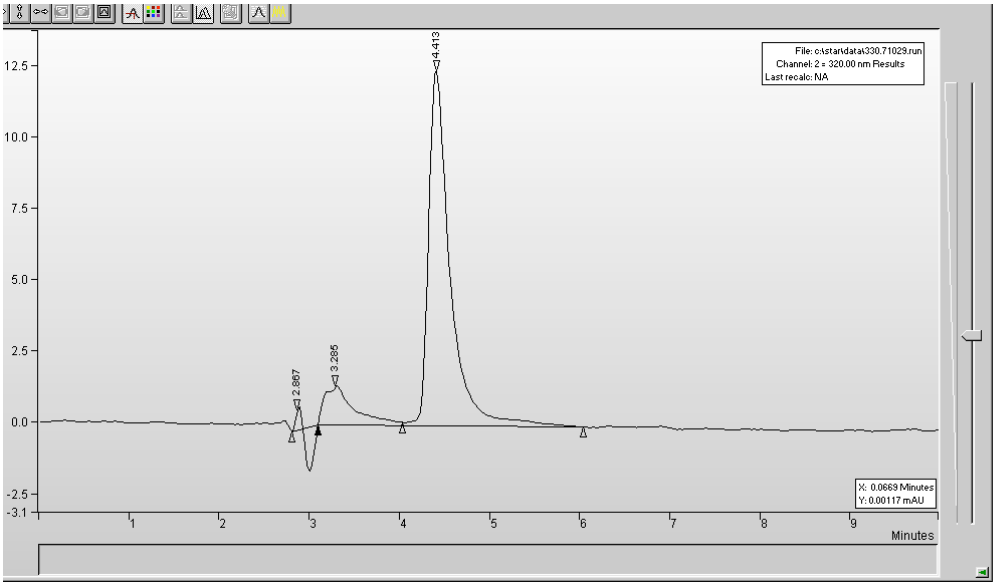


**Figure 43.** HPLC trace of BHQ-ATP

BHQ-ATP
BHQ-ATP

Automation directory: /export/home/walkup/vnmrsys/data/auto_2008.06.20
Sample id : s_20080516_005
Sample : zy4-202c

Pulse Sequence: PRESAT

Solvent: d2o
Ambient temperature
Operator: yzhu
File: zy4-202c_Presat_20080516_02
Mercury-400BB "chemnmr"

Relax. delay 0.020 sec
Pulse 45.0 degrees
Acq. time 1.998 sec
Width 6402.0 Hz
32 repetitions
OBSERVE H1, 400.1502871 MHz
DATA PROCESSING
Line broadening 0.2 Hz
FT size 65536
Total time 2 min, 5 sec

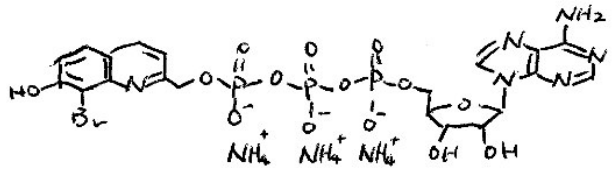


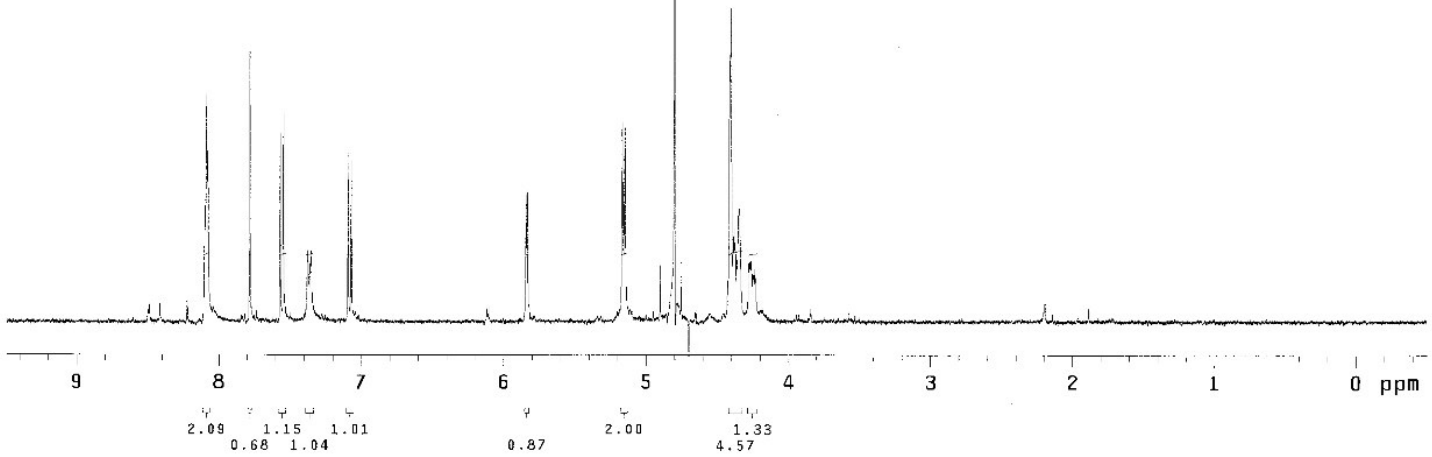

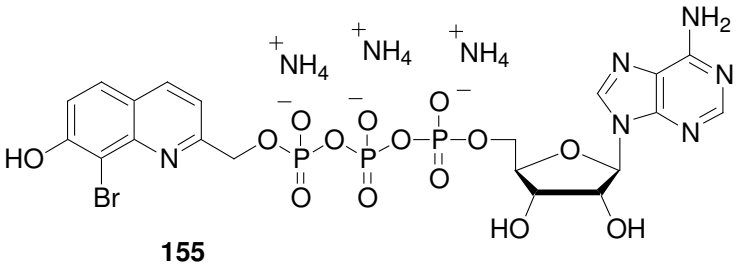

**155**

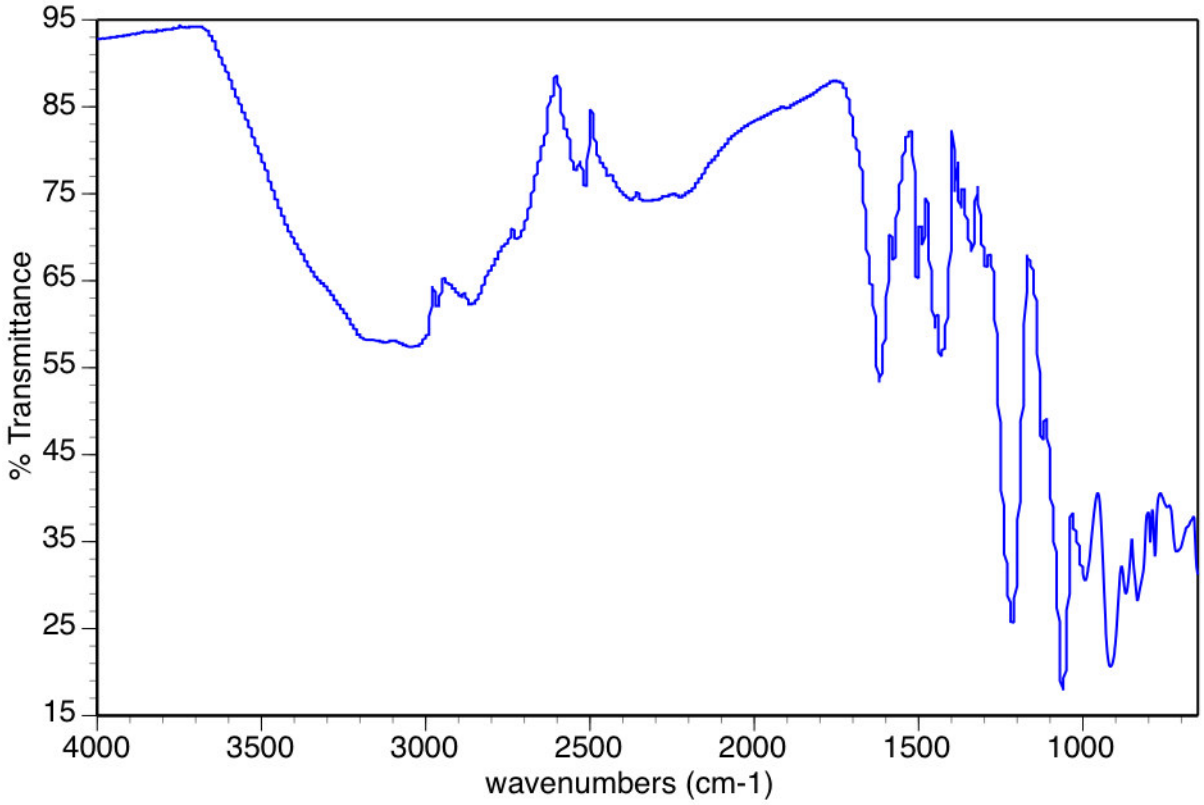
95
85
75
65
55
45
35
25
15
% Transmittance
4000
3500
3000
2500
2000
1500
1000
wavenumbers (cm-1)

***Determination of the quantum efficiency for one-photon photolysis***

KMOPS-buffered solutions (3 mL) of the substrates (100 μM) in quartz cuvettes (21-Q-10, Starna, Atascadero, CA) were irradiated with 365-nm UV light from a mercury lamp (Spectroline SB-100P; Spectronics, Westbury, NY) with a light filter. The spectral output of the lamp after the glass filters (CS0-52 and CS7-60, Ace Glass, Vineland, NJ) has a band between 350 and 380 nm. The duration of each irradiation period ranged from 5 to 60 s. After each period of irradiation, a 20-μL aliquot of the solution was removed for analysis by HPLC, using an external standard method to determine concentrations.

**Table 8.** HPLC solvent conditions for analysis of quinoline-caged compounds

| quinoline-caged compounds | Retention time of reactant (observing wavelength) | Retention time of product (observing wavelength) | Solvent conditions |
|---|---|---|---|
| **115** | 5.8 min (320 nm) | | 50/50 (0.1% TFA water/acetonitrile) |
| **118** | 5.8 min (300 nm) | 3.5 min (300 nm) | 50/50 (0.1% TFA water/acetonitrile) |
| **124** | 5.4 min (330 nm) | | 60/40 (0.1% TFA water/acetonitrile) |
| **127** | 6.4 min (332 nm) | | 50/50 (0.1% TFA water/acetonitrile) |
| **128** | 7.4 min (332 nm) | 3.4 min (260 nm) | 50/50 (0.1% TFA water/acetonitrile) |
| **143** | 7.9 min (320 nm) | | 65/35 (0.1% TFA water/acetonitrile) |
| **144** | 6.4 min (320 nm) | | 65/35 (0.1% TFA water/acetonitrile) |
| **145** | 6.8 min (438 nm) | | 60/40 (0.1% TFA water/acetonitrile) |
| **146** | 6.2 min (445 nm) | | 50/50 (0.1% TFA water/acetonitrile) |
| **147** | 5.8 min (330 nm) | | 65/35 (0.1% TFA water/acetonitrile) |
| **155** | 4.2 min (310 nm) | 2.8 min (253 nm) | 85/15 (25 mM $KH_2PO_4$ water solution/methanol) |

The analytes were eluted isocratically (flow rate of 1 mL/min) with acetonitrile and water containing 0.1% TFA (Table 8). The only exception is that BHQ-caged ATP **94** was eluted with methanol and 25 mM $KH_2PO_4$ buffer (pH = 6.2). The progress curves were plotted and fit to a single exponenial decay curve. Quantum efficiencies were calculated using equation (2).[140,141] The UV intensity of the lamp *I* was measured by potassium ferrioxalate actinometry[142] in the same setup. Piperonylic acid, 1-phenthioxypropane-2,3-diol, and ATP were monitored for their formation during the process, plotted, and fit to an exponential rise to max curve.

***Stern-Volmer triplet quenching experiment***

Sodium 2-naphthalensulfonate or potassium sorbate was dissolved in methanol and diluted to generate a 10 mM solution in KMOPS buffer. A 30-μL, 60-μL, and 90-μL aliquot was added to each of 3 different KMOPS-buffered solutions of BHQ-OAc (3 mL, 100 μM). The quantum efficiencies were determined as described for one-photon photolysis.

***Determination of the dark hydrolysis rate***

Substrates were dissolved in KMOPS and stored in the dark at room temperature. Samples for HPLC analysis were carried out periodically and injected as described for one-photon photolysis. Data were fit to single exponential decay curves from which the time constant, τ, was calculated.

***Measurement of the two-photon uncaging action cross-section***

Measurements were carried out in microcuvettes (10×1×1 mm illuminated dimensions) with an effective filling volume of 20 μL (26.10F-Q-10, Starna, Atascadero, CA). The IR laser

used was from a fs-pulsed and mode-locked Ti:sapphire laser (Mira 900 pumped by a Verdi, Coherent, Santa Clara, CA or a Chameleon Ultra II) focused on the center of the cuvette chamber with a 25-mm focal length lens optimized for IR lasers (06LXP003/076, Melles-Griot, Irvine, CA). The pulse width of the laser was 144 fs for Mira 900.

The KMOPS-buffered solutions of the substrates (20 μL) were irradiated by the IR laser in the microcuvette for a period of 5 to 40 min, and analyzed by HPLC, with the same methods and conditions as in the one-photon photolysis experiments. The progress curves were plotted, and fit to a single exponential decay curve. The formation of piperonylic acid, 1-phenthioxypropane-2,3-diol, and ATP were monitored, plotted, and fit to a single exponential rise to max curve.

The dark hydrolyses of DMAQ-OAc (**145**), DMAQ-Cl-OAc (**146**), and TQ-OAc (**147**) were fast comparing to other quinoline-caged compounds. The dark hydrolyzed percentage of the photolyzed sample was calculated using the determined dark hydrolysis rate and the waiting time for injection, and this value was subtracted from the result of HPLC analysis. And the corrected values were plotted and fit to a single exponential decay curve.

The two-photon uncaging cross-section ($\delta_u$) was determined using Tsien's method.[15] Referencing to fluorescein, which has a known fluorescence quantum yield ($Q_{fF}$ = 0.9 mol/ein) and absorbance cross-section ($\delta_{aF}$ = 30 GM at 740 nm),[116,143] using equation (1). The time-averaged fluorescent photon flux <F(t)> was calculated from the fluorescence of fluorescein, it emitted at a right angle to the beam and passed though a 535/45 nm bandpass filter (Chroma Technologies, Brattleboro, VT) was measured by an SED033 detector on an IL–1700 (International Light, Newburyport, MA). The number of molecules that undergo photochemical transformation $N_p$ was determined by simulation of one-second photolysis using the exponential decay curve acquired from the HPLC analyses.

***Oxygen-18 Labeling Experiment***

A 100-μM solution of BHQ-OAc in water was irradiated at 365 nm from a mercury lamp (Spectroline SB-100P; Spectronics, Westbury, NY) for 2.5 min as described for one-photon photolysis. The reaction mixture was analyzed by LC-MS (Biobasic 4 column, 150 × 1 mm, 50 μm, 300 Å; gradient elution of acetonitrile and water/TFA, 0 min 0% acetonitrile, 8 min 40% acetonitrile, 40 min 70% acetonitrile, 45 min 100% acetonitrile; analysis at 214 nm), selecting the peak corresponding to BHQ-OH for mass analysis. A 100-μM solution of BHQ-OAc in $^{18}$O-labeled water was irradiated for 2.5 min, and the reaction was analyzed by LC-MS using the same conditions as in the control experiment.

***Photolysis in dry acetonitrile-$d_3$ and acetonitrile-$d_3$ with trace water***

BHQ-OAc (5 mg) was dissolved in 1 mL dry acetonitrile–$d_3$ (or acetonitrile–$d_3$ with addition of 50 μL water) and charged to a quartz NMR tube. An $^1$H NMR spectrum was acquired as time 0. The sample was irradiated at 254 nm in a Rayonet photoreactor. Periodically, the photolysis was stopped to acquire an $^1$H NMR spectrum to monitor the reaction progress.

## References


(1) Engels, J.; Schlager, E.-J. Synthesis, Structure, and Reactivity of Adenosine Cyclic 3′,5′-Phosphate Benzyl Triesters. *J. Med. Chem.* **1977**, *20*, 907-011.

(2) Kaplan, J. H.; Forbush, B., III; Hoffman, J. F. Rapid photolytic release of adenosine 5′-triphosphate from a protected analogue: Utilization by the Na:K pump of human red blood cell ghosts. *Biochemistry* **1978**, *17*, 1929-1935.

(3) Greene, T. W.; Wuts, P. G. M. *Protective Groups in Organic Synthesis*; 3rd ed.; John Wiley & Sons: New York, **1999**.

(4) *Caged Compounds*; Marriott, G., Ed.; Academic Press: New York, **1998**; Vol. 291.

(5) Adams, S. R.; Tsien, R. Y. Controlling cell chemistry with caged compounds. *Annu. Rev. Physiol.* **1993**, *55*, 755-784.

(6) Pelliccioli, A. P.; Wirz, J. Photoremovable protecting groups: reaction mechanisms and applications. *Photochem.Photobio. Sci.* **2002**, *1*, 441-458.

(7) Bochet, C. G. Photolabile Protecting Groups and Linkers. *J. Chem. Soc, Perk. Trans. 1* **2002**, 125-142.

(8) Il'ichev, Y. V.; Schwoerer, M. A.; Wirz, J. Photochemical Reaction Mechanisms of 2-Nitrobenzyl Compounds: Methyl Ethers and Caged ATP. *J. Am. Chem. Soc* **2004**, *126*, 4581-4595.

(9) Papageorgiou, G. L.; Matthew, L.; Wan, P.; Corrie, J. E. T. An antenna triplet sensitiser for 1-acyl-7-nitroindolines improves the efficiency of carboxylic acid photorelease. *Photochem. Photobiol. Sci.* **2004**, *3*, 366-373.

(10) Walker, J. W.; Reid, G. P.; McCray, J. A.; Trentham, D. R. Photolabile 1-(2-nitrophenyl)ethyl phosphate esters of adenine nucleotide analogs. Synthesis and mechanism of photolysis. *J. Am. Chem. Soc*. **1988**, *110*, 7170-7177.

(11) Corrie, J. E. T.; Trentham, D. R. Caged Nucleotides and Neurotransmitters. In *Biological Applications of Photochemical Switches*; Morrison, H., Ed.; John Wiley & Sons: New York, **1993**, p 243-305.

(12) Kiskin, N. I.; Chillingworth, R.; McCray, J. A.; Piston, D.; Ogden, D. The efficiency of two-photon photolysis of a "caged" fluorophore, *o*-1-(2-nitrophenyl)ethylpyranine, in relation to photodamage of synaptic terminals. *Eur. Biophys. J.* **2002**, *30*, 588-604.

(13) Echevarria, W.; Leite, M. F.; Guerra, M. T.; Zipfel, W. R.; Nathanson, M. H. Regulation of calcium signals in the nucleus by a nucleoplasmic reticulum. *Nat. Cell Biol.* **2003**, *5*, 440-446.

(14) Gurney, A. M.; Lester, H. A. Light-Flash Physiology with Synthetic Photosensitive Compounds. *Physiol. Rev.* **1987**, *67*, 583-617.

(15) Furuta, T.; Wang, S. S. H.; Dantzker, J. L.; Dore, T. M.; Bybee, W. J.; Callaway, E. M.; Denk, W.; Tsien, R. Y. Brominated 7-hydroxycoumarin-4-ylmethyls: photolabile protecting groups with biologically useful cross-sections for two photon photolysis. *Proc. Natl. Acad. Sci. USA* **1999**, *96*, 1193-1200.

(16) Billington, A. P.; Walstrom, K. M.; Ramesh, D.; Guzikowski, A. P.; Carpenter, B. K.; Hess, G. P. Synthesis and photochemistry of photolabile *N*-glycine derivatives and effects of one on the glycine receptor. *Biochemistry* **1992**, *31*, 5500-5507.

(17) Milburn, T.; Matsubara, N.; Billington, A. P.; Udgaonkar, J. B.; Walker, J. W.; Carpenter, B. K.; Webb, W. W.; Marque, J.; Denk, W.; McCray, J. A.; Hess, G. P. Synthesis, photochemistry, and biological activity of a caged photolabile acetylcholine receptor ligand. *Biochemistry* **1989**, *28*, 49-55.

(18) Wieboldt, R.; Gee, K. R.; Niu, L.; Ramesh, D.; Carpenter, B. K.; Hess, G. P. Photolabile precursors of glutamate: synthesis, photochemical properties, and activation of glutamate receptors on a microsecond time scale. *Proc. Natl. Acad. Sci. USA* **1994**, *91*, 8752-8756.

(19) Wang, L.; Corrie, J. E. T.; Wootton, J. F. Photolabile Precursors of Cyclic Nucleotides with High Aqueous Solubility and Stability. *J. Org. Chem.* **2002**, *67*, 3474-3478.

(20) Pollock, J.; Crawford, J. H.; Wootton, J. F.; Corrie, J. E. T.; Scott, R. H. A comparison between the distinct inward currents activated in rat cultured dorsal root ganglion neurones by intracellular flash photolysis of two forms of caged cyclic guanosine monophosphate. *Neurosci. Lett.* **2003**, *338*, 143-146.

(21) Ordoukhanian, P.; Taylor, J. S. Caged Single and Double Strand Breaks. *Bioconjug. Chem.* **2000**, *11*, 94-103.

(22) Zhang, K.; Taylor, J. S. Phototriggered Formation and Repair of DNA Containing a Site-Specific Single Strand Break of the Type Produced by Ionizing Radiation or AP Lyase Activity. *Biochemistry* **2001**, *40*, 153-159.

(23) Schaper, K.; Mobarekeh, S. A. M.; Grewer, C. Synthesis and Photophysical Characterization of a New, Highly Hydrophilic Caging Group. *Eur. J. of Org. Chem.* **2002**, 1037-1046.

(24) Rossi, F. M.; Margulis, M.; Tang, C. M.; Kao, J. P. Y. N-Nmoc-L-glutamate, a new caged glutamate with high chemical stability and low pre-photolysis activity. *J. Biol. Chem.* **1997**, *272*, 32933-32939.

(25) Sundberg, S. A.; Barrett, R. W.; Pirrung, M.; Lu, A. L.; Kiangsoontra, B.; Holmes, C. P. Spatially-Addressable Immobilization of Macromolecules on Solid Supports. *J. Am. Chem. Soc*. **1995**, *117*, 12050-12057.

(26) Pirrung, M.; Huang, C. Y. A General Method for the Spatially Defined Immobilization of Biomolecules on Glass Surfaces Using "Caged" Biotin. *Bioconjug. Chem.* **1996**, *7*, 317-321.

(27) Sreekumar, R.; Pi, Y. Q.; Huang, X. P.; Walker, J. W. Stereospecific protein kinase C activation by photolabile diglycerides. *Bioorg. Med. Chem. Lett.* **1997**, *7*, 341-346.

(28) Rossi, F. M.; Kao, J. P. Y. Nmoc-DBHQ, a new caged molecule for modulating sarcoplasmic/endoplasmic reticulum Ca2+ ATPase activity with light flashes. *J. Biol. Chem.* **1997**, *272*, 3266-3271.

(29) Wootton, J. F.; Corrie, J. E. T.; Capiod, T.; Feeney, J.; Trentham, D. R.; Ogden, D. C. Kinetics of cytosolic Ca2+ concentration after photolytic release of 1-D-myo-inositol 1,4-bisphosphate 5-phosphorothioate from a caged derivative in guinea pig hepatocytes. *Biophys. J.* **1995**, *68*, 2601-2607.

(30) Khan, S.; Castellano, F.; Spudich, J. L.; McCray, J. A.; Goody, R. S.; Reid, G. P.; Trentham, D. R. Excitatory signaling in bacterial probed by caged chemoeffectors. *Biophys. J.* **1993**, *65*, 2368-2382.

(31) Barth, A.; Corrie, J. E. T. Characterization of a New Caged Proton Capable of Inducing Large pH Jumps. *Biophys. J.* **2002**, *83*, 2864-2871.

(32) Ellis-Davies, G. C. R.; Kaplan, J. H.; Barsotti, R. J. Laser photolysis of caged calcium: rates of calcium release by nitrophenyl-EGTA and DM-nitrophen. *Biophys. J.* **1996**, *70*, 1006-1016.

(33) Krafft, G. A.; Sutton, W. R.; Cummings, R. T. Photoactivable fluorophores. 3. Synthesis and photoactivation of fluorogenic difunctionalized fluoresceins. *J. Am. Chem. Soc* **1988**, *110*, 301-303.

(34) Canepari, M.; Nelson, L.; Papageorgiou, G.; Corrie, J. E. T.; Ogden, D. Photochemical and pharmacological evaluation of 7-nitroindolinyl-and 4-methoxy-7-nitroindolinyl-amino acids as novel, fast caged neurotransmitters. *J.Neurosci. Methods* **2001**, *112*, 29-42.

(35) Amit, B.; Ben-Efraim, D. A.; Patchornik, A. Light-sensitive amides. The photosolvolysis of substituted 1-acyl-7-nitroindolines. *J. Am. Chem. Soc* **1976**, *98*, 843-844.

(36) Pass, S.; Amit, B.; Patchornik, A. Racemization-free photochemical coupling of peptide segments. *J. Am. Chem. Soc*. **1981**, *103*, 7674-7675.

(37) Papageorgiou, G.; Ogden, D. C.; Barth, A.; Corrie, J. E. T. Photorelease of carboxylic acids from 1-acyl-7-nitroindolines in aqueous solution: Rapid and efficient photorelease of L-glutamate. *J. Am. Chem. Soc*. **1999**, *121*, 6503-6504.

(38) Morrison, J.; Wan, P.; Corrie, J. E. T.; Papageorgiou, G. Mechanisms of photorelease of carboxylic acids from 1-acyl-7-nitroindolines in solutions of varying water content. *Photochem. Photobiol. Sci.* **2002**, *1*, 960-969.

(39) Papageorgiou, G.; Corrie, J. E. T. Effects of aromatic substituents on the photocleavage of 1-acyl-7-nitroindolines. *Tetrahedron* **2000**, *56*, 8197-8205.

(40) Papageorgiou, G.; Corrie, J. E. T. Regioselective nitration of 1-acyl-4-methoxyindolines leads to efficient synthesis of a photolabile L-glutamate precursor. *Syn. Comm.* **2002**, *32*, 1571-1577.

(41) Adams, S. R.; Kao, J. P. Y.; Tsien, R. Y. Biologically useful chelators that take up calcium(2+) upon illumination. *J. Am. Chem. Soc*. **1989**, *111*, 7957-7968.

(42) Hiller, K. O.; Masloch, B.; Goebl, M.; Asmus, K. D. Mechanism of the hydroxyl radical induced oxidation of methionine in aqueous solution. *J. Am. Chem. Soc*. **1981**, *103*, 2734-2743.

(43) Sheehan, J. C.; Wilson, R. M.; Oxford, A. W. Photolysis of methoxy-substituted benzoin esters. Photosensitive protecting group for carboxylic acids. *J. Am. Chem. Soc.* **1971**, *93*, 7222-7228.

(44) Givens, R. S.; Park, C.-H. Hydroxyphenacyl ATP: a new phototrigger. V. *Tetrahedron Lett.* **1996**, *37*, 6259-6262.

(45) Corrie, J. E. T.; Trentham, D. R. Caged Nucleotides and Neurotransmitters. In *Biological Applications of Photochemical Switches*; Morrison, H., Ed.; John Wiley & Sons: New York, **1994**, p 243-305.

(46) Sokolov, V. S.; Apell, H.-J.; Corrie, J. E. T.; Trentham, D. R. Fast Transient Currents in Na,K-ATPase Induced by ATP Concentration Jumps from the P3-[1-(3',5'-Dimethoxyphenyl)-2-Phenyl-2-Oxo]ethyl Ester of ATP. *Biophys. J.* **1998**, *74*, 2285-2298.

(47) Corrie, J. E. T.; Katayama, Y.; Reid, G. P.; Anson, M.; Trentham, D. R. The development and application of photosensitive caged compounds to aid time-resolved structure determination of macromolecules. *Philos. Trans. R. Soc. Lond., Ser. A* **1992**, *340*, 233-244.

(48) Shi, Y.; Corrie, J. E. T.; Wan, P. Mechanism of 3',5'-Dimethoxybenzoin Ester Photochemistry: Heterolytic Cleavage Intramolecularly Assisted by the Dimethoxybenzene Ring Is the Primary Photochemical Step. *J. Org. Chem.* **1997**, *62*, 8278-8279.

(49) Rajesh, C. S.; Givens, R. S.; Wirz, J. Kinetics and Mechanism of Phosphate Photorelease from Benzoin Diethyl Phosphate: Evidence for Adiabatic Fission to a -Keto Cation in the Triplet State. *J. Am. Chem. Soc*. **2000**, *122*, 611-618.

(50) Givens, R. S.; Lee, J.-I. The *p*-hydroxyphenacyl photoremovable protecting group. *J. Photosci.* **2003**, *10*, 37-48.

(51) Anderson, J. C.; Reese, C. B. A photo-induced rearrangement involving aryl participation. *Tetrahedron Lett.* **1962**, *3*, 1-4.

(52) Givens, R. S.; Kueper, L. W. Photochemistry of phosphate esters. *Chem. Rev.* **1993**, *93*, 55-66.

(53) Park, C.-H.; Givens, R. S. New Photoactivated Protecting Groups. 6. *p*-Hydroxyphenacyl: A Phototrigger for Chemical and Biochemical Probes. *J. Am. Chem. Soc.* **1997**, *119*, 2453-2463.

(54) Zhang, K.; Corrie, J. E. T.; Munasinghe, V. R. N.; Wan, P. Mechanism of Photosolvolytic Rearrangement of p-Hydroxyphenacyl Esters: Evidence for Excited-State Intramolecular

Proton Transfer as the Primary Photochemical Step. *J. Am. Chem. Soc*. **1999**, *121*, 5625-5632.

(55) Fischer, M.; Wan, P. *m*-Quinone Methides from m-Hydroxy-1,1-Diaryl Alkenes via Excited-State (Formal) Intramolecular Proton Transfer Mediated by a Water Trimer. *J. Am. Chem. Soc*. **1998**, *120*, 2680-2681.

(56) Kandler, K.; Katz, L. C.; Kauer, J. A. Focal photolysis of caged glutamate produces long-term depression of hippocampal glutamate receptors. *Nat. Neurosci.* **1998**, *1*, 119-123.

(57) Givens, R. S.; Weber, J. F. W.; Conrad, P. G., II; Orosz, G.; Donahue, S. L.; Thayer, S. A. New Phototriggers 9: *p*-Hydroxyphenacyl as a C-Terminal Photoremovable Protecting Group for Oligopeptides. *J. Am. Chem. Soc*. **2000**, *122*, 2687-2697.

(58) Barltrop, J. A.; Schofield, P. Photosensitive Protecting Groups. *Tetrahedron Lett.* **1962**, *3*, 697-699.

(59) Chamberlain, J. W. Use of the 3,5-Dimethoxybenzyloxycarbonyl Group as a Photosensitive N-Protecting Group. *J. Org. Chem.* **1966**, *31*, 1658-1660.

(60) Zimmerman, H. E.; Sandel, V. R. Mechanistic Organic Photochemistry. II.1,2 Solvolytic Photochemical Reactions. *J. Am. Chem. Soc*. **1963**, *85*, 915-922.

(61) Givens, R. S.; Matuszewski, B.; Levi, N.; Leung, D. Photodecarboxylation. A labeling study. Mechanistic studies in photochemistry. 15. *J. Am. Chem. Soc*. **1977**, *99*, 1896-1903.

(62) Pincock, J. A. The photochemistry of Esters of Carboxylic Acids. In *Handbook of Organic Photochemistry and Photobiology* **2003**.

(63) Schade, B.; Hagen, V.; Schmidt, R.; Herbich, R.; Krause, E.; Eckardt, T.; Bendig, J. Deactivation behavior and excited state properties of (coumarin-4-yl)methyl derivatives. 1.

Photocleavage of (7-methoxycoumarin-4-yl)methyl-caged acids with fluorescence enhancement. *J. Org. Chem.* **1999**, *64*, 9109-9117.

(64) Hagen, V.; Bendig, J.; Frings, S.; Eckardt, T.; Helm, S.; Reuter, D.; Kaupp, U. B. Highly Efficient and Ultrafast Phototriggers for cAMP and cGMP by Using Long-Wavelength UV/Vis-Activation. *Angew. Chem., Int. Ed.* **2001**, *40*, 1046-1048.

(65) Schmidt, R.; Geissler, D.; Hagen, V.; Bendig, J. Mechanism of Photocleavage of (Coumarin-4-yl)methyl Esters. *J. Phys. Chem. A* **2007**, *111*, 5768-5774.

(66) Furuta, T.; Torigai, H.; Sugimoto, M.; Iwamura, M. Photochemical Properties of New Photolabile cAMP Derivatives in a Physiological Saline Solution. *J. Org. Chem.* **1995**, *60*, 3953-3956.

(67) Hagen, V.; Bendig, J.; Frings, S.; Weisner, B.; Schade, B.; Helm, S.; Lorenz, D.; Kaupp, U. B. Synthesis Photochemistry and Application of (7-Methoxycoumarin-4-yl)methyl-caged 8-bromoadenosine cyclic 3',5'-monophosphate and 8-Bromoguanosine cyclic 3',5'-monophosphate Photolyzed in the Nanosecond Time Region. *J. Photochem. Photobiol. B:* **1999**, *53*, 91-102.

(68) Eckardt, T.; Hagen, V.; Schade, B.; Schmidt, R.; Schweitzer, C.; Bendig, J. Deactivation Behavior and Excited-State Properties of (Coumarin-4-yl)methyl Derivatives. 2. Photocleavage of Selected (Coumarin-4-yl)methyl-Caged Adenosine Cyclic 3´,5´-Monophosphates with Fluorescence Enhancement. *J. Org. Chem.* **2002**, *67*, 703-710.

(69) Schönleber, R. O.; Bendig, J.; Hagen, V.; Giese, B. Rapid Photolytic Release of Cytidine 5´-Diphosphate from a Coumarin Derivative: a New Tool fo the Investigation of Ribonucleotide Reductases. *Bioorg. & Med. Chem. Lett.* **2002**, *10*, 97-101.

(70) Geissler, D.; Kresse, W.; Wiesner, B.; Bendig, J.; Kettenmann, H.; Hagen, V. DMACM-caged adenosine nucleotides: Ultrafast phototriggers for ATP, ADP, and AMP activated by long-wavelength irradiation. *ChemBioChem* **2003**, *4*, 162-170.

(71) Goard, M.; Aakalu, G.; Fedoryak, O. D.; Quinonez, C.; St. Julien, J.; Poteet, S. J.; Schuman, E. M.; Dore, T. M. Light-Mediated Inhibition of Protein Synthesis. *Chem. Biol.* **2005**, *12*, 685-693.

(72) Suzuki, A. Z.; Watanabe, T.; Kawamoto, M.; Nishiyama, K.; Yamashita, H.; Ishii, M.; Iwamura, M.; Furuta, T. Coumarin-4-ylmethoxycarbonyls as phototriggers for alcohols and phenols. *Org. Lett.* **2003**, *5*, 4867-4870.

(73) Lin, W.; Lawrence, D. S. A strategy for the construction of caged diols using a photolabile protecting group. *J. Org. Chem.* **2002**, *67*, 2723-2726.

(74) Lu, M.; Fedoryak, O. D.; Moister, B. R.; Dore, T. M. Bhc-diol as a photolabile protecting group for aldehydes and ketones. *Org. Lett.* **2003**, *5*, 2119-2122.

(75) Hagen, V.; Frings, S.; Wiesner, B.; Helm, S.; Kaupp, U. B.; Bendig, J. [7-(Dialkylamino)coumarin-4-yl]methyl-caged compounds as ultrafast and effective long-wavelength phototriggers of 8-bromo-substituted cyclic nucleotides. *ChemBioChem* **2003**, *4*, 434-442.

(76) Karpen, J. W.; Zimmerman, A. L.; Stryer, L.; Baylor, D. A. Gating Kinetics of the Cyclic-GMP-Activated Channel of Retinal Rods: Flash Photolysis and Voltage-Jump Studies. *Proc. Natl. Acad. Sci. USA* **1988**, *85*, 1287-1291.

(77) Gauss, R.; Seifert, R.; Kaupp, U. B. Molecular identification of a hyperpolarization-activated channel in sea urchin sperm. *Nature* **1998**, *393*, 583-587.

(78) Seifert, R.; Scholten, A.; Gauss, R.; Mincheva, A.; Lichter, P.; Kaupp, U. B. Molecular characterization of a slowly gating human hyperpolarization-activated channel predominantly expressed in thalamus, heart, and testis. *Proc. Natl. Acad. Sci. USA* **1999**, *96*, 9391-9396.

(79) Brown, E. B.; Shear, J. B.; Adams, S. R.; Tsien, R. Y.; Webb, W. W. Photolysis of caged calcium in femtoliter volumes using two-photon excitation. *Biophys. J.* **1999**, *76*, 489-499.

(80) DelPrincipe, F.; Egger, M.; Ellis-Davies, G. C. R.; Niggli, E. Two-photon and UV-laser flash photolysis of the $Ca^{2+}$ cage, dimethoxynitrophenyl-EGTA-4. *Cell Calcium* **1999**, *25*, 85-91.

(81) Kaplan, J. H.; Ellis-Davies, G. C. R. Photolabile chelators for the rapid photorelease of divalent cations. *Proc. Natl. Acad. Sci. USA* **1988**, *85*, 6571-6575.

(82) Ellis-Davies, G. C. R.; Kaplan, J. H. A new class of photolabile chelators for the rapid release of divalent cations: generation of caged Ca and caged Mg. *J. Org. Chem.* **1988**, *53*, 1966-1969.

(83) Adams, S. R.; Lev-Ram, V.; Tsien, R. Y. A new caged $Ca^{2+}$, azid-1, is far more photosensitive than nitrobenzyl-based chelators. *Chem. Biol.* **1997**, *4*, 867-878.

(84) Troullier, A.; Gerwert, K.; Dupont, Y. A time-resolved Fourier transformed infrared difference spectroscopy study of the sarcoplasmic reticulum Ca(2+)-ATPase: kinetics of the high-affinity calcium binding at low temperature. *Biophys. J.* **1996**, *71*, 2970-2983.

(85) Denk, W. Two-photon scanning photochemical microscopy: Mapping ligand-gated ion channel distributions. *Proc. Natl. Acad. Sci. USA* **1994**, *91*, 6629-6633.

(86) Matsuzaki, M.; Ellis-Davies, G. C. R.; Nemoto, T.; Miyashita, Y.; Iino, M.; Kasai, H. Dendritic spine geometry is critical for AMPA receptor expression in hippocampal CA1 pyramidal neurons. *Nat. Neurosci.* **2001**, *4*, 1086-1092.

(87) Smith, M. A.; Ellis-Davies, G. C. R.; Magee, J. C. Mechanism of the distance-dependent scaling of Schaffer collateral synapses in rat CA1 pyramidal neurons. *J. Physiol.* **2003**, *548*, 245-258.

(88) Sakmann, B.; Neher, E. *Single-channel Recording*; 2nd ed.; Plenum Press: New York, **1995**.

(89) Arias, H. R. Role of local anesthetics on both cholinergic and serotonergic ionotropic receptors. *Neurosci. Biobehavioral Rev.* **1999**, *23*, 817-843.

(90) Adams, P. R. Drug blockage of open end-plate channels. *J. Physiol.* **1976**, *260*, 531-552.

(91) Grewer, C.; Hess, G. P. On the mechanism of inhibition of a nicotinic acetylcholine receptor by the anticonvulsant MK-801 investigated by laser pulse photolysis in the microsecond-to-millisecond time region. *Biochemistry* **1999**, *38*, 7837-7846.

(92) Hess, G. P.; Ulrich, H.; Breitinger, H.-G.; Niu, L.; Gameiro, A. M.; Grewer, C.; Srivastava, S.; Ippolito, J. E.; Lee, S.; Jayaraman, V.; Coombs, S. E. Mechanism-based discovery of ligands that prevent inhibition of the nicotinic acetylcholine receptor by cocaine and MK-801. *Proc. Natl. Acad. Sci. USA* **2000**, *97*, 13895-13900.

(93) Hess, G. P.; Gameiro, A. M.; Schoenfeld, R. C.; Chen, Y.; Ulrich, H.; Nye, J. A.; Sit, B.; Carroll, F. I.; Ganem, B. Reversing the action of noncompetitive inhibitors (MK-801 and cocaine) on a protein (nicotinic acetylcholine receptor)-mediated reaction. *Biochemistry* **2003**, *42*, 6106-6114.

(94) Patchornik, A.; Amit, B.; Woodward, R. B. Photosensitive protecting groups. *J. Am. Chem. Soc*. **1970**, *92*, 6333-6335.

(95) Rusiecki, V. K.; Warne, S. A. Synthesis of N-Fmoc-N-Nvoc-Lysine and use in the preparation of selectively functionalized peptides. *Bioorg. Med. Chem. Lett.* **1993**, *3*, 707-710.

(96) Church, G.; Ferland, J. M.; Gauthier, J. Photolabile *p*-methoxyphenacyloxycarbonyl group for the protection of amines. *Tetrahedron Lett.* **1989**, *30*, 1901-1904.

(97) Pirrung, M. C.; Nunn, D. S. Synthesis of photodeprotectable serine derivatives. "Caged serine". *Bioorg. Med. Chem. Lett.* **1992**, *2*, 1489-1492.

(98) Kalbag, S. M.; Roeske, R. W. Photolabile protecting group for histidine. *J. Am. Chem. Soc.* **1975**, *97*, 440-441.

(99) Shigeri, Y.; Tatsu, Y.; Yumoto, N. Synthesis and application of caged peptides and proteins. *Pharmacol. Ther.* **2001**, *91*, 85-92.

(100) Marriott, G.; Roy, P.; Jacobson, K. Preparation and light-directed activation of caged proteins. *Methods Enzymol.* **2003**, *360*, 274-288.

(101) Walker, J. W.; Gilbert, S. H.; Drummond, R. M.; Yamada, M.; Sreekumar, R.; Carraway, R. E.; Ikebe, M.; Fay, F. S. Signaling Pathways Underlying Eosinophil Cell Motility Revealed by Using Caged Peptides. *Proc. Natl. Acad. Sci. USA* **1998**, *95*, 1568-1573.

(102) Zou, K.; Miller, W. T.; Givens, R. S.; Bayley, H. Caged thiophosphotyrosine peptides. *Angew. Chem. Int. Ed.* **2001**, *40*, 3049-3051.

(103) Pan, P.; Bayley, H. Caged cysteine and thiophosphoryl peptides. *FEBS Lett.* **1997**, *405*, 81-85.

(104) Lawrence, D. S. The preparation and in vivo applications of caged peptides and proteins. *Curr. Opin. Chem. Biol.* **2005**, *9*, 570-575.

(105) Humphrey, D.; Rajfur, Z.; Vazquez, M. E.; Scheswohl, D.; Schaller, M. D.; Jacobson, K.; Imperiali, B. *In Situ* Photoactivation of a caged phosphotyrosine peptide derived from focal adhesion kinase temporarily halts lamellar extension of single migrating tumor cells. *J. Biol. Chem.* **2005**, *280*, 22091-22101.

(106) Loudwig, S.; Bayley, H. Light-activated Proteins: An Overview. In *Dynamic Studies in Biology*; Goeldner, M., Givens, R. S., Eds. **2005**.

(107) Endo, M.; Nakayama, K.; Majima, T. Design and Synthesis of Photochemically Controllable Restriction Endonuclease BamHI by Manipulating theSalt-Bridge Network in the Dimer Interface. *J. Org. Chem.* **2004**, *69*, 4292-4298.

(108) Chaulk, S. G.; MacMillan, A. M. Separation of Spliceosome Assembly from Catalysis with Caged pre-mRNA Substrates. *Angew. Chem. Int. Ed.* **2001**, *40*, 2149-2152.

(109) Ando, H.; Furuta, T.; Tsien, R. Y.; Okamoto, H. Photo-mediated gene activation using caged RNA/DNA in zebrafish embryos. *Nat. Gene.* **2001**, *28*, 317-325.

(110) Göppert-Mayer, M. Über Elementarakte mit zwei Quantensprüngen. *Annalen der Physik* **1931**, *9*, 273-294.

(111) Göppert-Mayer, M. Über die Wahrscheinlichkeit des Zusammenwirkens zweier Lichtquanten in einem Elementarakt. *Naturwissenschaften* **1929**, *17*, 932.

(112) Kaiser, W.; Garrett, C. G. B. Two-photon excitation in $CaF_2$:$Eu^{2+}$. *Phys. Rev. Lett.* **1961**, *7*, 229-231.

(113) Denk, W.; Strickler, J. H.; Webb, W. W. Two-photon laser scanning fluorescence microscopy. *Science* **1990**, *248*, 73-76.

(114) Xu, C.; Zipfel, W.; Shear, J. B.; Williams, R. M.; Webb, W. W. Multiphoton fluorescence excitation: new spectral windows for biological nonlinear microscopy. *Proc. Natl. Acad. Sci. USA* **1996**, *93*, 10763-10768.

(115) Xu, C.; Webb, W. W. Multiphoton Excitation of Molecular Fluorophores and Nonlinear Laser Microscopy. In *Topics in Fluorescence Spectroscopy: Nonlinear and Two-Photon-Induced Fluorescence*; Lakowicz, J., Ed.; Plenum Press: New York, **1997**; Vol. 5, p 471-540.

(116) Xu, C.; Webb, W. W. Measurement of two-photon excitation cross sections of molecular fluorophores with data from 690 to 1050 nm. *J. Opt. Soc. Am. B: Opt. Phys.* **1996**, *13*, 481-491.

(117) Song, J. M.; Inque, T.; Kawazumi, H.; Ogawa, T. Determination of Two Photon Absorption Cross Section of Fluorescein Using a Mode Locked Titanium Sapphire Laser. *Anal. Sci.* **1999**, *15*, 601-605.

(118) Momotake, A.; Lindegger, N.; Niggli, E.; Barsotti, R. J.; Ellis-Davies, G. C. R. The nitrodibenzofuran chromophore: a new caging group for ultra-efficient photolysis in living cells. *Nat. Methods* **2006**, *3*, 35-40.

(119) Albota, M.; Beljonne, D.; Bredas, J.-L.; Ehrlich, J. E.; Fu, J.-Y.; Heikal, A. A.; Hess, S. E.; Kogej, T.; Levin, M. D.; Marder, S. R.; McCord-Maughon, D.; Perry, J. W.; Rockel, H.; Rumi, M.; Subramaniam, G.; Webb, W. W.; Wu, X.-L.; Xu, C. Design of organic molecules with large two-photon absorption cross sections. *Science* **1998**, *281*, 1653-1656.

(120) Reinhardt, B. A.; Brott, L. L.; Clarson, S. J.; Dillard, A. G.; Bhatt, J. C.; Kannan, R.; Yuan, L.; He, G. S.; Prasad, P. N. Highly active two-photon dyes: Design, synthesis, and characterization toward application. *Chem. Mat.* **1998**, *10*, 1863-1874.

(121) Aujard, I.; Benbrahim, C.; Gouget, M.; Ruel, O.; Baudin, J.-B.; Neveu, P.; Jullien, L. o-Nitrobenzyl Photolabile Protecting Groups with Red-Shifted Absorption: Syntheses and Uncaging Cross-Sections for One- and Two-Photon Excitation. *Chem. Eur. J.* **2006**, *12*, 6865-6879.

(122) Gug, S.; Charon, S.; Specht, A.; Alarcon, K.; Ogden, D.; Zietz, B.; Leonard, J.; Haacke, S.; Bolze, F.; Nicoud, J.-F.; Goeldner, M. Photolabile Glutamate Proecting Group with High One- and Two-Photon Uncaging Efficiencies. *ChemBioChem* **2008**, *9*, 1303-1307.

(123) Furuta, T.; Takeuchi, H.; Isozaki, M.; Takahashi, Y.; Kanehara, M.; Sugimoto, M.; Watanabe, T.; Noguchi, K.; Dore, T. M.; Kurahashi, T.; Iwamura, M.; Tsien, R. Y. Bhc-cNMPs as either water-soluble or membrane-permeant photo-releasable cyclic nucleotides for both one and two-photon excitations. *ChemBioChem* **2004**, *5*, 1119-1128.

(124) Geissler, D.; Antonenko, Y. N.; Schmidt, R.; Keller, S.; Krylova, O. O.; Wiesner, B.; Bendig, J.; Pohl, P.; Hagen, V. (Coumarin-4-yl)methyl Esters as Highly Efficient, Ultrafast Phototriggers for Protons and Their Application to Acidifying Membrane Surfaces. *Angew. Chem. Int. Ed.* **2005**, *44*, 1195-98.

(125) Gagey, N.; Neveu, P.; Jullien, L. Two-Photon Uncaging with the Efficient 3,5-Dibromo-2,4-dihydroxycinnamic Caging Group. *Angew. Chem. Int. Ed.* **2007**, *46*, 2467-2469.

(126) Gagey, N.; Neveu, P.; Benbrahim, C.; Goetz, B.; Aujard, I.; Baudin, J.-B.; Jullien, L. Two-photon Uncaging with Fluorescence Reporting: Evaluation of the o-Hydroxycinnamic Platform. *J. Am. Chem. Soc*. **2007**, *129*, 9986-9998.

(127) Turner, A. D.; Pizzo, S. V.; Rozakis, G. Photoreactivation of irreversibly inhibited serine proteinases. *J. Am. Chem. Soc*. **1988**, *110*, 244-250.

(128) Kantevari, S.; Hoang, C. J.; Ogrodnik, J.; Egger, M.; Niggli, E.; Ellis-Davies, G. C. R. Synthesis and two-photon photolysis of 6-(ortho-nitroveratryl)-caged IP3 in living cells. *ChemBioChem* **2006**, *7*, 174-180.

(129) Sarkisov, D.; Gelber, S.; Walker, J. W.; Wang, S. S.-H. Synapse Specificity of Calcium Release Probed by Chemical Two-photon Uncaging of Inositol 1, 4, 5-Trisphosphate. *J. Biol. Chem.* 2007, ***282***, 25517-25526.

(130) Neveu, P.; Aujard, I.; Benbrahim, C.; Le Saux, T.; Allemand, J.-F.; Vriz, S.; Bensimon, D.; Jullien, L. A Caged Retinoic Acid for One- and Two-Photon Excitation in Zebrafish Embryos. *Angew. Chem. Int. Ed.* **2008**, *47*, 3744-3746.

(131) Montgomery, H. J.; Perdicakis, B.; Fishlock, D.; Lajoie, G. A.; Jervis, E.; Guillemette, J. G. Photo-control of nitric oxide synthase activity using a caged isoform specific inhibitor. *Bioorg. Med. Chem.* **2002**, *10*, 1919-1927.

(132) Perdicakis, B.; Montgomery, H. J.; Abbott, G. L.; Fishlock, D.; Lajoie, G. A.; Guillemette, J. G.; Jervis, E. Photocontrol of nitric oxide production in cell culture using a caged isoform selective inhibitor. *Bioorg. Med. Chem.* **2005**, *13*, 47-57.

(133) Lin, W.; Peng, D.; Wang, B.; Long, L.; Guo, C.; Yuan, J. A Model for Light-Triggered Porphyrin Anticancer Prodrugs Based on an o-Nitrobenzyl Photolabile Group. *Eur. J. Org. Chem.* **2008**, *5*, 793-796.

(134) Dore, T. M. Multiphoton Phototriggers for Exploring Cell Physiology. In *Dynamic Studies in Biology: Phototriggers, Photoswitches, and Caged Biomolecules*; Givens, R. S., Goeldner, M., Eds.; Wiley-VCH: Weinheim, Germany, **2005**, p 435-459.

(135) Fedoryak, O. D.; Dore, T. M. Brominated hydroxyquinoline as a photolabile protecting group with sensitivity to multiphoton excitation. *Org. Lett.* **2002**, *4*, 3419-3422.

(136) Egri, G.; Kolbert, A.; Balint, J.; Fogassy, E.; Novak, L.; Poppe, L. Baker's yeast mediated stereoselective biotransformation of 1-acetoxy-3-aryloxypropan-2-ones. *Tetrahedron: Asym.* **1998**, *9*, 271-283.

(137) Yale, H. L.; Pribyl, E. J.; Braker, W.; Bernstein, J.; Lott, W. A. Muscle-relaxing compounds similar to 3-(*o*-toloxy)-1,2-propanediol. II. Substituted alkanediols. *J. Am. Chem. Soc*. **1950**, *72*, 3716-3718.

(138) Bardez, E. Excited-state proton transfer in bifunctional compounds. *Isr. J. Chem.* **1999**, *39*, 319-332.

(139) Bardez, E.; Fedorov, A.; Berberan-Santos, M. N.; Martinho, J. M. G. Photoinduced Coupled Proton and Electron Transfers. 2. 7-Hydroxyquinolinium Ion. *J. Phys. Chem. A* **1999**, *103*, 4131-4136.

(140) Adams, S. R.; Kao, J. P. Y.; Grynkiewicz, G.; Minta, A.; Tsien, R. Y. Biologically useful chelators that release $Ca^{2+}$ upon illumination. *J. Am. Chem. Soc.* **1988**, *110*, 3212-3220.

(141) Livingston, R. Behavior of Photochromic Systems. In *Photochromism*; Brown, G. H., Ed.; Wiley: New York, **1971**, p 13-44.

(142) Hatchard, C. G.; Parker, C. A. A new sensitive chemical actinometer. II. Potassium ferrioxalate as a standard chemical actinometer. *Proc. R. Soc. London, Ser. A* **1956**, *235*, 518-536.

(143) Xu, C.; Guild, J.; Webb, W. W.; Denk, W. Determination of absolute two-photon excitation cross sections by *in situ* second-order autocorrelation. *Opt. Lett.* **1995**, *20*, 2372-2374.

(144) Simons, J. P. *Photochemistry and Spectroscopy*; Wiley-Interscience: New York, **1971**.

(145) Zhu, Y.; Pavlos, C. M.; Toscano, J. P.; Dore, T. M. 8-Bromo-7-hydroxyquinoline as a Photoremovable Protecting Group for Physiological Use: Mechanism and Scope. *J. Am. Chem. Soc.* **2006**, *128*, 4267-4276.

(146) Kwok, W. M.; An, H.-Y.; Xue, J.; Ma, C.; Du, Y.; Nganga, J. L.; Zhu, Y.; Dore, T. M.; Phillips, D. L. Time-Resolved Spectroscopic Studies of the Photodeprotection of 8-Bromo-7-hydroxyquinoline Caged Acetate. Unpublished work

(147) Zhu, Y.; Reddie, K.; Davis, M. J.; Kragor, C.; Wilson, H.; Dore, T. M. Unpublished work.

(148) Kiskin, N. I.; Ogden, D. Two-photon excitation and photolysis by pulsed laser illumination modelled by spatially non-uniform reactions with simultaneous diffusion. *Eur. Biophys. J.* **2002**, *30*, 571-587.

(149) Haugland, R. P.; Gee, K. R. Preparation α-carboxy amino acids and nucleotides caged with a photo-removable *o*-nirobenzyl group. US Patent US 5635608, 19970603, 1997.

(150) Wootton, J. W.; Trentham, D. R. Caged compounds to probe the dynamics of cellular processes: synthesis and properties of some novel photosensitive P-2-nitrobenzyl esters of nucleotides. *NATO ASI Ser., Ser. C* **1989**, *272*, 277-296.

(151) Goldman, Y. E.; Hibbred, M. G.; Trentham, D. R. Relaxation of rabbit psoas muscle fibres from rigor by photochemical generation of adenosine 5'-triphosphate. *J. Physiol.* **1984**, *354*, 577-604.

(152) Borejdo, J.; Shepard, A.; Akopova, I.; Grudzinski, W.; Malicka, J. Rotation of the lever Arm of Myosin in Contracting Skeletal Muscle Fiber Measured by Two-Photon Anisotropy. *Biophys. J.* **2004**, *87*, 3912-3921.